

**The influence of coagulation system on early leukocyte
recruitment and acute microcirculatory injury after
extended hepatectomy**



Yunjie Zhang

aus Shanghai, P.R China

2023

Aus der Klinik für Allgemein-, Viszeral-
und Transplantationschirurgie

Klinik der Universität München
Direktor: Prof. Dr. Jens Werner

**The influence of coagulation system on early leukocyte
recruitment and acute microcirculatory injury after
extended hepatectomy**

Dissertation
zum Erwerb des Doktorgrades der Medizin
an der Medizinischen Fakultät der
Ludwig-Maximilians-Universität zu München

vorgelegt von

Yunjie Zhang

aus Shanghai, P.R China

2023

Mit Genehmigung der Medizinischen Fakultät
der Universität München

Berichterstatter:	Prof. Dr. Andrej Khandoga
Mitberichterstatter:	Prof. Dr. Christian Schulz Prof. Dr. Michael Spannagl Prof. Dr. Fritz Krombach
Mitbetreuung durch den promovierten Mitarbeiter:	Dr. med. Maximilian Lerchenberger
Dekan:	Prof. Dr. med. Thomas Gudermann
Tag der mündlichen Prüfung:	26.10.2023

Meiner Familie

Inhaltsverzeichnis

<i>Zusammenfassung</i>	4
<i>Abstract</i>	6
<i>Abbreviations</i>	8
1. Background	10
1.1 The importance of liver resection in liver surgery	10
1.2 Post-hepatectomy liver failure: a dangerous complication after hepatectomy	11
1.3 Current preventive strategies of the PHLF are not promising	12
1.4 Hepatic perfusion	14
1.5 Portal hyperperfusion and microcirculatory injury after extended liver resection	15
1.6 Sterile inflammation of the liver	16
1.7 The potential role of leukocytes in PHLF	17
1.7.1 Leukocytes	17
1.7.2 Leukocyte recruitment	18
1.7.3 Current knowledge on the role of leukocytes in PHLF	21
1.8 Blood coagulation and liver injury	22
1.8.1 Serine proteases	23
1.8.2 Platelets	24
1.8.3 Protease-activated receptors	26
1.8.4 Fibrinogen	26
1.9 Hypotheses	27
2. Objectives	28
3. Materials and Methods	30
3.1 Ethics	30
3.2 Animal models	30
3.3 Anesthesia	30
3.4 General preparation	31
3.5 Surgical preparation for 60% PH	32
3.6 Surgical preparation for 90% PH	33

3.7 Surgical preparation for sham-operated animals.....	33
3.8 Basic setting for <i>in vivo</i> imaging	34
3.9 Blood and tissue sampling.....	35
3.10 Epifluorescence microscopy	35
3.11 Microcirculatory parameters	37
3.12 Study I: the role of SPs in the acute-phase liver injury after PH	37
3.12.1 Experimental groups.....	37
3.12.2 Protocol of inhibitor treatment	38
3.12.3 Experimental protocol.....	38
3.13. Study II: the impact of platelets on the acute-phase liver injury after PH.....	39
3.13.1 Experimental design and groups.....	39
3.13.2 Protocol of platelet depletion.....	40
3.13.3 Experimental protocol.....	40
3.14. Study III: the impact of PAR-4 on platelet aggregation and neutrophil-platelet interaction in the acute-phase injury after PH	41
3.14.1 Experimental design and groups.....	41
3.14.2 Experimental protocol.....	42
3.14.3 Two-photon microscope	43
3.15 Study IV: fibrinogen deposition in the acute phase after PH.....	45
3.15.1 Experimental groups.....	45
3.15.2 Experimental protocol.....	45
3.15.3 Assessment of fibrinogen deposition in the acute phase after extended liver resection <i>in vivo</i>	46
3.16 Histology.....	47
3.16.1 Paraffinization of the tissue	47
3.16.2 Immunohistochemistry (IHC)	48
3.16.3 Antibodies and reagents	49
3.17 Biochemical analysis of the liver function	50
3.18 Statistics	50
4. Results	51
4.1 Study I: the role of SPs in the acute-phase liver injury after PH	51
4.1.1 Macrohemodynamic parameters	51
4.1.2 Microcirculatory parameters.....	52
4.1.3 Bilirubin, AST and ALT.....	55
4.2 Study II: the role of platelets on the acute-phase liver injury after PH	56
4.2.1 Macrohemodynamic parameter	56
4.2.2 Platelet counts.....	57
4.2.3 Microcirculatory parameters.....	58
4.2.4 IHC analysis	61
4.2.5 Bilirubin, AST, ALT and GLDH.....	62

4.3 Study III: the impact of PAR-4 on platelet aggregation and neutrophil-platelet interaction in the acute-phase liver injury after 60% PH	63
4.3.1 Macrohemodynamic parameter	64
4.3.2 Microcirculatory parameters.....	64
4.3.3 Two-photon-microscopic analysis.....	67
4.3.4 AST, ALT and GLDH.....	71
4.4 Study IV: Fibrinogen deposition in the acute phase after PH	72
4.4.1 Macrohemodynamic parameters	72
4.4.2 Fibrinogen deposition after PH	72
5. Discussion	74
5.1 Animal models	75
5.1.1 Approximate 60%-PH model for <i>in vivo</i> imaging.....	75
5.1.2 Approximate 90%-PH model for <i>in vivo</i> imaging.....	76
5.1.3 Approximate 60%-PH with platelet-depletion model	76
5.1.4 The setting for <i>in vivo</i> imaging.....	77
5.2 Epifluorescence microscopy	79
5.3 Two-photon microscopy	80
5.4 results	81
5.4.1 Study I	81
5.4.2 Study II.....	83
5.4.3 Study III.....	86
5.4.4 Study IV.....	88
5.5 Conclusions	89
6. References	90
<i>Danksagung</i>	102
<i>Affidavit</i>	104
<i>Lebenslauf</i>	105

Zusammenfassung

Das hepatektomie-induzierte Leberversagen ist ein potentiell tödliches Krankheitsbild nach erweiterter Leberresektion oder Leberteiltransplantation. Dieses Versagen scheint einerseits durch eine supraphysiologische Belastung der Restleber, andererseits durch die hyperperfusionsbedingten Mikrozirkulationsverletzungen und eine verhinderte Leberregeneration verursacht zu werden. Der genaue pathophysiologische Mechanismus der mikrovaskulären Schädigung in der akuten Phase konnte jedoch bisher noch nicht entschlüsselt werden.

Im Rahmen der vorliegenden Doktorarbeit wurden die Einflüsse der wichtigen Bestandteile der Koagulationskaskade bei akuter Leberschädigung nach partieller Hepatektomie mittels intravitalmikroskopischer Methoden sowie weiterführender laborchemischer Untersuchungen und (immun-)histochemischer Aufarbeitung der Leberpräparate untersucht.

Zuerst wurde ein Mausmodell für die intravitalmikroskopische Untersuchung etabliert. Nach erweiterter Hepatektomie wurde neben einer Perfusionsstörung eine ausgeprägte Endothel-Leukozyten-Interaktion beobachtet. Die Serinproteasen beeinflussten sowohl die Mikroperfusion wie auch die Leberschädigung durch eine frühe Leukozytenrekrutierung nach partieller Hepatektomie.

Mittels eines Thrombozytendepletionsmodells wurde der Einfluss der Thrombozyten nach erweiterter Hepatektomie untersucht. Die Ergebnisse deuteten darauf hin, dass Thrombozyten die Rekrutierung der verschiedenen Leukozytensubpopulationen durch eine ICAM-1-abhängige Endothel-Leukozyten-Interaktion regulierten. Zudem führte die Depletion der Thrombozyten zu einer signifikant verminderten Verschlechterung der Leberfunktion.

Infolgedessen wurde die Rolle des PAR-4, ein Aktivator der Thrombozyten, in der Bildung von Mikrothrombosen als Ursache der Perfusionsstörung nach partieller Hepatektomie mithilfe der Zwei-Photon-Mikroskopie untersucht. Die Thrombozytenaktivierung über PAR-4 induzierte Mikrothrombosen und vermehrte Neutrophil-Thrombozyten-Interaktionen in hepatischen Sinusoiden, wodurch eine Akutelechschädigung nach partieller Hepatektomie verschlimmert wurde.

Schlussendlich wurde die Fibrinogenbindung am hepatischen Endothel nach partieller Hepatektomie beobachtet. Die deutliche Ablagerung des Fibrinogens in der Lebermikrozirkulation bewies eine Aktivierung und Beanspruchung des Koagulationssystems unter einem stark gesteigerten Scherstress unmittelbar nach der Leberresektion.

In dieser Studie wurde der Pathomechanismus des Leberversagens nach Hepatektomie mit Hilfe der in-vivo-Mikroskopie und verschiedener Mausmodelle innovativ untersucht. Dies war auch die erste Beschreibung einer intravitalen Zwei-Photonen-Mikroskopie-Studie im Zusammenhang mit dem hepatektomie-induzierten Leberversagen. Die klinische Relevanz der vorgestellten Komponenten der Koagulationskaskade für therapeutische Interventionen bleibt in weiterführenden Studien zu überprüfen.

Abstract

Post-hepatectomy liver failure or Small-for-size syndrome is a potentially fatal complication after extended liver resection or partial liver transplantation. This is caused by supraphysiologic perfusion in the remnant liver and microcirculatory injury. However, the exact pathophysiological mechanism of microvascular injury in the acute phase is still unclear.

In the present work, the impact of important components from the coagulation cascade was investigated in acute liver injury after partial hepatectomy.

First, a mouse model suitable for intravital microscopic examination was established. After extended hepatectomy, an increased endothelial-leukocyte interaction was observed in addition to perfusion failure. Serine proteases affected both microperfusion and liver injury by inducing early leukocyte recruitment after partial hepatectomy.

A platelet depletion model was used to investigate the influence of platelets after extended hepatectomy. The results indicated that platelets regulated the recruitment of different leukocyte subpopulations through an ICAM-1-dependent pattern. In addition, the platelet depletion resulted in significantly improved liver function.

Furtherly, the role of PAR-4, an activator of platelets, was investigated using two-photon microscopy. Platelet activation via PAR-4 induced microthrombosis and increased neutrophil-platelet interactions in hepatic sinusoids, exacerbating acute liver injury after partial hepatectomy.

Finally, fibrinogen deposition to hepatic endothelium after partial hepatectomy was investigated. The deposition of fibrinogen in the liver microcirculation reflected the activation of the coagulation system under increased shear stress immediately after liver resection.

In this study, the pathomechanism of post-hepatectomy liver failure was innovatively investigated by utilizing *in vivo* microscopy and different murine models. This was also the first description of *in vivo* two-photon microscopy study in the context of post-hepatectomy liver failure. The clinical relevance of the presented components of the coagulation cascade as therapeutic interventions remains to be verified in further studies.

Abbreviations

2PM	two-photon microscope
ALT	alanine aminotransferase
AST	aspartate aminotransferase
CCD	charge-coupled device
DAMPs	damage-associated molecular patterns
FITC	fluorescein isothiocyanate
GLDH	glutamate dehydrogenase
GP	glycoprotein
HABR	hepatic arterial buffer response
HCC	hepatocellular carcinoma
ICAM-1	intercellular adhesion molecule 1
ICAM-2	intercellular adhesion molecule 2
ICC	intrahepatic cholangiocarcinoma
IHC	immunohistochemistry
IL	interleukin
IRI	ischemia-reperfusion injury
LFA-1	leukocyte function associated molecule-1

MAP	mean arterial pressure
MMP-9	matrix metalloproteinase-9
MPO	myeloperoxidase
NF- κ B	nuclear factor kappa-light-chain-enhancer of activated B cells
NK	natural killer
PAR4	protease-activated receptor 4
PH	partial hepatectomy
PHLF	post-hepatectomy liver failure
Plg	plasminogen
SEM	standard error of the mean
SFSS	small-for-size syndrome
SP	serine protease
TCR	T cell receptor
TxA2	Thromboxane A2
tPA	tissue-type plasminogen activator
TXA	tranexamic acid
uPA	urokinase-type plasminogen activator
vWF	von Willebrand Factor

1. Background

1.1 The importance of liver resection in liver surgery

Liver resection or hepatectomy is a widely practiced surgical procedure treating many major hepatic diseases¹. Primary liver cancer, for example, is the fifth most common cancer and the second leading cause to cancer deaths worldwide². The most common histological type is hepatocellular carcinoma (HCC, approximately 80%), followed by intrahepatic cholangiocarcinoma (ICC, approximately 15%)³. The incidence of liver cancer has considerably risen in India, Oceania, America, and most European countries in recent years⁴. Globally, the incidence of HCC increased nearly four folds in the last four decades (1.6 per 100 000 in 1975-1977 to 4.8 per 100 000 in 2005-2007)⁵ according to an End Results population-based cancer registry. The overall 5-year survival rate of HCC is 18.4%. The incidence of ICC in America averaged 1.6 per 100 000/ per year since 2000, with an overall 5-year survival rate of 10% and 30-35% for the operable patients^{6,7}. Surgical liver resection is the standard curative treatment of non-metastatic and resectable tumors in patients suffering from HCC and ICC.

Other than primary liver cancer, colorectal cancer is the second most common cancer type in females and third in males. Approximately 70% of patients diagnosed with colorectal cancer will eventually develop hepatic metastasis⁸. Increasing evidence suggests that liver resection is also a successful treatment for patients suffering from colorectal hepatic metastasis^{9,10}. The operability rate of hepatic metastasis is 20-30%¹¹. The progressive resection of metastasis results

in a 5-year survival rate of approximately 30% to 47%¹². However, recurrence occurs in up to 75% of patients after liver resection¹³. Resection of the metastasis is the only curative treatment that has been proven to contribute to patient survival¹⁴.

Liver resection is also performed in the split liver and living-donor liver transplantation¹⁵. Liver transplantation has been developed to treat patients with end-stage liver disease with 1- and 5-year survival rates of 90% and 80%, respectively¹⁶. Liver transplantation improved the 3-year survival rate to 80% from HCC patients who were selected according to Milan criteria¹⁷ and the 5-year survival rate up to 42% in patients with ICC¹⁸. In 2015, 1489 candidates were added to the waiting list in Germany, but only 894 liver transplantations were performed, in which 48 of the transplanted organs were from living donors¹⁹. However, organ shortage is always a major limitation. The United Network for Organ Sharing database showed that of 81592 listed patients, 11284 (13.8%) died on the waitlist from 2002-2013²⁰.

1.2 Post-hepatectomy liver failure: a dangerous complication after hepatectomy

Nevertheless, the practice of hepatectomy is largely restricted because extended resection might cause post-hepatectomy liver failure (PHLF)²¹, also known as small-for-size syndrome (SFSS) in the area of transplantation, which is associated with a mortality rate up to 30%²². The incidence of PHLF is reported differently between 1.2 to 32%, according to various centers²³ and is correlated with the volume of remnant liver or the graft-to-recipient weight ratio regarding liver transplantation²⁴. Clinically, PHLF was generally defined as the occurrence of

hyperbilirubinemia, coagulopathy, ascites, and encephalopathy in the first week postoperatively (Table 1)²⁵⁻²⁷. Microscopically, the cholestasis, hemorrhagic necrosis, and ballooning of hepatocytes can be found in the parenchymal tissue with the PHLF²⁸. Three grades of PHLF were defined by the International Study Group of Liver Surgery based on its impact on clinical management.

grade	definition
a	PHLF resulting in abnormal laboratory parameters but requiring no change in the clinical management of the patient.
b	PHLF resulting in a deviation from the regular clinical management but manageable without invasive treatment.
c	PHLF resulting in a deviation from the regular clinical management and requiring invasive treatment.

Table 1: grading of PHLF according to a consensus from the international study group of liver surgery²³.

1.3 Current preventive strategies of the PHLF are not promising

The surgical intervention, such as hemiportocaval shunt^{29,30}, meso-renal shunt³¹, delayed ligation of spontaneous portosystemic shunts³²⁻³⁴, splenectomy^{35,36}, splenic artery embolization/ligation³⁷, and preoperative transjugular intrahepatic portosystemic shunt³⁸⁻⁴⁰ can prevent or decrease the incidence of the PHLF postoperatively. These approaches mainly divert the portal blood to reduce the portal hyperperfusion, but they fail to provide a promising outcome to

prevent the occurrence of PHLF⁴¹. Many have been reported to cause adverse events such as surgical complications and increased incidence of infection due to the immune defect after the splenectomy (Table 2)⁴². Pharmacological approaches aiming at tuning portal perfusion were only described in animal-based experiments. Application of Prostaglandin E1⁴³, Nitric oxide⁴⁴, Octreotide⁴⁵, and Endothelin A receptor antagonist⁴⁶ showed positive effects of ameliorating microcirculatory damage and improving liver regeneration in different animal models. The pathophysiological details of the PHLF remains unclear. The imbalance between liver regeneration and the overwhelming demand for the liver function is believed as the principal pathogenesis of PHLF⁴⁷. The unmasking of the underlying mechanisms might improve the postoperative management of patients with PHLF and indirectly ease the long-presented liver graft shortage.

approaches	advantages	disadvantages	citations
1. <i>portal-systemic (porto-caval, mesorenal or meso-caval) shunt</i>	effective in decreasing portal vein pressure	surgical complications portal vein thrombosis encephalopathy insufficient hepatic perfusion liver graft atrophy	Yamada <i>et al.</i> ²⁹ Botha <i>et al.</i> ³⁰ Sato <i>et al.</i> ³¹
2. <i>delayed ligation of spontaneous portal-systemic shunt</i>	sufficient hepatic perfusion	complicated surgical procedures lack of studies with large sample size	Sato <i>et al.</i> ³² Cescon <i>et al.</i> ³³ Shirouzu <i>et al.</i> ³⁴
3. <i>splenectomy</i>	may reduce acute rejection effective in decreasing portal vein pressure	increased risk of hemorrhage increased risk of infection surgical difficulties portal vein thrombosis	Ren <i>et al.</i> ³⁵ Eipel <i>et al.</i> ³⁶

4. <i>splenic artery embolization/ligation</i>	without increased risk of bleeding and infection	splenic abscess/infarction	Umeda <i>et al.</i> ³⁷
5. <i>preoperative transjugular intrahepatic portosystemic shunt</i>	no need of additional surgery	controversial outcomes	Rosado <i>et al.</i> ³⁸ Sellers <i>et al.</i> ³⁹ Saad <i>et al.</i> ⁴⁰

Table 2: comparison of surgical approaches to prevent SFSS/PHLF

1.4 Hepatic perfusion

The human liver receives approximately 25% of the cardiac output and is the organ with the highest blood supply in the body. The liver has a dual blood supply. The primary inflows of the liver are the portal vein and the hepatic artery, which are accompanied by the common hepatic duct, lymphatic vessels, and nerves (sympathetic nerve and vagus nerve). The portal vein supplies with 75-80% of the total inflow of the liver, whereas the remaining 20-25% originates from the hepatic artery⁴⁸. The oxygen supply of the liver is provided half by portal venous blood and half from the hepatic artery⁴⁹. The total blood inflow of the portal vein is determined by the outflow of splanchnic organs, namely, the splenic vein and superior mesenteric vein.

The hepatic blood inflow is dynamic hemostasis regulated by the hepatic arterial buffer response (HABR). Lauth *et al.* described this phenomenon for the first time that the hepatic arterial inflow can compensate for the change of portal venous flow to maintain a physiological liver perfusion⁵⁰. HABR is also seen in the denervated liver⁵¹, a transplanted human liver, and resected remnant liver⁵². A hypothesis of the HABR is the “washout” theory of adenosine. Adenosine is produced in liver sinusoids at a constant rate. It serves as a potent dilator of the

hepatic artery. A decreased portal blood flow may result in a relatively reduced “washout” of adenosine. The accumulated adenosine can dilate the hepatic artery. This can compensate for the decrease in portal blood flow. Vice versa, a high portal blood flow will “washout” the adenosine, which results in a contraction of the hepatic artery⁵³. However, in the context of extended hepatectomy, the HABR fails to compensate for the portal inflow. The constant hepatic hyperperfusion will cause an increment of hepatic microvascular shear stress. This shear stress increment is an essential trigger of liver regeneration. Excessive shear stress, however, leads to endothelial injury and necrosis, which hinders liver function and regeneration⁵⁴⁻⁵⁶.

1.5 Portal hyperperfusion and microcirculatory injury after extended liver resection

To explain the cause of PHLF, the “portal vein hyperperfusion” hypothesis is widely used by many clinical and animal studies^{24,57}. Under the pathological condition after liver resection, HABR fails to compensate for the portal inflow. The relatively high portal blood inflow received by the limited hepatic volume can disturb liver homeostasis⁵⁸. Clinically, the mean portal flow is 130mL/min/100g weight of graft, according to Paulsen *et al.*⁵⁹. The early elevation of the portal vein pressure (≥ 20 mmHg) after the liver transplantation is associated with poor outcomes^{60,61}. The portal hyperperfusion and a poor arterial inflow caused by the HABR might also contribute to the hypoxia and ischemia and worsen the parenchymal injury⁶².

Shear stress is a force that causes layers or parts to slide upon each other in opposite directions. In the context of blood, blood shear stress is mainly associated with blood viscosity and velocity⁶³. Exaggerated shear stress due to excessive resection can damage hepatic endothelial cells and cause hemorrhagic necrosis⁵⁵. Man *et al.* reported a significantly increased portal pressure in the first 20 minutes after reperfusion using a rat partial liver transplantation model. The hepatic microcirculatory blood flow rose during the first 40 minutes after reperfusion⁶⁴. Morphological changes of the hepatic microstructure, such as disruption of the liver endothelial lining in sinusoids, sinusoidal congestion, and collapse of the space of Disse, were reported by using electron microscopy⁶⁴. In another animal-based study, the shrink of the sinusoidal lumen and impairment of the liver endothelial lining could be observed already ten minutes after the 80% partial hepatectomy (PH)⁶⁵. Several clinical studies and systematic reviews concluded that clinically significant portal hypertension had a negative impact on both of the short- and long-term prognoses after PH^{66,67}.

1.6 Sterile inflammation of the liver

Hepatic endothelial injury and impairment of the hepatic microstructure due to hyperperfusion following extended hepatectomy can lead to a sterile inflammation of the liver. The term “sterile inflammation” is a type of inflammation resulting from such as ischemia-reperfusion injury (IRI), crush injury, or chemically induced injury in the absence of any pathogens⁶⁸. The trigger of this type of inflammation is called “damage-associated molecular patterns” (DAMPs) released from the injured cells. Many different DAMPs have been identified, such as adenosine triphosphate, Defensins, High-Mobility-Group-Protein B1, Heat Shock Protein, and nuclear DNA, etc⁶⁹.

Liver IRI is, as an example, a hepatic injury resulting from sterile inflammation and oxidative stress following the restoration of oxygen delivery to previously ischemic liver microcirculation. The lack of oxygen during ischemia results in ATP depletion and the loss of metabolic homeostasis in hepatic cells. After receiving the DAMPs from the damaged hepatic cells, Kupffer cells are activated. They can release reactive oxygen species (ROS) provoking cell damage and a variety of cytokines such as interleukin(IL)-1- β , tumor necrosis factor (TNF)- α , interferon- γ , and IL-12 which leads to the recruitment of pro-inflammatory leukocytes like neutrophils, macrophages ,and CD4+ T-cells. CD4+ T-cells can activate endothelium and facilitate platelet adherence via CD40-CD40L and CD28-B7-dependent pathways⁷⁰. This is followed by the swelling of sinusoidal endothelial cells, which causes narrowing of the hepatic sinusoidal lumen and microcirculatory injury. The narrowing of sinusoidal lumen also contributes to the accumulation of neutrophils, which induces further tissue damage by releasing ROS and proteases⁷¹.

1.7 The potential role of leukocytes in PHLF

1.7.1 Leukocytes

Leukocytes are a group of blood cells stemming from hemopoietic stem cells in the bone marrow. They are a critical component of both innate and adaptive immune systems⁷². Leukocytes are further divided into two main groups, namely granulocytes and agranulocytes. The granulocytes include neutrophils, basophils, eosinophils, and mast cells. The cytoplasmic granules in these cells contain enzymes that can directly digest pathogens. The other type is agranulocytes, also called mononuclear leukocytes, such as lymphocytes, macrophages, monocytes, and dendritic cells. They

are involved in both innate and adaptive immunity⁷³. Leukocytes play a critical role in the inflammatory response of many liver diseases, including cirrhosis, IRI, sepsis- or endotoxin-induced liver failure, viral and alcoholic hepatitis, graft rejection, and cholestasis^{70,74-78}.

Neutrophil granulocytes, also called neutrophils, are polymorphonuclear leukocytes with a mean diameter of 9 to 15 μm . They constitute 50-70% of leukocytes in human circulation. Neutrophils are well recognized as the first group of leukocytes reacting to acute inflammation and recruited to the inflammatory site⁷⁹. As a type of granulocytes, neutrophils can eliminate pathogens by both intra- and extracellular mechanisms. 1) Neutrophils can phagocytose the pathogens and release ROS to kill them directly.⁸⁰ 2) Neutrophils can release antibacterial proteins (lysozyme, defensins, lactoferrin und cathepsins) into the extracellular milieu.⁸¹ 3) Neutrophils can form neutrophil extracellular traps (NETs) containing histones and enzymes that immobilize pathogens like bacteria and facilitate the killing process via antibacterial proteins⁸². Neutrophils are also highly functional cells in sterile inflammation, like the process of tissue injury and repair⁸². Early neutrophil recruitment can be triggered by DAMPs and by chemokines due to tissue injury. After arriving at the injured site, neutrophils phagocytose the necrotic cell debris and release proteolytic enzymes and antimicrobial proteins for the further clearance of injured tissue. The phagocytosis can also trigger the neutrophils to release pro-regenerating cytokines such as transforming growth factor- β and IL-10⁸³.

1.7.2 Leukocyte recruitment

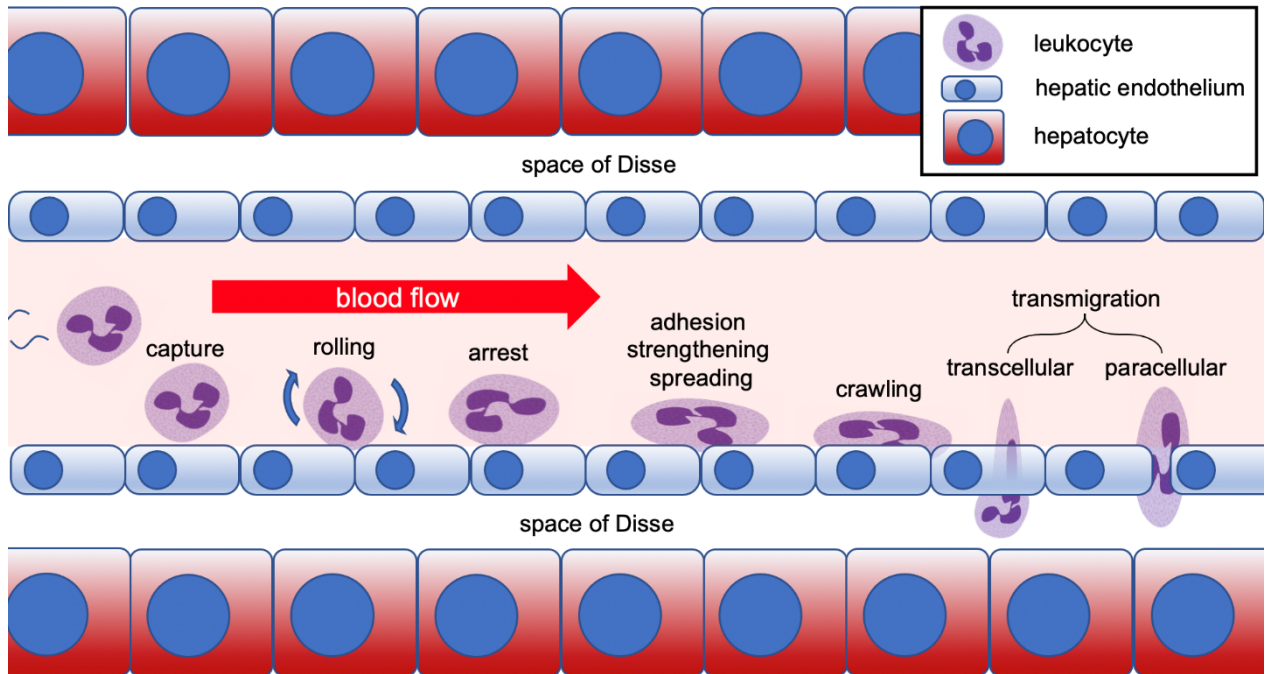
The leukocyte recruitment process enables leukocytes, mainly neutrophils, to leave the intravascular compartment to get to the inflammation site. This process happens predominantly in postcapillary venules starting with capturing the free-flowing leukocytes in the blood to the

endothelial wall. There are generally six major steps for a free-flowing leukocyte to transmigrate into the tissue, namely (I) capture or tethering, (II) rolling, (III) arrest, (IV) adhesion strengthening and spreading, (V) intraluminal crawling, and (VI) transmigration (Figure 1)⁸⁴.

The selectin family, namely P-, E-, L-selectin, is essential to initiate the capture of leukocytes and to reduce the velocity of the leukocyte rolling movement⁸⁵⁻⁸⁷. P-selectin is stored in the Weibel-Palade bodies and constitutively expressed by endothelial cells⁸⁸. Histamine and different inflammatory mediators stimulate the translocation of P-selectin to the luminal surface of endothelial cells. P-selectin on the vessel wall can bind to P-selectin glycoprotein ligand 1 expressed on leukocytes. This binding secures the connection between leukocytes and endothelial cells, which facilitates leukocyte capture and tethering. The tethering enables a cell to roll at a velocity of 10-15 $\mu\text{m/s}$ ⁸⁹. During the rolling process, the integrins on leukocytes can be activated by chemotactic cytokines in an inflammatory environment. The activation of integrins leads to the changes in individual integrin heterodimers, which increases ligand-binding energy⁸⁴.

Leukocyte arrest is triggered by chemokines. During inflammatory processes, activated endothelial cells and leukocytes can secrete a broad range of chemokines. They can bind to chemokine receptors on the endothelium. Binding of chemokines to their receptors activates phospholipase C, which activates cytoskeletal regulatory kinases and mediate chemotaxis⁹⁰. Activated platelets can also deposit CC-chemokine ligand 5 and CXC-chemokine ligand 4 and 5 onto the endothelium and trigger the leukocyte arrest⁹¹. Leukocyte arrest is mainly executed

by the intercellular adhesion molecules-1 (ICAM-1) and vascular cell-adhesion molecule 1 (VCAM-1). ICAM-1 is a molecule constitutively expressed by endothelial cells, which interact



with β_2 -integrin lymphocyte function-associated antigen-1 (LFA-1, also known as $\alpha_L\beta_2$ -integrin). VCAM-1 interacts with β_1 -integrin very late antigen 4 (VLA-4, also known as $\alpha_4\beta_1$ -integrin)^{92,93}.

Figure 1: a schematic overview of the leukocyte adhesion in hepatic sinusoids. Under certain shear stress, the free-flowing leukocytes are captured with the help of selectin-family. As shear force pushes the captured leukocytes forwards, the tethers break off at the rear, new tethers are formed in the front, which enables the leukocytes to roll on the endothelial wall. During the rolling, leukocytes can be activated by chemokines released by endothelium, which expands the expression of integrins leading to the arrest of leukocytes. The adhesion force further increases while crawling to find appropriate sites for the transmigration either in a transcellular or by a paracellular manner.

A firmly adherent leukocyte will then transmigrate through the endothelial wall either by the paracellular route (80-95%) through the endothelial junction^{84,94} or by the transcellular route

(5-20%) directly “through” a single endothelial cell⁹⁵. Ligation of ICAM-1 leads to increased intracellular Ca²⁺ and activation of MAPK and Rho-GTPase, collectively induces endothelial contraction and the opening of intercellular contacts. The transmigration is then mediated by the junctional molecules expressed by endothelial cells. Platelet/endothelial-cell adhesion molecule (PECAM-1) is responsible for homophilic interactions; junctional adhesion molecule A, B, and C (JAM-A, JAM-B, and JAM-C) regulate both homophilic and integrin interaction⁹¹.

1.7.3 Current knowledge on the role of leukocytes in PHLF

What has been generally accepted is that leukocytes, especially polymorphonuclear neutrophils, prompts the inflammatory response in the acute phase after liver resection⁹⁶. They might cause further circulatory and parenchymal damage^{97,98}, despite their positive effect on liver regeneration^{99,100}. Most of the research has been focused on the impact of leukocyte function on liver regeneration⁹⁹⁻¹⁰⁴. Less effort has been made to address what triggers the recruitment of leukocyte and the role of different subsets of leukocyte^{98,105-107}.

Ohashi *et al.* found that six hours after 70% PH, matrix metalloproteinase-9 (MMP-9) facilitated the neutrophils to migrate from the sinusoids into the tissue, which promoted inflammation¹⁰⁵. Inhibition of MMP-9 significantly attenuated the inflammatory response and parenchymal damage from SFSS⁹⁷. Rudich *et al.* reported that focal necrosis could be found as early as two hours following 70% PH. T, natural killer (NK), and NKT cells were recruited to the liver in the early phase¹⁰⁶. Unlike neutrophils, a significantly increased number of CD3+ T cells was firstly found two days after PH¹⁰⁷. The proportion of CD4+ cells was mildly increased

by about 10% during the first day after PH¹⁰⁴. A series of studies from Toru Abo and colleagues showed that the T cell receptor (TCR)⁺ CD3⁺ T cells with high expressions of IL-2R β and leucocyte function-associated molecule-1 (LFA-1), along with the NK cells (TCR⁻ IL-2R β ⁺) were the dominant subsets of T cell in the normal liver¹⁰⁷. By analyzing the subset of lymphocytes in the post-PH liver, the most expanded subset was NKT cell (NK1.1⁺ intermediated CD3), which dramatically expanded during the first day after PH. The expansion of these subsets was also associated with sympathetic nerve activation¹⁰⁴. Later, using NKT cell-deficient mice, the same group revealed that NKT cell and granulocytes participated in the hepatic inflammation after PH¹⁰⁸. The cellular immune response mechanism in SFSS is only partially unveiled. The complex network of cellular interaction and the complete picture of the immune process is still uncertain.

1.8 Blood coagulation and liver injury

The blood coagulating system contains abundant cellular and humoral components that are exhibiting hemostatic functions. They help to seal vascular damage and prevent the invasion of pathogens. In recent decades, huge interest has been drawn to answer a novel cross-talk between the blood coagulating system and inflammation¹⁰⁹. The endothelial cell injury or activation could induce a hypercoagulable state. The activation of some key factors in blood coagulating systems, such as serine proteases (SPs) and platelets, was proven to enhance the inflammation¹¹⁰.

1.8.1 Serine proteases

SPs are endopeptidases that cleave peptide bonds in proteins. The catalytic triad, namely histidine, aspartate, and serine, can be found in the catalytic site of all SPs. Each amino acid plays a pivotal role in protein cleaving¹¹¹. There are four clans of SPs, namely, chymotrypsin, subtilisin, carboxypeptidase Y, and Clp protease. SPs are recognized as one of the critical components of the coagulation system. SP members, such as plasmin and thrombin, can mediate inflammation and regeneration processes in various liver diseases¹¹²⁻¹¹⁵. As one of the most prominent SPs, plasmin is formed in the liver as a zymogen known as plasminogen (Plg). The Plg is synthesized in the liver and predominantly activated by tissue-type Plg activator (tPA), urokinase-type Plg activator (uPA), and kallikrein, which are also SPs. This process is negatively regulated by plasminogen activator inhibitor-1 (PAI-1). After activation, plasmin can target tPA and uPA, which forms a positive feedback loop. α_2 -antiplasmin is the primary inhibitor of plasmin. α_2 -macroglobulin can also inhibit plasmin to a lesser extent¹¹⁶.

An important and well-described function of plasmin in the fibrinolytic system is that it cleaves insoluble fibrin clot into soluble fibrin degradation product¹¹⁷. Additionally, plasmin splits other substrates such as prothrombin, fibrinogen, factors V, VIII, IX, XI, XII that can locally reduce the coagulability. Other than the well-known function of SPs in coagulation, SPs own a great impact on leukocyte recruitment in the inflammatory process. PAI-1 was reported to be rapidly deposited on the endothelial wall in IRI. It can cause conformational change in β_2 integrins of rolling neutrophils. This change promotes the hepatic IRI by facilitating neutrophil infiltration¹¹⁸. An *in vivo* chemotaxis assay using the murine cremaster model showed that the inhibition of SPs with aprotinin or the inhibition of plasmin with tranexamic acid could suppress intravascular neutrophil recruitment and transmigration¹¹⁹.

In the context of hepatectomy, the early activity of plasminogen activator was reported after hepatectomy in humans. The significant increase of plasminogen activator activity appeared when the remnant liver volume was smaller than 60% and was negatively correlated with the remnant liver volume¹²⁰. Mars *et al.* reported that activation of both uPA and uPA receptor was detected only one minute after PH¹²¹. Besides an immediate increase of uPA after PH, inhibition of PAI-1, a major physiological inactivator of uPA, could improve the survival of rats undergoing 95% PH¹²². The evidence above suggested that SPs, specifically plasmin/Plg, might play important roles in acute liver injury after liver resection. Notably, inhibition of SPs^{123,124}, as well as competitive inhibition of plasmin alone¹²⁵, resulted in attenuated inflammatory responses in patients undergoing both extended liver resection and other major surgical procedures through weakened neutrophil recruitment and complement activation.

The evidence above implied the engagement of SPs after extended hepatectomy demonstrated by both experimental and clinical studies. However, the detailed mechanism of microvascular injury concerning SPs in the acute phase after liver resection remains unclear.

1.8.2 Platelets

Platelets are anucleate cells with an average size of 2-3 μm stemming from megakaryocytes. The primary and well-described function is the maintenance of hemostasis. Platelets circulate in proximity to vascular walls and do not interact with endothelial cells under physiologic conditions. However, when the endothelial lining is disrupted, the initial tethering of the platelet to the endothelial wall occurs^{126,127}, which also leads to the rolling and adherence of the platelet. This process is mainly facilitated by the interaction of the subendothelial extracellular matrix and platelet receptors. The glycoprotein (GP) 1b/V/IX, a receptor on the platelet, can

bind to the von Willebrand factor (vWF), which serves as an adhesive GP. GPVI and α IIb β 1 receptors can bind to the exposed collagen from the subendothelial extracellular matrix¹²⁸. After firm adhesion, a platelet can bind to and incorporate other platelets from the microcirculation. This process is mediated by α IIb β 3 integrin (GP IIb/IIIa), and p-selectin in the α -granules. Platelets also release thromboxane A2 (TxA2) to constrict the vessel. In the site of injury, platelet can be activated by thrombin, surface stimulation, tissue factor, also called factor III, and platelet secretion products like ADP, TxA2¹²⁸. The activated platelets change into a pseudopodal form and becoming aggregated. Simultaneously, thrombin converts fibrinogen into fibrin, forming a fibrin network and strengthening the aggregated platelet¹²⁹.

It has been shown that these small cellular fragments own a variety of functions in conducting an inflammatory process after endothelial activation^{109,130}. As bridging molecules, such as α IIb β 3 integrin, vWF, ICAM-1, fibrinogen, fibronectin, and α V β 3 integrin, are largely engaged in this process¹³¹. Furthermore, platelets can bind to the injured/activated endothelial wall via GP α IIb as well as CD40L¹³². It was reported that the platelets could also interact with leukocytes via P-selectin/ P-selectin GP ligand-1, CD11b/CD18, and ICAM-2/LFA-11 interaction, during acute inflammation¹³³⁻¹³⁵. Several studies revealed that adhesion of platelets to the vascular wall could be initiated by a high shear rate depending on the GPIb-vWF pathway¹³⁶⁻¹³⁸. Early work of our group showed that platelet-mediated early leukocyte recruitment played a vital role in the inflammatory process of hepatic IRI¹³⁹⁻¹⁴². However, the role of platelet is still unclear in the acute pathophysiological condition of PHLF.

1.8.3 Protease-activated receptors

Protease-activated receptors (PAR) family consists of 4 members (PAR-1-4)¹⁴³. They are classically viewed as elegant mediators in the process of hemostasis. These receptors are G-protein coupled receptors but are unique in contrast to classical receptors because they can be activated by proteolytic cleavage that exposes the tethered ligand¹⁴⁴. PAR-1, PAR-3, and PAR-4 are activated by thrombin, whereas PAR-2 is primarily activated by FXa¹⁴⁵.

Platelets can be activated by thrombin via PARs¹⁴⁶. Human platelets express both PAR-1 and 4, whereas PAR-4 is the major thrombin receptor in murine platelets¹⁴⁷. The activation of the PAR-4 was reported to promote platelet-leukocyte interaction¹⁴⁸. Our group reported that inhibition of PAR-4 alleviates platelet-endothelial interaction and platelet migration to the liver in IRI¹³⁹. However, whether PAR-4 mediates the early immune response in the acute phase caused by portal hyperperfusion needs to be investigated.

1.8.4 Fibrinogen

Fibrinogen is a soluble GP synthesized in the liver. Under pathological conditions, such as hepatic IRI¹⁴² and vascular disruption¹⁴⁹, the concentration of fibrinogen in blood quickly increases¹⁵⁰. Fibrinogen is thus an acute-phase reactant. Two fibrinopeptides A and B from fibrinogen can be cleaved by thrombin under the coagulation cascade activation, allowing spontaneous formation of cross-linked fibrin. The cross-linked fibrin, together with platelets, are critical components of typical blood clots¹⁵¹. Via binding of the fibrinogen γ -chain and the α IIb β 3

integrin receptor on the platelet surface, the cross-links between platelets and fibrinogen are established. This cross-link facilitates the aggregation of platelets¹⁴⁹.

Fibrin(ogen) and its degradation products play a prominent role in regulating the inflammatory response in the liver¹⁴². Fibrin(ogen) can activate several pro-inflammatory pathways, such as NF- κ B (nuclear factor kappa-light-chain-enhancer of activated B cells) via CD11b/CD18 (also termed as Macrophage-1 antigen or Mac-1) by binding and activating a wide range of immune cells resulting in the expression of Tumor Necrosis Factor- α and IL-1 β ¹⁵². Hence, the early deposition of fibrinogen is a sign of the activation of the coagulation cascade. It can also be a sign of the initiation of the inflammatory response. The activity of fibrinogen in early-stage after major liver resection is by far unclear. As a bridge between SPs and platelet aggregation, the role of fibrinogen ought to be clarified.

1.9 Hypotheses

It was hypothesized in this work, that the sudden increase of shear stress in hepatic sinusoid due to the expanded hepatectomy can induce leukocyte recruitment and eventually perfusion failure in the liver microcirculation. The platelets and SPs prompt the leukocyte recruitment and perfusion failure after expanded hepatectomy. The platelets can be activated via PAR-4 and consequently form microthrombi to compromise the microcirculation and interact with neutrophils to induce ROS damage. Fibrinogen deposition appears immediately after the liver resection in response to the change of shear rate to facilitate the microthrombosis and leukocyte recruitment.

2. Objectives

To investigate the impact of different components in the coagulation system on acute liver injury after liver resection, the current work consists of four major parts (Figure 2):

Study I: to establish a suitable murine model of SFSS and to examine the role of SPs in the acute phase after liver resection. *(This part of the work is partially cited from the doctoral thesis from Patrick Huber in order to demonstrate the whole picture of the current study due to the unpublished state of the respective manuscript)*

Study II: to reveal the role of platelets in leukocyte recruitment and liver injury in the acute phase after liver resection.

Study III: to investigate the effect of PAR-4 on the leukocyte recruitment and neutrophil-platelet interaction in hepatic microcirculation in the acute phase after liver resection.

Study IV: to observe the early fibrinogen deposition in the acute phase after liver resection.

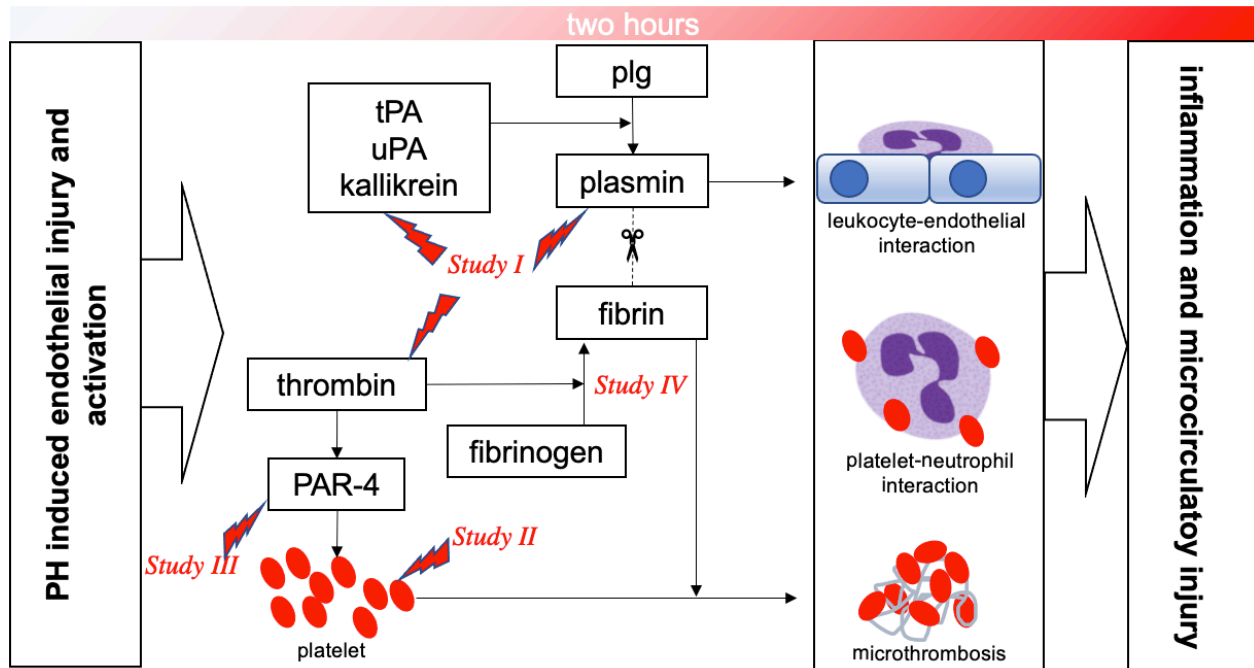


Figure 2: a schematic overview of the current work. Different checkpoints in the coagulation cascade were analyzed using an intravital microscope in the acute phase after liver resection. **Study I:** The effect of SPs on the leukocyte-endothelial interaction and microcirculatory impairment was evaluated. **Study II:** The role of platelets, one of the essential front-line responders of the coagulation cascade, was investigated. **Study III:** The impact of platelet activator PAR-4 on platelet aggregation and platelet-neutrophil interaction was analyzed. **Study IV:** Fibrinogen deposition in hepatic microcirculation as evidence of the activation of coagulation cascade was observed.

3. Materials and Methods

3.1 Ethics

The animal experiments from 2018-2020 were performed at the Walter-Brendel center of experimental medicine of Ludwig-Maximilians University (Munich, Germany) under the approval by the government of Oberbayern (Protocol no. 02-17-132) to ensure animal welfare.

3.2 Animal models

Female C57BL/6 mice were purchased from Charles River (Sulzfeld, Germany) at the age of 10-14 weeks and weighing 20-25g. The mice were housed under standard conditions (temperature: 22 ± 2 °C, humidity: 30 – 60%, light-dark cycle of 12 hours with lights on at 7 A.M.). The mice were caged 3 to 5 with a minimal space of 2-3 cm³/g bodyweight. Soft wooden granules (LIGNOCEL BK 8-15, J. Rettenmaier & Soehne, Rosenberg, Germany) were used as litter. Clean water and foods (Nr. 1324, 10 mm Pellets, Altromin, Lage, Germany) were provided ad libitum.

3.3 Anesthesia

General anesthesia was used for all experiments. The mixture of midazolam (Domitor, Ismaning, Germany) /medetomidine (Ratiopharm, Ulm, Germany) /fentanyl (Dechra, Aulendorf, Germany) with a dosage of 5mg/kg, 0.5mg/kg, and 0.05mg/kg, respectively, was injected intraperitoneally as induction. One-third of dosage/hour was administered i.v. to maintain the anesthetic status. The surgical tolerance of the mice was tested using interdigital reflex.

3.4 General preparation

After anesthesia and proof of negative interdigital reflex, the animals were placed in a supine position on a heating pad. The body temperature was kept at 36-37 °C. Oxygen was supplied with a mask at the concentration of 1L/min.

The surgical area was shaved with a scalpel (Feather disposable scalpel 11#, Electron Microscopy Sciences, PA, USA) after disinfection (Hqut-Desinfiziens, Bode Chemie, Hamburg, Germany). The right jugular vein was dissected. A polyethylene catheter (PE 50, ID 0.28mm; Portex, Hythe, UK) connecting with a needle (30G, Sterican®, B. Braun, Hessen, Germany) and a 1ml syringe (Injekt®-F, B. Braun, Hessen, Germany) was inserted into the jugular vein and fixed by using 7-0 suture (Silk braided suture, Pearsalls Ltd, Taunton, England) serve as venous access. The right carotid artery was then separated from the vagus nerve. A polyethylene catheter (PE 50, ID 0.28mm; Portex, Hythe, UK) connecting with an invasive blood pressure measuring system was then inserted in the carotid artery and fixed using 7-0 suture (Pearsalls Ltd, Taunton, England). The incision for catheterization was then sutured using 5-0 PROLENE suture (Ethicon Somerville, NJ, USA).

The invasive blood pressure measuring system consisted of a transducer (ADInstruments, Sydney, Australia), an amplifier (ADInstruments), Powerlab (ADInstruments), a set of calibration

kit, and connected to a notebook (HP, California, USA) using the proposed program (LabChart, ADInstruments) for continuous recording.

3.5 Surgical preparation for 60% PH

The approximal 60% PH was performed using a modified technique reported by Tomohide Hori *et al.*¹⁵³. After a median laparotomy, liver lobes were mobilized. A small LIGACLIP MCA clip (Ethicon Endo-Surgery, Cincinnati, Ohio, USA) was applied to ligate one branch of the portal vein supplying the right liver lobe. The inferior right lobe was resected by placing a 2-0 polyester suture (Ethicon) in the root. The median lobe was ligated by 2-0 polyester suture (Ethicon) and resected with caution to avoid compromising the left lateral lobe (LLL). The superior right lobe was resected by placing a medium LIGACLIP MCA clip close to the vena cava.

According to the approximate proportion of each liver lobe from mice (Table 3), the median, right upper, and lower lobes were ligated. The proportion of hepatectomy was about 55%.

lobes	percent of total
left lateral lobe	35.6
right lobe	24.6
left median lobe	10.2
right median lobe	22.2
caudate lobe	9.3

Table 3: the proportion of each liver lobes from C57BL/6¹⁵⁴

3.6 Surgical preparation for 90% PH

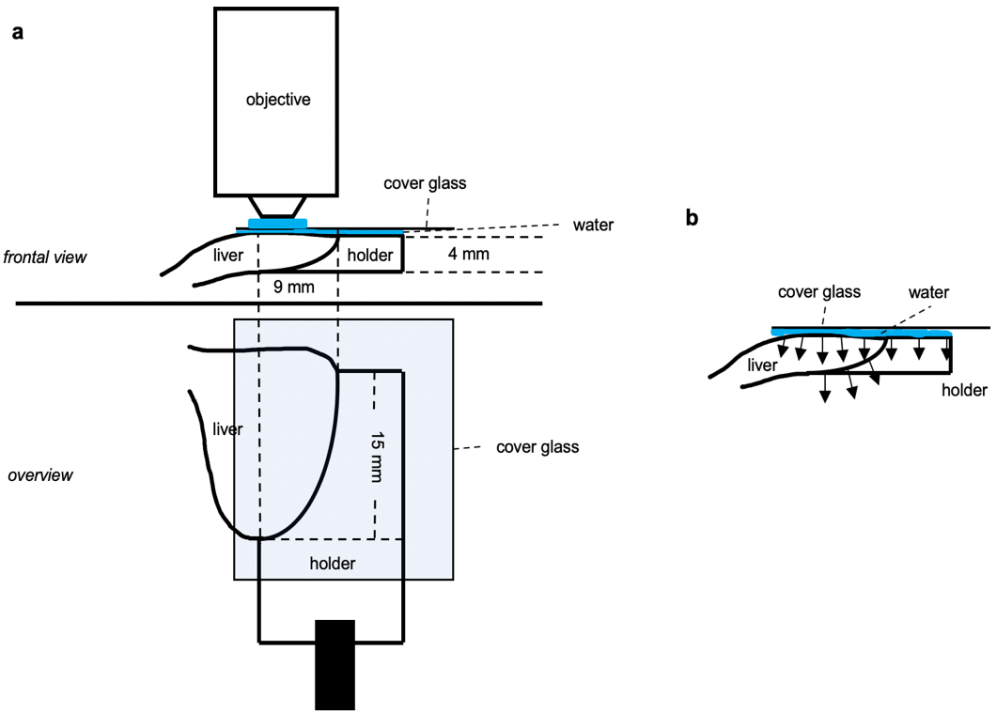
Approximately 90% PH was performed by additionally ligating the lateral lobe with 2-0 polyester suture (Ethicon) based on the 60%-PH model. According to Table 3, the proportion of remnant liver was about 9.3%.

3.7 Surgical preparation for sham-operated animals

Only catheterization and laparotomy were performed in sham-operated animals.

3.8 Basic setting for *in vivo* imaging

A mosquito forceps was used to expose the lateral lobe by extracting xiphoid cranially. The liver of mice was held by a customized retaining device. This device had the following features (Figure 3). First, the shape was designed to suit the dorsal surface of the liver anatomically so that the curved front surface can be presented flatly. Second, a horizontal platform scattered the weight of cover glass from squeezing the liver and kept the cover glass in a horizontal position. These features can disperse the pressure from the cover glass so that the microperfu-



sion was disrupted at a minimal level. A small amount of saline was then injected under the cover glass.

Figure 3: depiction of the customized retaining device. **a:** The cavity sized 15*9*4 mm (length*width*thickness) was designed to compensate for the curved dorsal contour anatomically. This size can be generally applied to the liver lobe from female mice weighing 20-25g. **b:** The arrows represent the force from cover glass, which might be concentrated on the bulge of the liver surface. The shattering of the force from the side platform, together with the flat ventral surface, enabled a shattering of the pressure. The microcirculation could thus be maximally preserved.

3.9 Blood and tissue sampling

At the end of the experiment, the blood was collected from the vena cava. The vena cava was punctured by a 1ml pre-heparinized syringe (Injekt®-F) with a 20G needle (BD Microlance™, Becton Dickinson, NJ, USA). The collected blood was aliquoted to perform a complete blood count with the full blood and a liver enzyme test with the serum.

The complete blood count was performed immediately after the experiment with a hematological analyzer (XN-1000, Sysmex, Norderstedt, Germany). The lateral lobe was excised and put into a 1.5ml tube (Eppendorf, Hamburg, Germany). The rest of the full blood was centrifuged at 3000g for 5min. The serum was extracted. Together with liver tissues, serums were preserved in a -80°C refrigerator for further analysis of liver function.

3.10 Epifluorescence microscopy

Immediately and at two hours after PH, intravital microscopic observations were performed using the technique of epi-illumination. A Leitz Orthoplan Microscope (Leitz, Wetzlar, Germany) was supplied with a Ploemo-Pak light source and a 100 W HBO Mercury lamp (OSRAM GmbH, München, Deutschland). The microscope was also equipped with an I_{2/3} filter block

(excitation: 450-490 nm, emission: >515nm; Leitz), N2 filter block (excitation: 530-560 nm, emission: >580nm, Leitz) and a 25x water immersed objective (W 25x/0,6; Leitz) enabling 500 times magnification. The image of the microscope would be processed by a charge-coupled device (CCD) camera (FK 6990, CoHu, Prospective Measurements, San Diego, USA) and transferred the signal to a digital cassette recorder (Sony, Tokyo, Japan) which presented the image on a computer screen (Flatron, LG, Seoul, South Korea). The video player recorded the live image into a video cassette as documentation. All of the documentation would be digitalized using MAGIX video easy (MAGIX Software GmbH, Berlin, Germany).

To visualize the leukocytes and the leukocyte-endothelial interaction, rhodamine 6G (0.05%, 50µl, Sigma-Aldrich) was systemically applied. Fluorescein isothiocyanate (FITC)-labeled Dextran (100µl, 5%, MW 150.000, Sigma-Aldrich) was administrated i.v. to visualize liver perfusion. FluoSpheres™ Sulfate Microspheres, 2.0 µm, yellow-Green fluorescent (505/515), 2% solids (10µl diluted in 50ul Saline, Invitrogen, Carlsbad, CA, USA) were injected i.v. allowing the determination of centerline blood velocity in postsinusoidal venules.

During intravital imaging, five to seven randomly chosen postsinusoidal venules were observed by 30 seconds each field with diameters ranging from 15 to 30 µm. Ten fields of randomly chosen sinusoids were observed by 5 seconds each field.

3.11 Microcirculatory parameters

The digitalized live images were analyzed off-line using ImageJ. The following parameters were quantified:

- 1) The diameter of postsinusoidal venules;
- 2) The number of rolling leukocytes with the observation time of 30 seconds in postsinusoidal venules;
- 3) The number of firmly adherent leukocytes located within postsinusoidal venules and without moving at least 20 seconds.
- 4) The shear rate of postsinusoidal venules wall, according to the Newtonian definition [$\gamma = 8 * \text{centerline velocity} / 1.6 / \text{diameter}$] where the centerline velocity was measured using MtrackJ plugin
- 5) The perfusion failure rate: percentage of sinusoids with no perfusion.

3.12 Study I: the role of SPs in the acute-phase liver injury after PH

3.12.1 Experimental groups

In the first set of experiments, the leukocyte recruitment and microcirculatory failure induced by PH were studied. In two additional groups, the effect of SP activity in the acute phase of SFSS was investigated by applying systemic SP inhibitors aprotinin.

group number	surgical process	intervention	animals (n)
1	sham operation	vehicle	11
2	60% PH	vehicle	11
3	90% PH	vehicle	11
4	60% PH	aprotinin	11

Table 4: overview of the experimental groups in study I

3.12.2 Protocol of inhibitor treatment

Aprotinin, a broad-spectrum SPs inhibitor (100,000 KIU kg⁻¹ h⁻¹, Sigma-Aldrich, St. Louis, MO, USA) were infused intravenously separately in two groups starting from 5min before hepatectomy. A second dose of inhibitor would be infused one hour after the initial dose to keep the blood concentration. Mice in other groups receiving saline as a vehicle.

3.12.3 Experimental protocol

The experiments were carried out according to the following protocol:

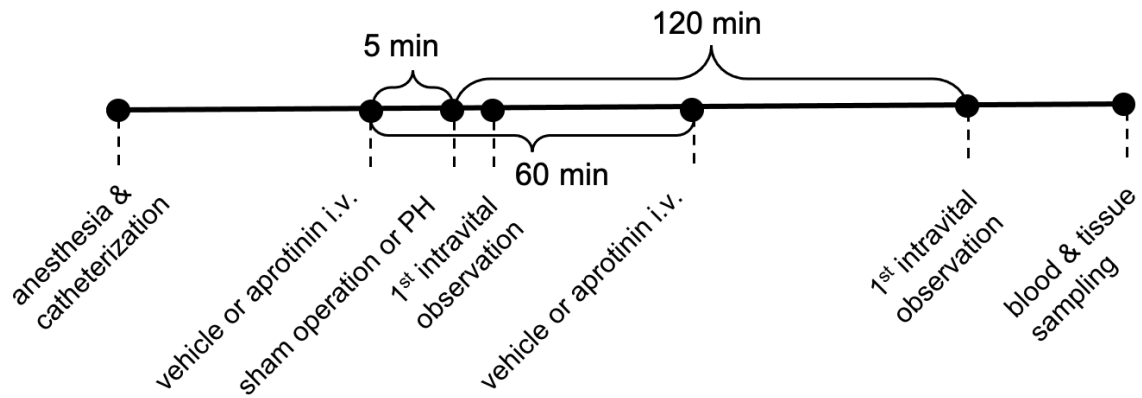


Figure 4: the experimental protocol to analyze the effect of SP activity in the acute phase after PH. After successful anesthesia and catheterization, aprotinin was infused intravenously 5 min before the liver resection. Immediately after the PH, and after 120 min, intravital imaging was performed using an epifluorescence microscope. The second dose of aprotinin would be infused 1 hour after the initial doses. Blood and liver were harvested after the second imaging.

3.13. Study II: the impact of platelets on the acute-phase liver injury after PH

3.13.1 Experimental design and groups

In this set of experiments, two groups were performed to address the effect of platelets in the acute phase of SFSS.

group number	surgical process	intervention	animals (n)
1	60% PH	vehicle	6
2	60% PH	platelet depletion	6

Table 5: overview of the experimental groups in study II

3.13.2 Protocol of platelet depletion

The depletion of platelets was carried out 24 hours and six hours before PH by using an anti-GPIb α (CD42b) mAb, clone Xia.B2; 50 μ g, i.v. (Emfret Analytics, Eibelstadt, Germany) via the tail vein. The sham-operated animals received saline as vehicle 24 hours and six hours before PH via the tail vein. The platelet count was validated by the aforementioned hematological analyzer.

3.13.3 Experimental protocol

The experiments were carried out according to the following protocol.

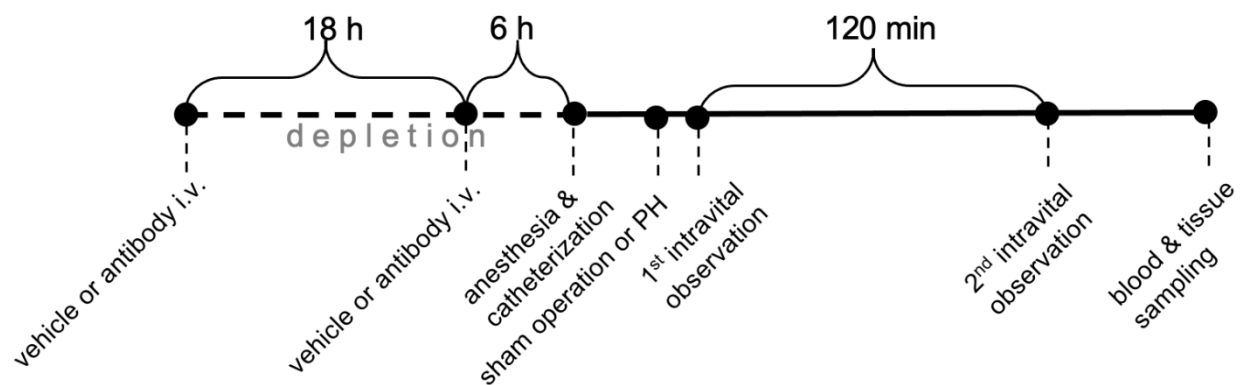


Figure 5: the experimental protocol to analyze the role of platelets in the acute phase after PH. The depletion of platelets started 24 hours and six hours before the surgery. After successful anesthesia and catheterization, intravital observation with two time points was performed as described in Study I.

3.14. Study III: the impact of PAR-4 on platelet aggregation and neutrophil-platelet interaction in the acute-phase injury after PH

3.14.1 Experimental design and groups

In this set of experiments, the leukocyte-endothelial interaction and microcirculatory injury were analyzed by using an epifluorescence microscope. The neutrophil-platelet interaction in the acute phase after PH was investigated by using a two-photon microscope (2PM).

group number	surgical process	intervention	animals (n)
1	60% PH	vehicle	6
2	60% PH	tcY-NH ₂	6

Table 6: overview of the experimental groups analyzed by epifluorescence microscope in study III

group number	surgical process	intervention	animals (n)
1	sham operation	vehicle	6
2	60% PH	vehicle	6
3	60% PH	tcY-NH ₂	6

Table 7: overview of the experimental groups analyzed by 2PM in study III

3.14.2 Experimental protocol

The experiments were carried out according to the following protocols.

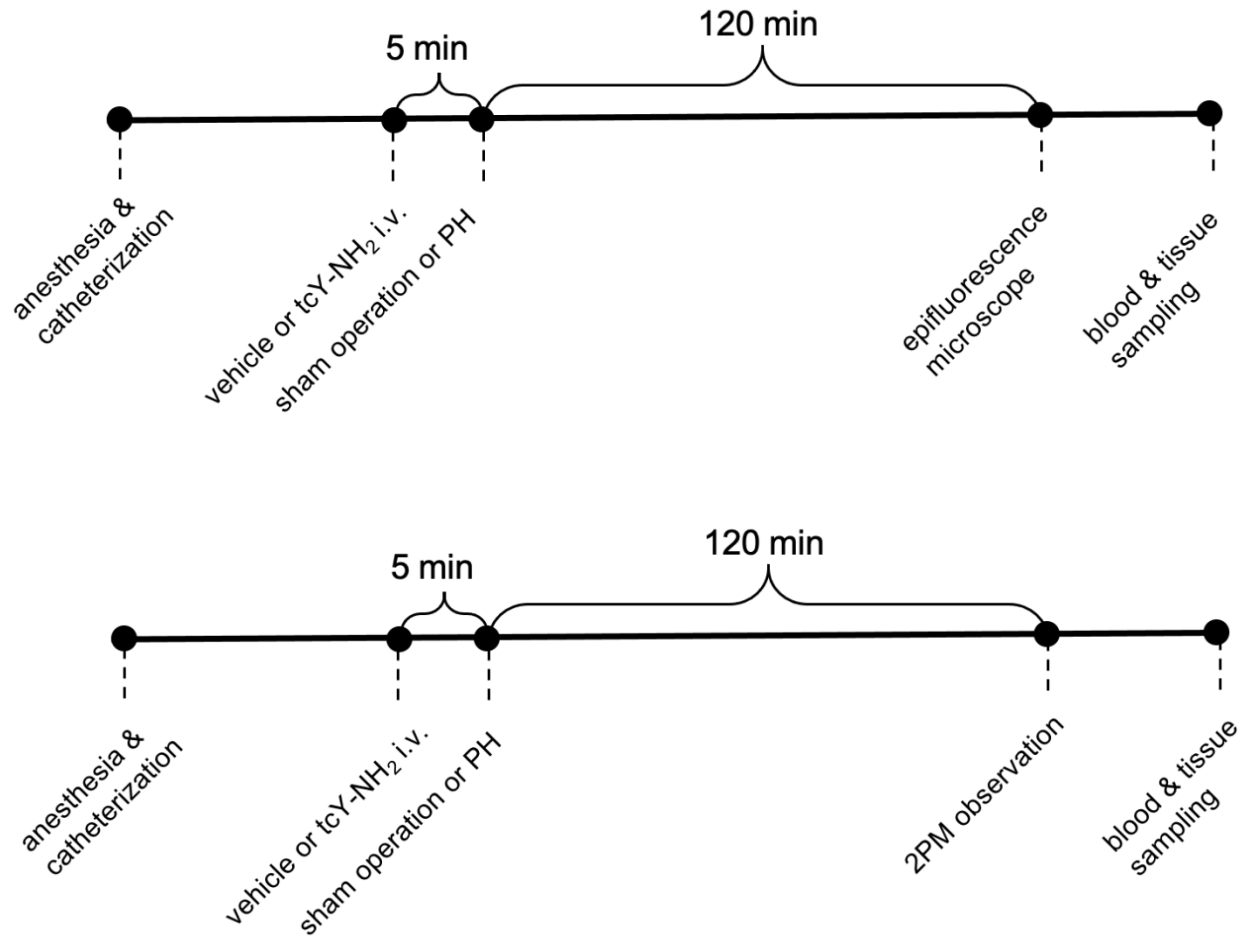


Figure 6: experimental protocols to analyze the role of PAR-4 in the acute phase after PH. After successful anesthesia and catheterization. The tcY-NH₂, the PAR-4 inhibitor, was infused 5 min before PH. The leukocyte-endothelial interaction and microcirculatory injury were investigated by using an epifluorescence microscope. The neutrophil-platelet interaction in acute phase after PH was analyzed by using 2PM

3.14.3 Two-photon microscope

An upright microscope with a water immersion objective (20 x 0.95 NA; Olympus, Tokyo, Japan) connecting to a TriM Scope I 2PM (LaVision Biotech, Gottingen, Germany) was used to perform *in vivo* imaging. The laser was generated (Mai Tai, Spectra-Physics, CA, USA) with a wavelength of 810 nm. Four photomultiplier tubes detected the emission from the tissue

through filters LP494, BP525/50, LP 560, and LP665. The software ImSpector (LaVision Biotech, Bielefeld, Germany) was used for image processing. In this set of experiments, the sinusoids were colorized using FITC (Sigma-Aldrich), neutrophils were stained using PE anti-mouse Ly-6G (Biolegend, CA, USA), and platelets were stained using X649 (Emfret).

Six random selected fields sized 450*450 μ m were taken using the resolution of 1024x1024. For each selected field, 20 consecutive images were taken with an interval of 1.4s / frame. The focus was chosen on the liver surface (depth < 30 μ m) to achieve the best image quality.

ImageJ¹⁵⁵ was then used to merge the three channels of images. The sinusoids, neutrophils, and platelets were colorized in green, red, and blue, respectively. The 3-channel-overlapped signals (purple) were autofluorescence of Kupffer cells. The following parameters were then quantified:

- 1) Neutrophils: number of Ly-6G-positive cells in one high-power field.
- 2) Microthrombi: number of GPIb-V-IX-positive clots that were stable in sinusoids throughout ten frames (1.4s each frame) in one high-power field.
- 3) Neutrophils interacting with platelets: Ly-6G-positive cells that were colocalized with GPIb-V-IX throughout ten frames (1.4s each frame) in one high-power field.

3.15 Study IV: fibrinogen deposition in the acute phase after PH

3.15.1 Experimental groups

In this set of experiments, two groups were performed to exam the activation of the coagulation system in the acute phase after 60% PH.

group number	surgical process	intervention	animals (n)
1	sham operation	fibrinogen	3
2	60% PH	fibrinogen	3

Table 8: overview of the experimental groups in study IV

3.15.2 Experimental protocol

The experiments were carried out according to the following protocol.

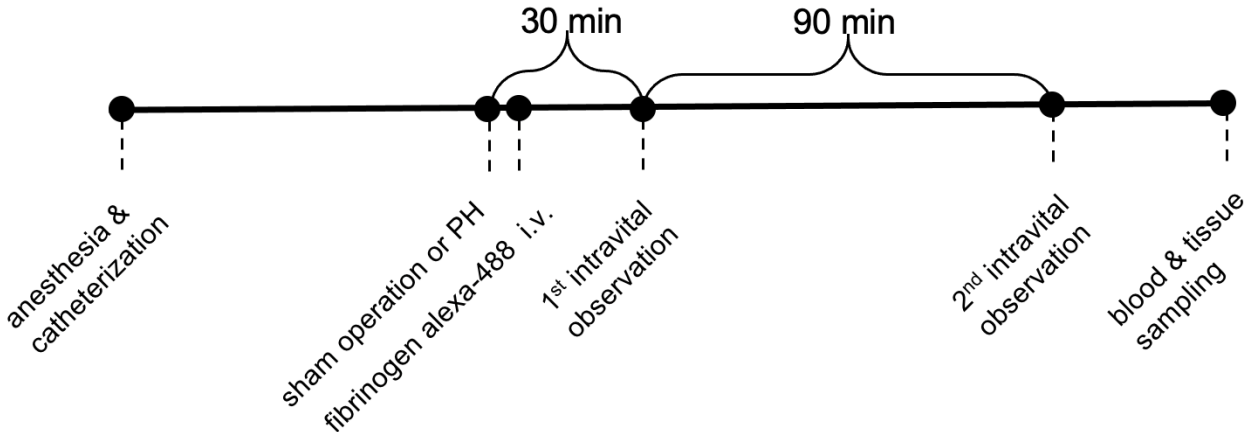
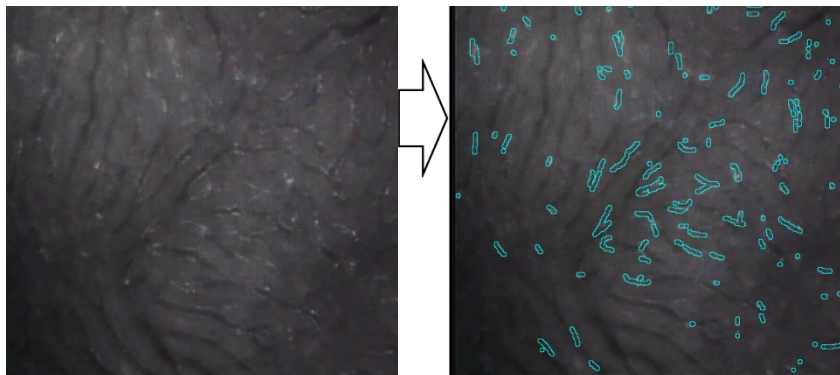


Figure 7: the experimental protocol used to observe the fibrinogen deposition in the acute phase after PH. After successful anesthesia and catheterization, PH was performed. Fibrinogen conjugated with Alexa-488 was infused immediately after PH. With an epifluorescence microscope, the *in vivo* imaging was performed 30 min and 120 min after PH.

3.15.3 Assessment of fibrinogen deposition in the acute phase after extended liver resection *in vivo*

To indirectly detect the activity of the coagulation system after PH, the deposition of fibrinogen in sinusoids was investigated *in vivo* by fluorescence microscopy¹⁴². Alexa 488-conjugated human fibrinogen (1.7 mg/kg; Molecular Probes, Eugene, OR) was applied intravenously immediately after hepatectomy. To evaluate the fluorescent signal from deposited fibrinogen, ten sinusoids were randomly taken both 30min and 120min after hepatectomy or sham operation. After digitalization, one frame with the best focus from each sinusoid was used for analysis. The fluorescent signals from fibrinogen in hepatic sinusoids were manually marked in a blind



manner using the selection function of ImageJ with a 5-pixel-sized marker¹⁵⁵.

Figure 8: quantification of fibrinogen deposition. Video frame was scaled with actual size. The visible deposition of alexa 488-conjugated fibrinogen was marked using a 5-pixel-sized marker. The final area was calculated by ImageJ (red frame) with the unit of μm^2 .

3.16 Histology

3.16.1 Paraffinization of the tissue

All tissues were thawed in 4°C 4% formaldehyde solution neutral buffer for 12 hours and were placed at room temperature for the next 12-24 hours. Fixed tissues were then transferred into a histological processing machine (Shandon, Thermo fisher scientific, Massachusetts, USA).

The machine automatically run the following protocols for animal tissues thinner than 4mm:

- | | |
|---|------------|
| 1) ethanol 70% (SAV Liquid Production,
Flintsbach am Inn, Germany) | 10 minutes |
| 2) ethanol 70% | 10 minutes |
| 3) ethanol 96% (SAV Liquid Production) | 10 minutes |
| 4) ethanol 96% | 10 minutes |
| 5) ethanol 96% | 10 minutes |
| 6) ethanol 99% (SAV Liquid Production) | 30 minutes |
| 7) ethanol 99% | 30 minutes |
| 8) ethanol 99% | 30 minutes |
| 9) xylene (Fisher Scientific, NH, USA) | 45 minutes |

10) xylene	45 minutes
11) paraffin (Sigma-Aldrich)	60 minutes
12) paraffin	60 minutes

The liver tissues from paraffin were then transferred to an embedding machine (Tissue-Tek, Sakura, CA, USA).

3.16.2 Immunohistochemistry (IHC)

The sections for IHC went through the following rehydrating protocol:

1) xylene:	five minutes (two times)
2) ethanol 99%:	five minutes
3) ethanol 96%:	five minutes
4) ethanol 70%:	five minutes
5) dH ₂ O rinse:	five minutes (two times)

Antigen retrieval was performed with a 20 min 95°C water bath with citrate buffer (Sigma-Aldrich), pH 6.0. The sections were left in the water bath for 30 min to cool down. The following protocol was used for the staining:

1) washing	five minutes (three times)
2) primary antibody	one hour
3) washing	five minutes (three times)
4) LINK	20 minutes

5) LABEL	20 minutes
6) 3,3'- diaminobenzidine	depended on the primary antibody
7) hematoxylin 1/10 conc.	20 seconds
8) tap water	one minute
9) 30%-HCL 70% ethanol	quick wash
10) tap water	one minute
11) ethanol 70%:	quick rinse
12) ethanol 96%	quick rinse
13) ethanol 99%	quick rinse
14) xylene:	five minutes
15) xylene:	five minutes
16) mounting	

3.16.3 Antibodies and reagents

CD45 antibody (1:200, Cell Signaling Technology, #70257), ICAM-1 antibody (1:2000, Abcam, 179707), Lymphocyte antigen 6 complex locus G6D (Ly-6G) antibody (1:1000, Biolegend, 127602), myeloperoxidase (MPO) antibody (1:200, Invitrogen, PA5-16672), CD3 antibody (1:150 Abcam 16669) and Ki-67 antibody (1:200, Cell Signaling Technology, D3B5) were used as primary antibodies. Secondary detection was performed by Super Sensitive detecting system (BioGenex, CA, USA). Counterstaining of the sections was performed using Mayer's hematoxylin (Merck, Darmstadt, Germany).

CD45, Ly-6G, MPO, CD3, and Ki-67 positive cells in sinusoids were counted in 10 high-power fields (at microscope magnification x400, Leica).

All cell counts were performed in a blinded manner. Analysis of ICAM-1 expression was performed semiquantitatively in a blinded fashion with a grading system of 0–3: 0, no staining; 1, weak staining; 2, mild staining; 3, strong staining.

3.17 Biochemical analysis of the liver function

Total bilirubin, serum aspartate aminotransferase (AST), alanine aminotransferase (ALT), and glutamate dehydrogenase (GLDH) activities were measured with an automated analyzer (AU 5800; Beckman Coulter, Brea, CA, USA) using standardized test systems (HiCo GOT and HiCo GPT; Roche Applied Sciences, Indianapolis, IN, USA).

3.18 Statistics

Data analysis was performed using a statistical software package (SigmaPlot 13.0, Systat Software, Erkrath, Germany). Analysis of variance on ranks followed by Student-Newman-Keuls methods was used to estimate stochastic probability in intergroup comparison. To issue the significance of differences between the two groups, the Kolmogorov–Smirnov test was performed to verify normality. If verified, the two-tailed independent t-test was performed to determine significance. If violated, the Mann–Whitney U test for independent samples was performed. The data was presented in mean values \pm standard error of the mean (SEM).

4. Results

4.1 Study I: the role of SPs in the acute-phase liver injury after PH

In Study I, the data are partially cited from the doctoral thesis from Patrick Huber in order to represent the whole structure of current research. These data are unpublished.

4.1.1 Macrohemodynamic parameters

No significant difference was found in the mean arterial pressures (MAPs) in the sham-operated mice (74.6 ± 1.7 mmHg) and the mice undergoing 60% PH (70.8 ± 0.8 mmHg). Due to the massive resection of the liver in the 90%-PH group (63.0 ± 1.8 mmHg), the MAP of this group was lower than that in the sham-operated mice. In all groups, the MAPs remained constant during the two-hour course.

4.1.2 Microcirculatory parameters

4.1.2.1 *Rolling leukocytes*

A significant increase in the average number of rolling leukocytes was found in postsinusoidal venules after 60% PH (baseline 9.1 ± 0.9 /30s and two hours 14.9 ± 1.2 /30s) and after 90% PH (baseline 11.3 ± 1.1 /30s and two hours 12.6 ± 1.2 /30s) compared to the number in sham-operated animals (baseline 3.7 ± 0.5 /30s and two hours 4.9 ± 0.4 /30s). Surprisingly, significantly fewer rolling leukocytes were found in postsinusoidal venules two hours after 90% PH than the number in animals undergoing 60% PH. A significant decrement in the number of rolling leukocytes was found in postsinusoidal venules after treating with aprotinin (baseline 6.7 ± 0.3 /30s and two hours 9.7 ± 1.0 /30s) compared to the number from saline-treated animals undergoing 60% PH (Figure 9a).

4.1.2.2 *Firmly adherent leukocytes*

The firmly adherent leukocytes were detected with an average count of 25.1 ± 6.4 /mm² in the sham-operated group in the baseline measurement. This number drastically increased to 120.4 ± 13.4 /mm² in mice receiving 60% PH immediately after PH. In the measurement after two hours, the number in the 60%-PH group treated with vehicle showed a dramatic three-fold increment to 535.6 ± 28.7 /mm² compared to the average from sham-operated animals (171.7 ± 30.6 /mm²). Interestingly, the average number of firmly adherent leukocytes after 90% PH (baseline 83.3 ± 33.6 /mm² and two hours 231.4 ± 30.1 /mm²) were found significantly greater than that in the 60%-PH group. In the baseline measurement, the number of firmly adherent

leukocytes significantly dropped in the aprotinin-treated mice undergoing 60% PH (22.2 ± 5.4 /mm²) compared to the number in the vehicle-treated animals undergoing 60% PH. After two hours, the increment of firmly adherent leukocytes caused by 60% PH was significantly repressed in the presence of aprotinin (199.4 ± 22.2 /mm², Figure 9b).

4.1.2.3 Perfusion failure rate

A significant perfusion injury was found in the 60%-PH group treated with vehicle in the baseline ($15.9 \pm 1.3\%$) and two-hour measurements ($21.8 \pm 1.0\%$) compared to the perfusion failure in sham-operated mice ($6.9 \pm 0.5\%$ and $12.5 \pm 1.2\%$, respectively). The animals undergoing 90% PH showed a further deteriorated perfusion injury (baseline $30.4 \pm 3.0\%$ and two hours $34.5 \pm 4.6\%$, respectively) compared to that of less invasively operated groups. The post-hepatectomy microcirculatory injury of the liver was alleviated after treating with aprotinin. No significant difference of perfusion failure was found from the animals treated with aprotinin in baseline ($8.5 \pm 0.4\%$ and $7.7 \pm 0.7\%$, respectively) and two-hour measurement ($15.6 \pm 0.9\%$ and $14.2 \pm 0.9\%$, respectively) after PH compared to that of sham-operated animals (Figure 9c).

4.1.2.4 Shear rate

The perfusion injuries appeared in line with a significant elevation of shear rate in postsinusoidal venules. The shear rate in postsinusoidal venules in sham-operated mice averaged 164.2 ± 12.7 /s in baseline and 143.3 ± 10.6 /s after two hours. The shear rate significantly elevated after 60% PH both in baseline and two-hour measurement (229.0 ± 15.8 /s and 209.5 ± 13.8 /s, respectively). The animals undergoing 90% PH showed a further significant increment ($321.1 \pm$

18.5 /s and 269.4 ± 9.1 /s, respectively). With the broad-spectrum inhibition of SPs, the shear rate in postsinusoidal venules was found significantly decreased (baseline 198.7 ± 13.2 /s and two hours 164.0 ± 12.9 /s) compared to that detected in the 60%-PH group (Figure 9d).

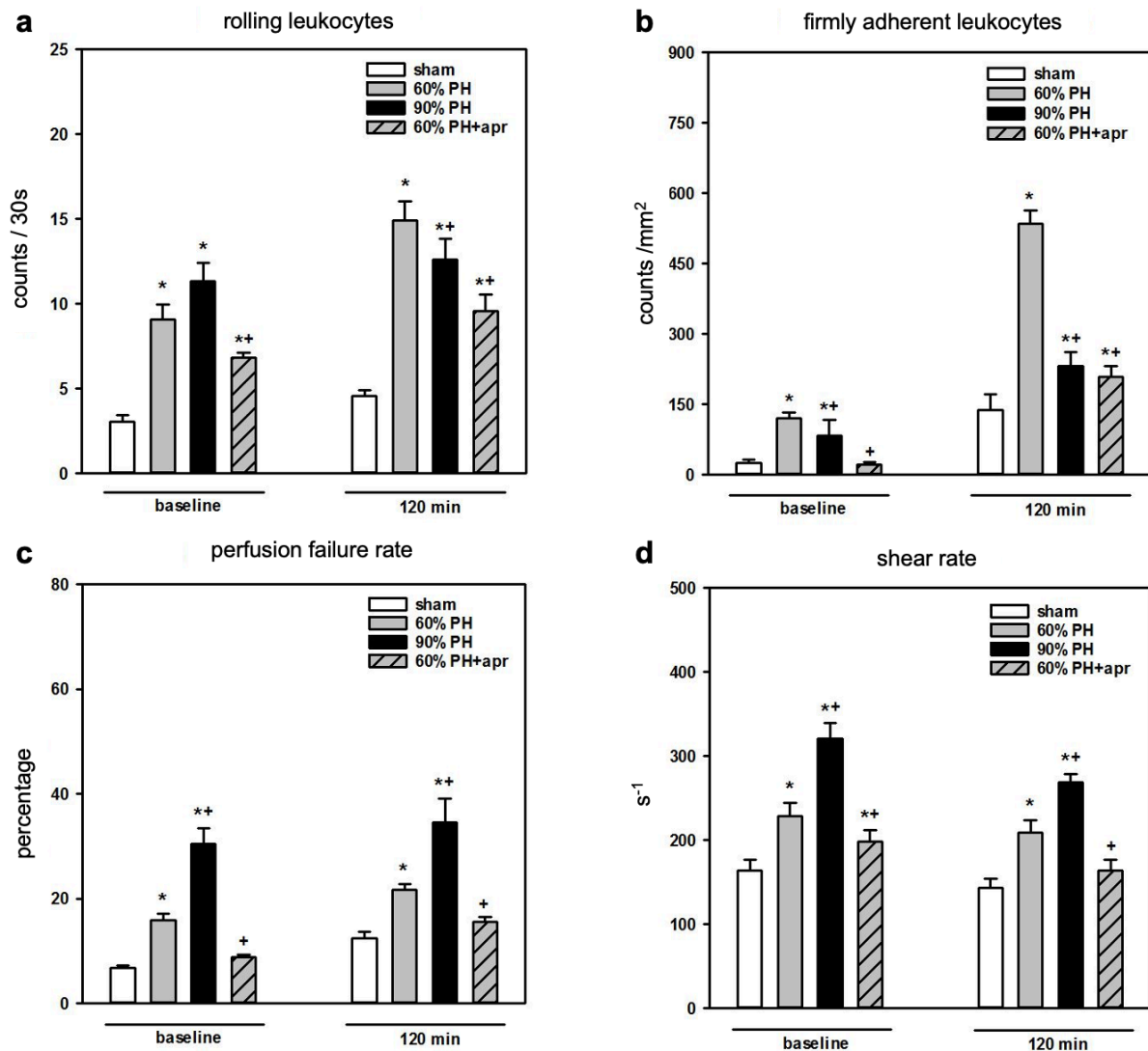


Figure 9: quantification of leukocyte recruitment and *in vivo* analysis of microvascular injury in sinusoids and shear rate in post-sinusoidal after PH. a and b: the numbers of rolling and firmly adherent leukocytes increased immediately after 60% and 90% PH. The application of aprotinin ameliorates this increment after 60%

PH. **c**: a significant perfusion failure was found in line with the extent of PHs. The microcirculation was improved after the application of aprotinin. **d**: the shear rate increased in line with the extent of PH. The shear rate significantly decreased with the treatment with aprotinin compared to that in vehicle-treated mice undergoing 60% PH n=11 animals per group, mean \pm SEM. *, $P < 0.05$, versus sham-operated group; +, $P < 0.05$, versus 60%-PH group.

4.1.3 Bilirubin, AST and ALT

The total bilirubin level in serum elevated significantly in line to the extent of PH (sham 0.72 ± 0.19 mg/dL; 60% PH 1.23 ± 0.19 mg/dL; 90% PH 1.90 ± 0.14 mg/dL) two hours after liver resection. The systemic application of aprotinin results in a significant improvement in the level of total bilirubin (aprotinin 0.88 ± 0.15 mg/dL). The level of liver enzyme in serum was determined as markers of hepatocellular injury. A significant increase in the level of hepatic transaminases (AST 1453 ± 133 ; ALT 974 ± 75 U/L) was found in the 60%-PH group treated with saline compared to that in the sham group (AST 339 ± 95 ; ALT 195 ± 59 U/L). The level of hepatic transaminases significantly decreased with aprotinin (AST 995 ± 137 ; ALT 704 ± 111 U/L). Surprisingly, in the 90%-PH group, the transaminase levels were significantly lower compared to the level from the animals receiving 60% PH.

groups	60% PH + saline	60% PH + CD42b
MAP (mmHg)	72.0 ± 1.7	67.8 ± 2.3

4.2 Study II: the role of platelets on the acute-phase liver injury after PH

4.2.1 Macrohemodynamic parameter

No significant difference was found in MAPs with platelet depletion and the group treated with saline.

Table 9: the MAP of each group, n=6, mean \pm SEM

4.2.2 Platelet counts

The average platelet count in mice with depletion protocols was approximately 4.8% from the mice receiving saline, which showed a successful depletion of platelets with anti-CD42b monoclonal antibody. The average count was 33.2 ± 11.1 $10^3/\mu\text{L}$ in mice with platelet depletion and 685.2 ± 24.9 $10^3/\mu\text{L}$ in vehicle-treated mice (Figure 10).

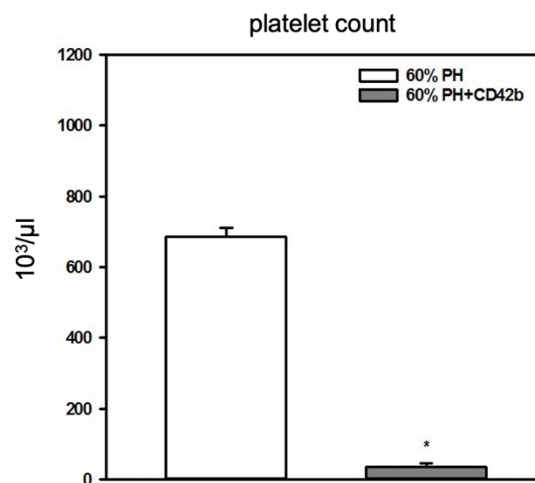


Figure 10: systemic platelet count. n=6 animals per group, mean \pm SEM. *, P < 0.001, versus vehicle-treated group.

4.2.3 Microcirculatory parameters

4.2.3.1 Venule diameters

The postsinusoidal venules analyzed from the animal undergoing 60% PH treated with saline had an average diameter of $19.6 \pm 0.8 \mu\text{m}$. The animal undergoing 60% PH after platelet depletion had an average diameter of $18.2 \pm 0.3 \mu\text{m}$. No significant difference was found between the two groups (Figure 11).

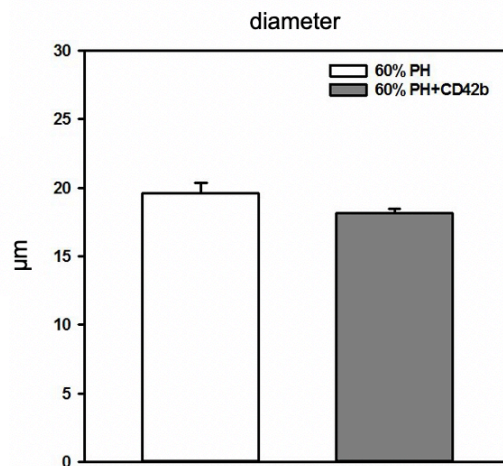


Figure 11: vessel diameter. No significant difference was found between the two groups. n=6 animals per group, mean ± SEM.

4.2.3.2 Rolling Leukocytes

The numbers of rolling leukocytes averaged $5.7 \pm 0.6 /30\text{s}$ and $9.6 \pm 0.7 /30\text{s}$ in baseline and two-hour measurements in mice receiving saline, respectively. The average numbers of rolling leukocytes were found significantly decreased after platelet depletion both in baseline ($3.5 \pm$

0.5 /30s) and two-hour measurements (6.5 ± 0.9 /30s) after PH compared to vehicle treated animals in postsinusoidal venules (Figure 12a).

4.2.3.3. *Firmly adherent leukocytes*

In the baseline measurement, the number of firmly adherent leukocytes was $83.8 \pm 18.1/\text{mm}^2$ in the vehicle-treated group and $46.3 \pm 36.2 /\text{mm}^2$ in the platelet-depleted group whereas no significant difference was found between two groups. After two hours, the number of firmly adherent leukocytes in vehicle-treated animals increased to $375.3 \pm 32.5 /\text{mm}^2$. A significant decrease was found after platelet depletion with an average of $208.2 \pm 29.3 /\text{mm}^2$ compared to the number in vehicle-treated animals. (Figure 12b)

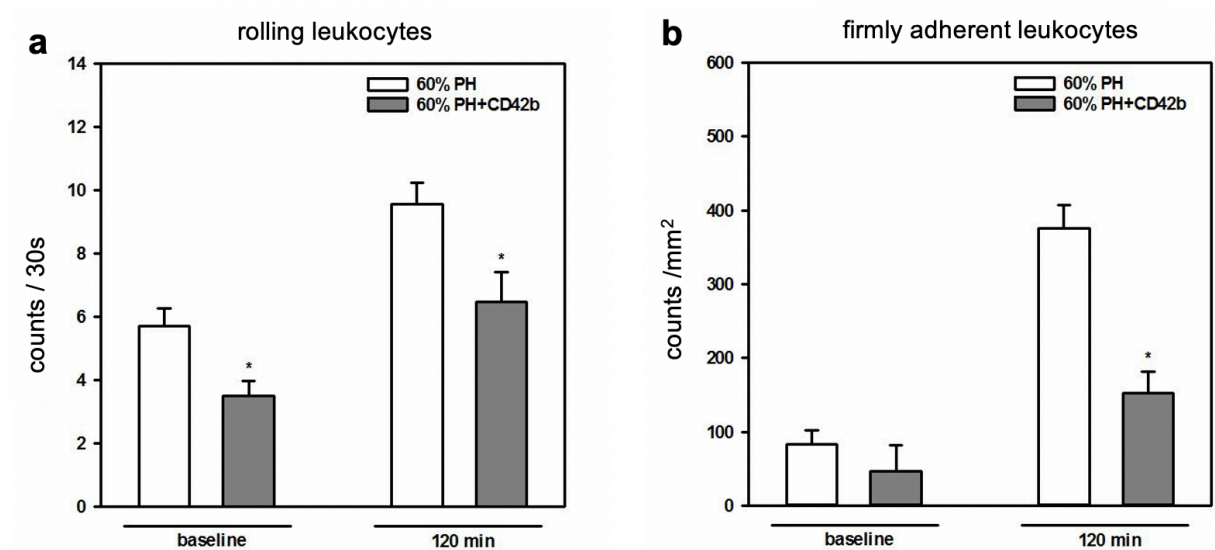


Figure 12: *quantification of leukocyte rolling and leukocyte firm adherence.* a: The number of rolling leukocytes was found significantly lower than that in the platelet-depleted animals both immediately and two hours after PH. b: A significant decrease was found in the number of firmly adherent leukocytes two hours after 60% PH. n=6 animals per group, mean \pm SEM. *, P < 0.05, versus vehicle-treated group.

4.2.3.4 Perfusion failure rate and shear rate

Extended Hepatectomy induced deterioration of sinusoidal in the group with normal platelet count (baseline $12.2 \pm 0.6\%$ and two hours $16.9 \pm 0.9\%$). After platelet depletion, however, significant improvement of sinusoidal perfusion was found immediately and two hours after 60% PH with platelet depletion (baseline $7.7 \pm 0.4\%$ and two hours $14.2 \pm 0.9\%$, Figure 13a).

Although the shear rate in depletion group was lower (baseline $209.4 \pm 8.1s^{-1}$ and two hours $213.1 \pm 7.1s^{-1}$), the difference was found insignificant compared to that in mice receiving vehicle (baseline $261.6 \pm 31.8s^{-1}$ and two hours $238.2 \pm 13.4s^{-1}$, Figure 13b).

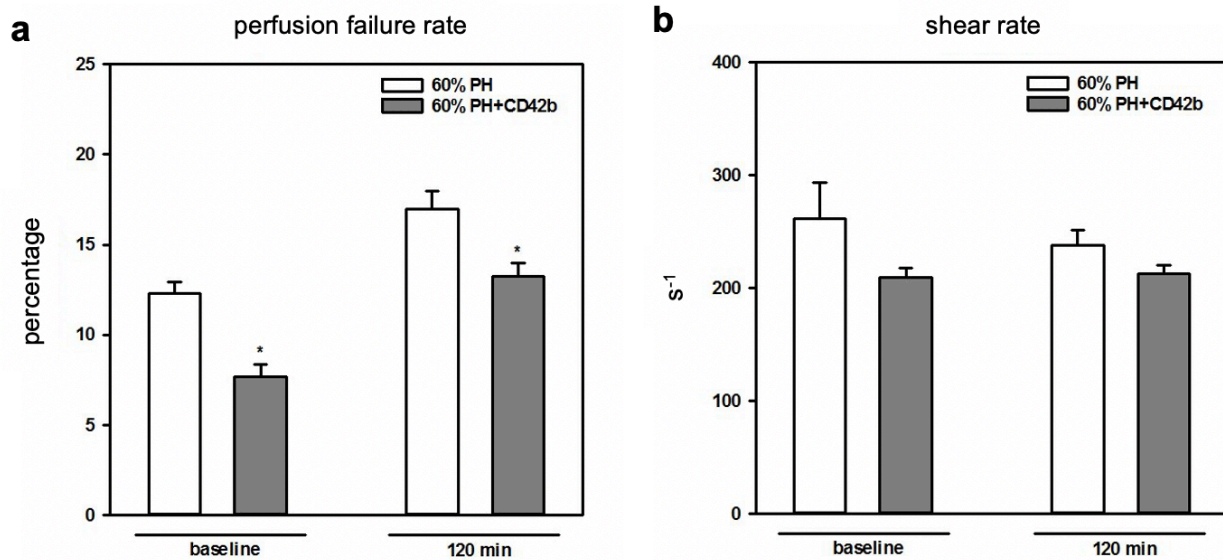


Figure 13: *in vivo* analysis of the microvascular injury and post-sinusoidal shear rate after 60% PH. a: Significant improvement in perfusion was found in platelet-depleted animals both immediately and two hours after PH. b: No significant difference in shear rate was found in postsinusoidal venules. n=6 animals per group, mean \pm SEM. *, P < 0.05, versus vehicle-treated group.

4.2.4 IHC analysis

4.2.4.1 Leukocyte subpopulations

The numbers of leukocytes (marked with CD45), neutrophils (marked with MPO), and T-cells (marked with CD3) were found significantly reduced in hepatic sinusoids in the platelet-depleted group two hours after 60%PH (Figure 14).

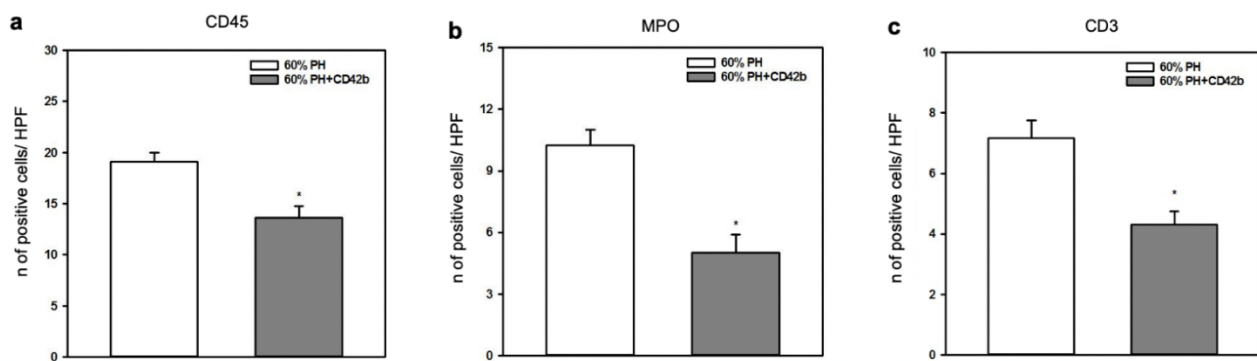
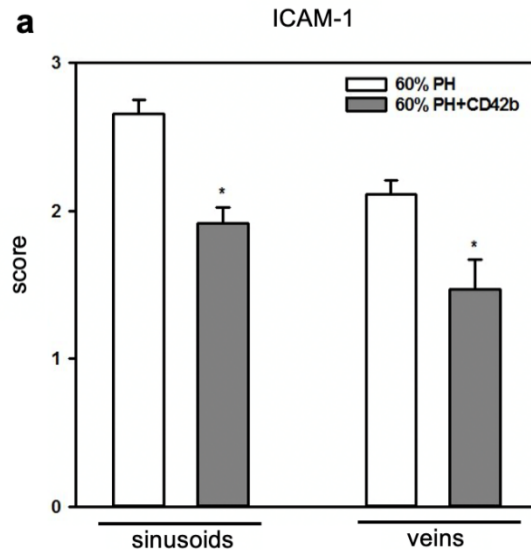


Figure 14: quantification of leukocyte subpopulations using IHC analysis. The number of all three types of cell were significantly decreased after the platelet depletion in the context of 60% PH. n=6 animals per group, mean \pm SEM. *, P < 0.05, versus 60%-PH group.

4.2.4.2 Expression of ICAM-1

After platelet depletion, significantly attenuated expression of ICAM-1 was found in sinusoids as well as hepatic veins compared to that the saline-treated group undergoing 60% PH (Figure



15).

Figure 15: IHC analysis of ICAM-1 expression. n=6 animals per group, mean \pm SEM. *, P < 0.05, versus 60%-PH group.

4.2.5 Bilirubin, AST, ALT and GLDH

The cholestasis reflected by bilirubin level in the acute phase after 60% PH was found improved after platelet depletion, although the difference was not significant (vehicle-treated group 1.0 ± 0.2 mg/dl; platelet-depleted group 0.5 ± 0.2 mg/dl). The necrotic injury reflected by AST, ALT, and GLDH was found significantly ameliorated after platelet depletion (716.0 ± 70.1 U/L, 489.3 ± 50.0 U/L, and 114.8 ± 26.6 U/L) compared to that in vehicle-treated mice (1100.6 ± 114.1 U/L, 723.3 ± 49.6 U/L, and 264.1 ± 46.2 U/L, respectively, Figure 16).

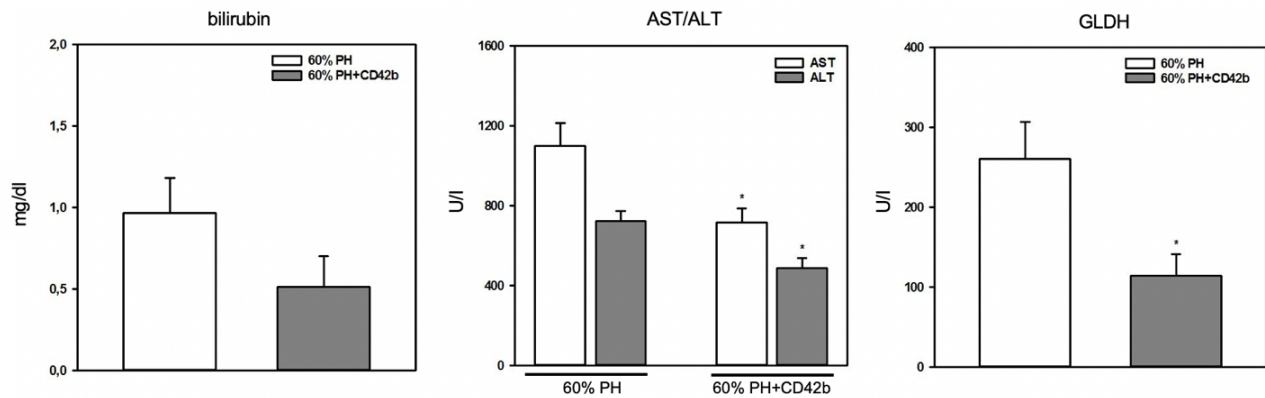


Figure 16: liver injury reflected by bilirubin and enzymes in animals undergoing 60% PH with vehicle and or platelet depletion. n=6 animals per group, mean \pm SEM. *, P < 0.05, versus 60%-PH group treated with vehicle.

4.3 Study III: the impact of PAR-4 on platelet aggregation and neutrophil-platelet interaction in the acute-phase liver injury after 60% PH

4.3.1 Macrohemodynamic parameter

No significant difference was found in the MAPs between the group with PAR-4 inhibition and the group treated with saline.

Table 10: the MAP of each group, n=6, mean \pm SEM

4.3.2 Microcirculatory parameters

groups	60% PH + saline	60% PH + tcY-NH ₂
MAP (mmHg)	75.1 \pm 3.3	75.7 \pm 2.3

4.3.2.1 Venule diameters

The analyzed postsinusoidal venules from the animal receiving 60% PH treated with saline had an average of $19.7 \pm 0.4 \mu\text{m}$. The mean diameter from the animal receiving 60% PH treated with tcY-NH₂ was $20.3 \pm 0.8 \mu\text{m}$. No significant difference was found between these two groups.

4.3.2.2 Rolling leukocytes

Two hours after the 60% PH, the number of rolling leukocytes in the postsinusoidal venules had an average of $10.3 \pm 1.2 /30\text{s}$ in the saline-treated animals and $9.9 \pm 1.3 /30\text{s}$ in the tcY-NH₂-treated animals. No significant difference was found between these two groups (Figure 17a).

4.3.2.3 Firmly adherent leukocytes

A significant decrease was found in the number of firmly adherent leukocytes in the animals treated with tcY-NH₂ ($134.7 \pm 11.3 / \text{mm}^2$) compared to the number from saline-treated animals ($215.4 \pm 14.2 / \text{mm}^2$) two hours after 60% PH (Figure 17b)

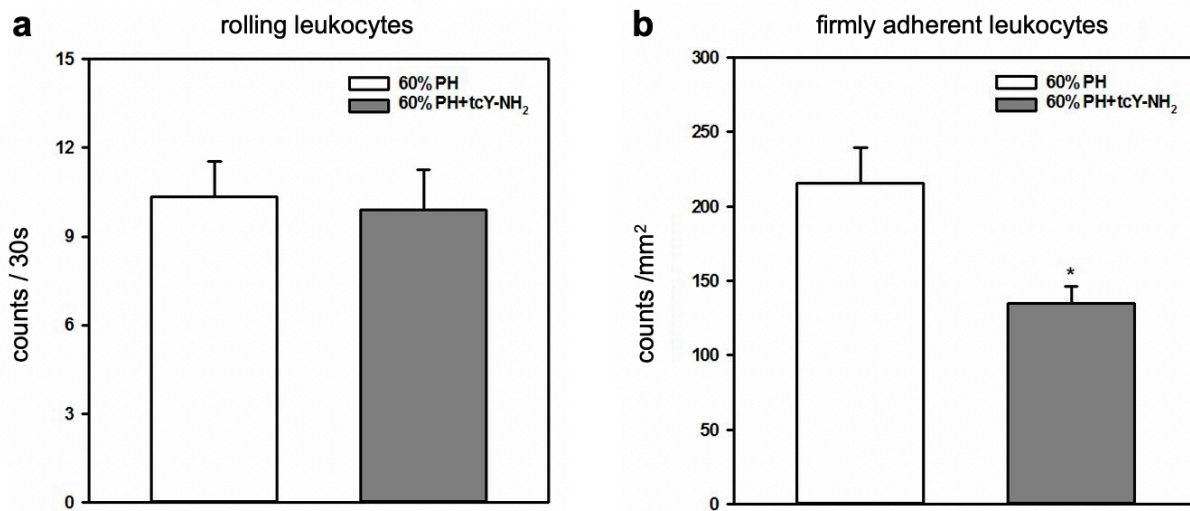


Figure 17: quantification of leukocyte rolling and leukocyte firm adherence. **a:** No significant difference was found in the number of rolling leukocytes in postsinusoidal venules two hours after PH. **b:** A significant decrease was found two hours after 60% PH in the number of firmly adherent leukocytes in postsinusoidal venules two hours after PH in the presence of tcY-NH₂. n=6 animals per group, mean \pm SEM. *, P < 0.05, versus vehicle-treated group.

4.3.2.4 Perfusion failure rate and shear rate

Two hours after 60% PH, the average perfusion failure rate in saline-treated animals was $13.9 \pm 1.2\%$; the average in animals treated with tcY-NH₂ was $10.9 \pm 1.1\%$. No significant difference was found between these two groups (Figure 18a).

The shear rate was slightly diminished in animals undergoing after treatment tcY-NH₂ compared to animals receiving vehicle treatment. However, no significant differences were detected after two hours between the two groups (saline-treated animals: $215.4 \pm 10.2 \text{ s}^{-1}$; tcY-NH₂-treated animals $185.4 \pm 10.1 \text{ s}^{-1}$, Figure 18b)

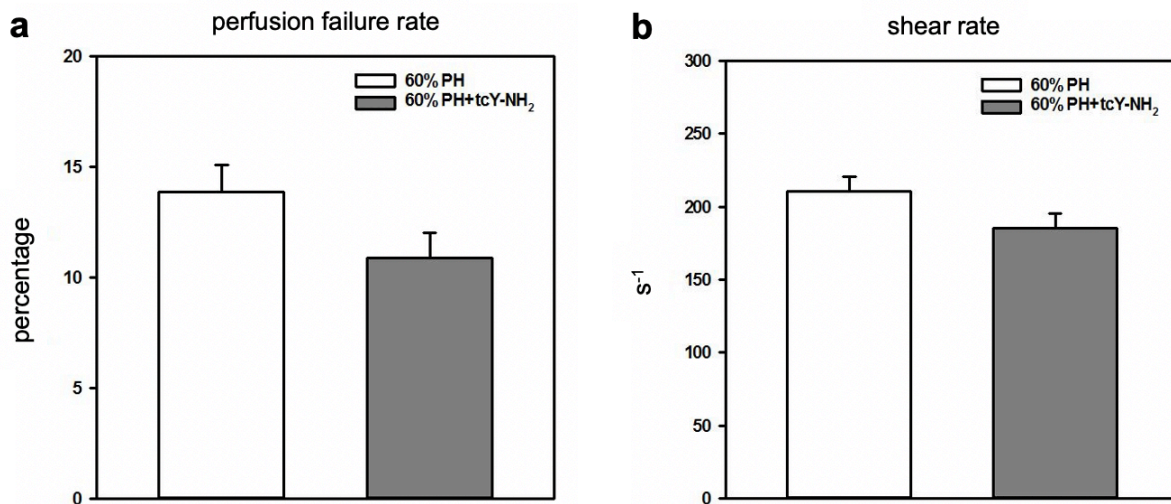


Figure 18: *in vivo* analysis of the microvascular injury and post-sinusoidal shear rate after 60% PH. n=6 animals per group, mean \pm SEM. *, $P < 0.05$, versus vehicle-treated group.

4.3.3 Two-photon-microscopic analysis

Consecutive pictures of hepatic microcirculation with high resolution were taken by 2PM to quantify the neutrophil recruitment, neutrophil-platelet interaction, and microthrombi in the hepatic sinusoids (as described earlier in method section, chapter 3.14.3, Figure 19).

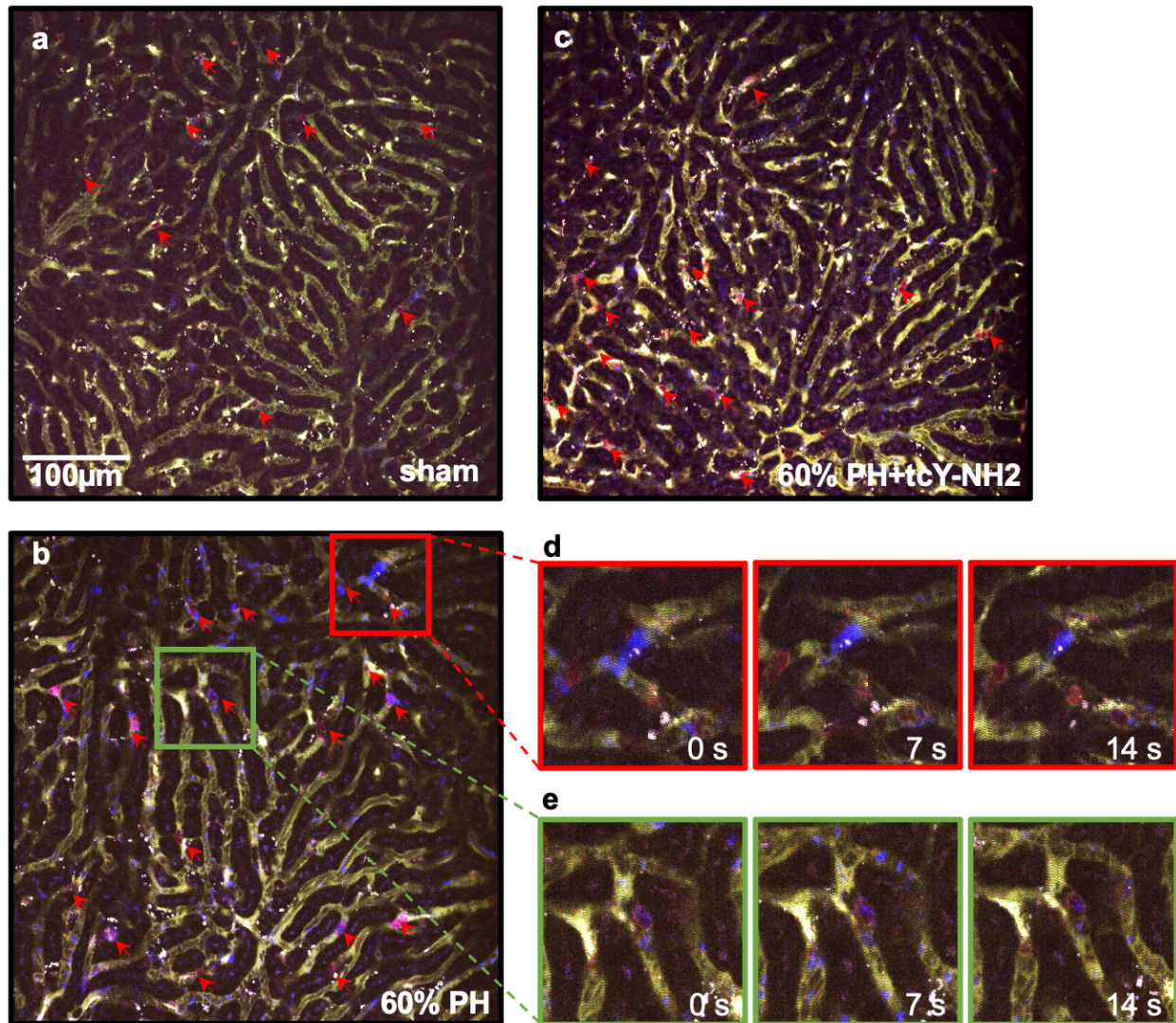


Figure 19: three-channel *in vivo* imaging from 2PM. Red: neutrophils (Ly-6G), blue: platelets(GPIIb-V-IX) and green: sinusoids (FITC). a: sham-operated animals. b: the 60%-PH group receiving saline as vehicle c: the 60%-PH group receiving tcY-NH₂. d: microthrombi from aggregated platelets marked with GPIIb-V-IX, which were stable in the same position throughout ten frames (1.4s/frame). e: colocalization of neutrophils and platelets, which could be constantly observed throughout ten frames (1.4s/frame), were considered as interaction.

4.3.3.1 Neutrophils

The number of neutrophils significantly expanded in sinusoids two hours after PH ($126.7 \pm 16.6 / \text{mm}^2$) compared to the number in the sham-operated animals ($40.4 \pm 9.3 / \text{mm}^2$). With the inhibition of PAR-4 by pretreating the animals with tcY-NH₂, positive counts insignificantly sank to $88.6 \pm 11.3 / \text{mm}^2$ compared to that in the mice undergoing 60% PH receiving saline (Figure 20).

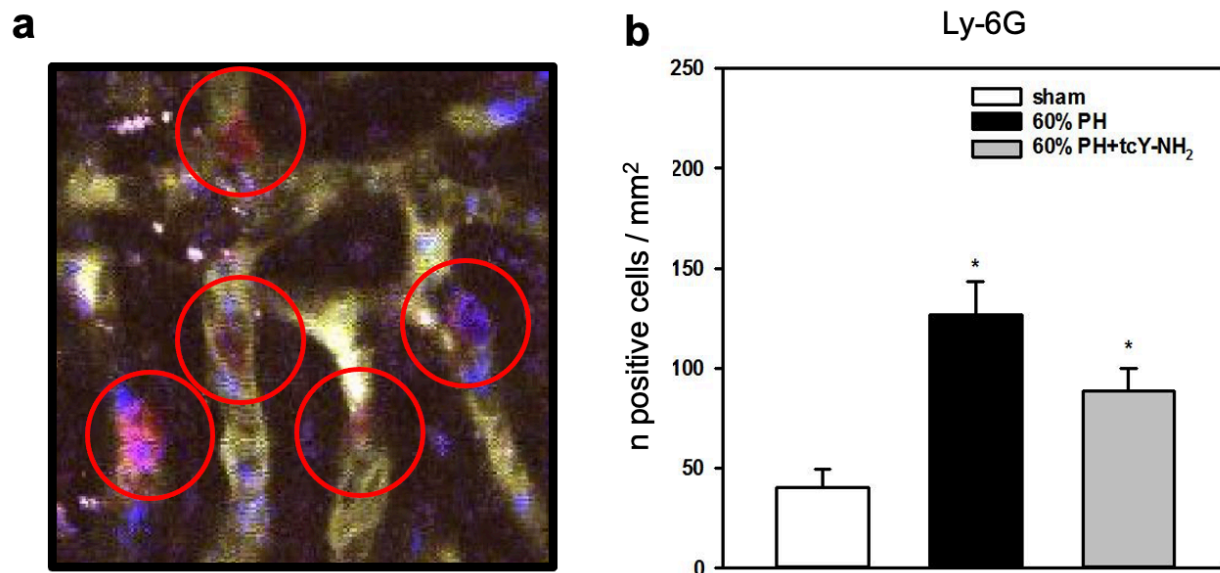


Figure 20: quantification of neutrophils in hepatic sinusoids marked with Ly-6G. a: Ly-6G⁺ cells (red circle) were quantified in hepatic sinusoids using 2PM. b: PH caused a significant increase in the number of neutrophil (Ly-6G⁺). This number insignificantly decreased in sinusoids after tcY-NH₂ treatment. n=6 animals per group, mean ± SEM. *, P < 0.05, versus sham-operated group; +, P < 0.05, versus 60%-PH group.

4.3.3.2 Neutrophil-platelet interaction

The 60% PH caused a significantly intensified neutrophil-platelet interaction reflected by the number of platelet-colocalized neutrophils $47.2 \pm 5.8 /\text{mm}^2$ compared to that in the sham-operated mice $9.9 \pm 2.6 /\text{mm}^2$. This increment was significantly suppressed after PAR-4 inhibition averaging $27.2 \pm 3.2 /\text{mm}^2$ (Figure 21).

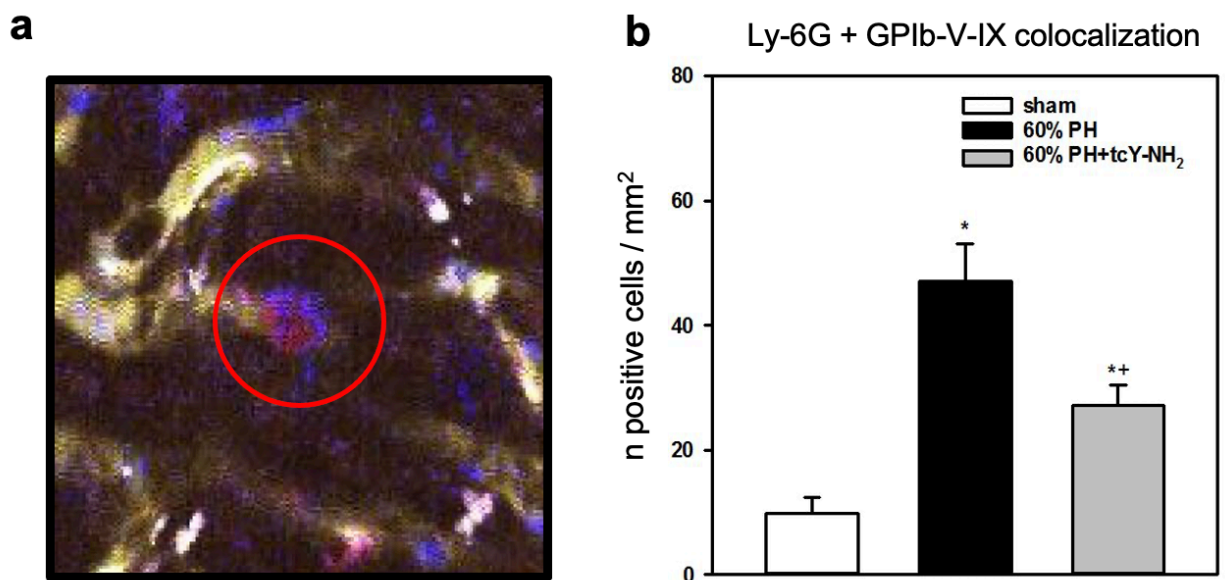


Figure 21: quantification of neutrophil-platelet interaction by counting the colocalization of Ly-6G and GPIb-V-IX. a: Ly-6G⁺ GPIb-V-IX⁺ cells (red circle) were quantified in hepatic sinusoids using 2PM. b: PH caused a significant increase in the number of platelet-colocalized neutrophils (Ly-6G⁺ GPIb-V-IX⁺). This number significantly decreased in sinusoids after tcY-NH₂ treatment. n=6 animals per group, mean ± SEM. *, P < 0.05, versus sham-operated group; +, P < 0.05, versus 60%-PH group.

4.3.3.3 Microthrombosis

Among the sham-operated animals, the microthrombi conformed by platelets in the microcirculation was rare to be found ($3.9 \pm 1.1 /\text{mm}^2$). A significant increase in microthrombi was found two hours after 60% PH ($21.5 \pm 2.6 /\text{mm}^2$). The number of microthrombi in sinusoids significantly decreased in the animals with PAR-4 inhibition ($12.1 \pm 2.4 /\text{mm}^2$, Figure 22).

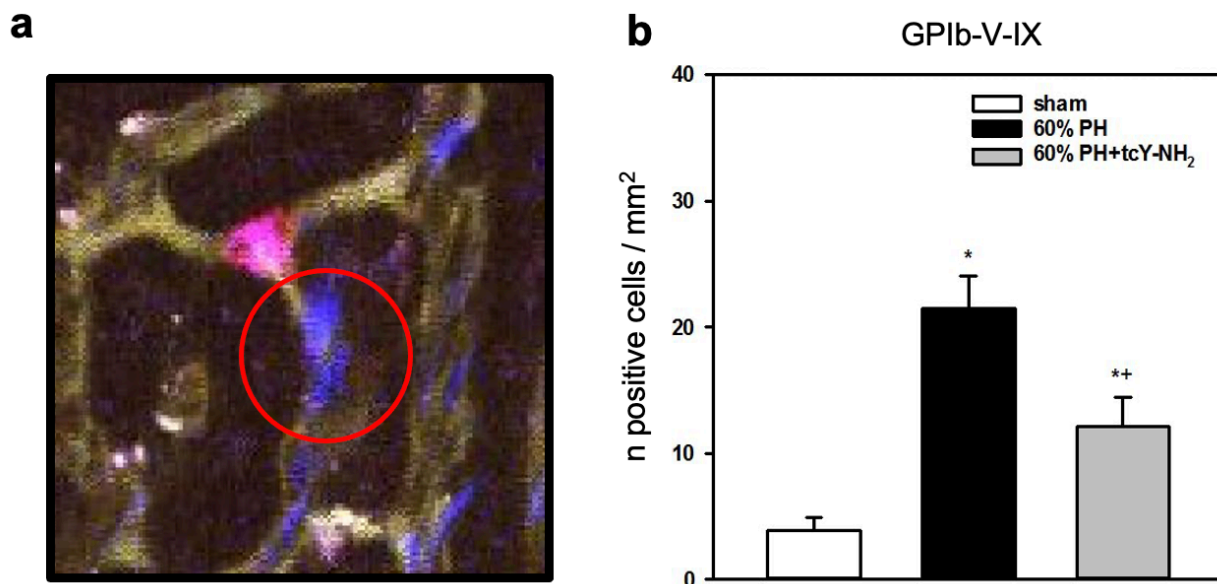


Figure 22: quantification of microthrombi marked with GPIb-V-IX. a: microthrombi from aggregated platelets marked with GPIb-V-IX (red circle) were stable in the same position throughout ten frames (1.4s/frame). **b:** PH caused a significant increase in the number of microthrombi (GPIb-V-IX⁺) in sinusoid. This number significantly decreased in sinusoids after tcY-NH₂ treatment. n=6 animals per group, mean ± SEM. *, P < 0.05, versus sham-operated group; +, P < 0.05, versus 60%-PH group.

4.3.4 AST, ALT and GLDH

Significant increments of AST, ALT, and GLDH were caused by the 60% PH (AST 847.6 ± 69.3 U/L; ALT 631.3 ± 59.2 U/L; GLDH 200.9 ± 49.1 U/L) after two hours compared to these in sham-operated mice (AST 46.5 ± 4.8 U/L; ALT 30.2 ± 4.3 U/L and GLDH 5.93 ± 1.4 U/L). This injury was significantly attenuated after inhibition of PAR-4 (AST 570.3 ± 56.5 U/L; ALT 472.1 ± 44.0 U/L and GLDH 98.6 ± 18.6 U/L, Figure 23).

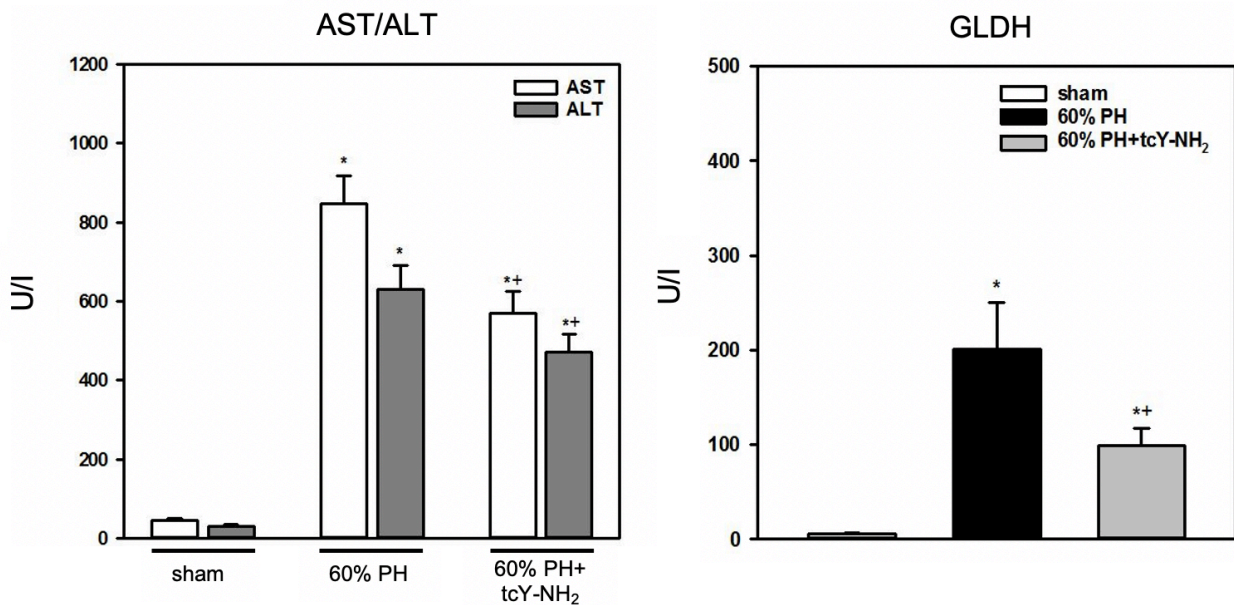


Figure 23: liver injury reflected by bilirubin and enzymes. Serum activity of liver enzyme demonstrated a significant necrotic injury two hours after 60% PH. The inhibition of PAR-4 significantly ameliorated liver injury after 60% PH. n=6 animals per group, mean \pm SEM. *, P < 0.05, versus sham-operated group; +, P < 0.05, versus 60%-PH group.

4.4 Study IV: Fibrinogen deposition in the acute phase after PH

4.4.1 Macrohemodynamic parameters

groups	sham	60% PH
MAP (mmHg)	74.3 ± 1.9	72.8 ± 1.5

There was no significant difference in MAP between the two experimental groups.

Table 11: MAP of each group, n=3, mean ± SD

4.4.2 Fibrinogen deposition after PH

Fibrinogen activation occurs in both inflammatory and hemorrhagic conditions. Fibrinogen is the main substrate of plasmin, which has been shown to play an important role in the induction of inflammatory processes following extended hepatectomy. To further address the role of the plasminogen-fibrinogen complex, fibrin(ogen) activity after extended hepatectomy was investigated *in vivo*. Fluorescence intensity was significantly increased after both 30 minutes and two hours after 60% PH ($2165.4 \pm 509.9 \mu\text{m}^2/500\text{x HPF}$ and $6467.3 \pm 1090.0 \mu\text{m}^2/500\text{x HPF}$, respectively) compared to the signal intensity in sham-operated animals (30 minutes $491.8 \pm 300.2 \mu\text{m}^2/500$ and two hours $2641.8.3 \pm 909.1 \mu\text{m}^2/500\text{x HPF}$, respectively, Figure 24). Notably, the fluorescent fibrinogen was mainly restricted to hepatic sinusoids.

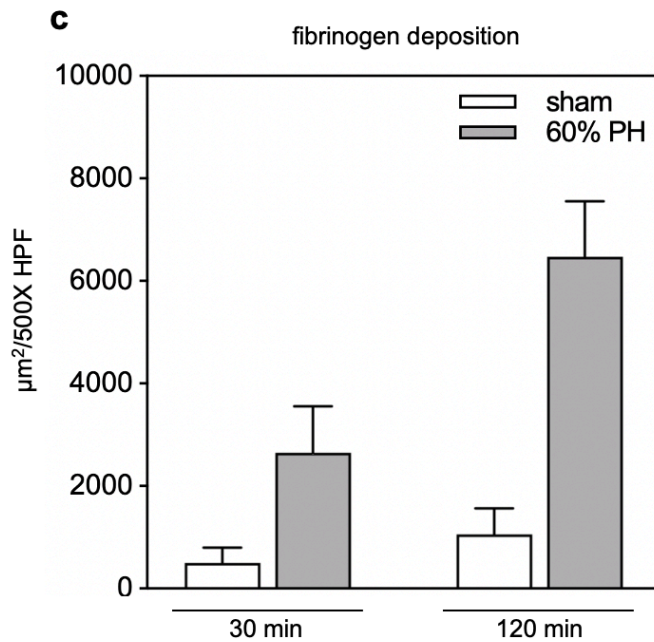
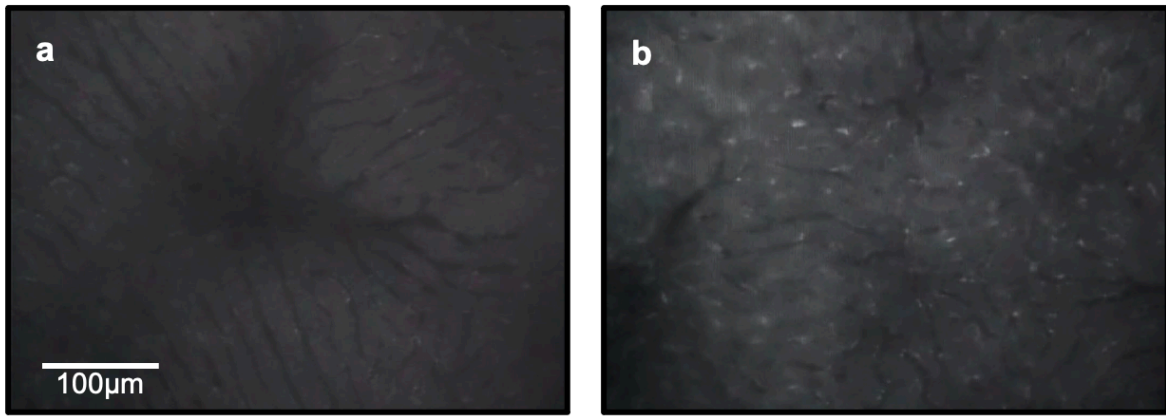


Figure 24: *in vivo* analysis of fibrinogen deposition. After infusion of Alexa-488-marked fibrinogen in sinusoids, **a**: Low deposition of fibrinogen was found in the sham-operated animals after two hours. **b**: The accumulation of fibrinogen in sinusoids in animals undergoing 60% PH after two hours. **c**: Significantly increased fibrinogen deposition was found at 30 and 120 minutes after PH compared to that in the sham-operated animals. Magnification 500x. n=3 animals per group, mean \pm SD. *, P < 0.001, versus sham-operated group.

5. Discussion

Facing an increasing demand for hepatectomy, effective treatments and preventions need to be developed to improve the outcome, reduce the life-threatening complication and avoid the occurrence of PHLF¹⁵⁶. As one of the most dangerous complications after extended liver resection, the pathophysiological mechanism for the development of PHLF is incompletely understood. Many studies focused on the mechanism of liver regeneration after major liver resection. In contrast, little effort has been paid to unveil the development of resection-induced liver injury^{105,106,157,158}.

A prominent physiological or, in most cases, pathological alternation after extended liver resection is the dramatically increased shear stress¹⁵⁹ due to the insufficient blood-vessel bed in the remnant liver. Studies showed that this “hyperperfusion” directly caused an injury of the hepatic endothelial wall and microvascular impairment. This microcirculatory injury can further induce perfusion failure and hepatic necrosis⁴⁹.

The activation of coagulation cascade is the first response after the injury of the hepatic endothelial cell wall^{160,161}. Other than the classic biological function of hemostasis, it has been recently reported that the coagulation cascade could induce the innate immune response and inflammation¹⁶². This study focused on the effect of coagulation cascade on leukocyte recruitment and microcirculatory injury in the acute phase after major liver resection.

5.1 Animal models

In this series of studies, C57BL/6 based murine models have been used to analyze the hepatic microstructure and essential immune cell components, such as leukocytes, neutrophils, and platelets. We applied different intravital imaging techniques to observe the live cell-cell interactions and the dynamic blood flow in the sinusoid. These complicated processes can only be presented in living organs. Many inhibitors and antibodies were used as interventions or to fluorescently stain the cell components. These reagents may be harmful and poisonous to the human body, so that it is necessary to use animal objects to achieve the scientific purpose. However due to the genetic difference between murine and human, further clinical study need to be conducted.

5.1.1 Approximate 60%-PH model for *in vivo* imaging

Higgins and Anderson have firstly described a reproducible two-thirds PH model in rats¹⁶³. Many other research groups have published various improvements and methods to achieve PH^{153,164,165}. Most of the protocols were targeted to investigate liver regeneration. Unlike what was described from other literature that the LLL of mice is mostly resected to enable the intravital imaging, the LLL was preserved in the current work. Our research group has found that the LLL owns sufficient liver surface area to present the liver microstructures, such as sinusoids, postsinusoidal venules, and presinusoidal arteries¹⁴². The MAPs of the experiments showed no significant difference indicating that this basic surgical model was reproducible.

A similar animal model with 70% PH for intravital microscopic investigation was also reported by Dold *et al.*, where Sprague-Dawley rats were used in the study. LLL and ML were resected to achieve an approximate 70% PH¹⁶⁶. The average size of mice's liver was much smaller than the size of the liver of rats. A flat and sufficient surface area is thus critical for a reproducible and representative mouse model. This is the reason to preserve the LLL in the current study.

5.1.2 Approximate 90%-PH model for *in vivo* imaging

The LLL was ligated additionally to observe the leukocyte-endothelial interaction and micro-circulatory injury in extreme pathophysiological conditions. The proportion of resected liver was about 92.7%. A smaller retaining device was made to present the caudal lobe. Because of the massive liver resection, the MAP of this group is inevitably lower than the 60%-PH groups and sham-operated animals. However, all of the animals survived in 2-hour courses. The SEMs showed a small intragroup variation.

5.1.3 Approximate 60%-PH with platelet-depletion model

A 24 hours + six-hour protocol was a classical method to deplete the platelet in our research group¹⁶⁷. The platelet counts showed a concrete >95% depletion of platelets. Because of the depletion of the platelets, the surgical difficulty of this model was huge. The combination of ligation and clip technique enabled the liver to be resected nearly without bleeding. However, due to the complicated catheterization process and the 2-hour courses, it was challenging to keep total bleeding as low as that from the mice with normal platelet counts. The MAP was

thus lower in the platelet-depletion mice than the mice with normal platelet counts, but the difference was not significant.

5.1.4 The setting for *in vivo* imaging

Many *in vivo* studies with murine liver have been reported for different purposes^{70,166}. Few described the paradox of fixing the liver under the microscope. Both epi-fluorescent and 2PM in our institution are up-right microscopes. Compared to an inverted microscope, where the mice might be placed over its liver, causing compression and breath-related liver movement¹⁶⁸, the advantage of presenting the liver with an up-right microscope was that it could avoid the major compression. The respiration-related liver movement could be improved by using a suitable liver retaining device.

The paradox of presenting the liver was that it was almost impossible to meet the following basic conditions.

1. a minimized movement caused by respiration
2. a flat and horizontal position to avoid concentrated compression from the cover glass provides an equally focused view under the objective to prevent the disturbing of micro-perfusion.

The anatomy of the mouse liver decided that the liver largely moves along with the respiration because the diaphragm and the liver are closely connected with a short trunk of superior vena cava¹⁶⁹. To avoid this micromovement, Gaertner *et al.*¹⁷⁰ used a vacuum device to fix the liver.

Park *et al.*¹⁷¹ applied glue to fix the liver on the glass. However, these techniques may cause the interruption of the microperfusion because of the solid fixation. Some groups tried to use the surface tension of the water to “suck” the liver onto the cover glass. Although there was almost no compression from the cover glass using the water surface tension, the respiration-caused micromovement was too strong, making the view under the microscope difficult to analyze. This model is thus difficult to be stably reproduced.

One of the goals of our study was to analyze the shear rate in postsinusoidal venules, which means that the microperfusion should not be disrupted. Thus, we applied our presenting system, as is described in **3.8**. There were several advantages to using this system.

1. The horizontal platform and specially designed cavity for the liver could enable the frontal surface of the liver to be flat enough and scattered the compression caused by a cover glass.
2. The friction under the liver (caudal surface) ensured the liver micromovement to be within a tolerable level without causing upper compression.
3. Repeatability. No glue was needed, which made the two-hour measurement after a baseline measurement possible.

5.2 Epifluorescence microscopy

Epi-illumination means the illumination from the surface of the specimen. This technique is widely used in all fields of life science. One basic instrument of epi-illumination is the fluorescence microscope. It is a conventional compound microscope that has been equipped with a strong light source that produces a broad-spectrum of light. A narrow range of wavelengths is selected by passing a filter. This excitation is then reflected by a beam splitter and passes through the objective lens onto the sample. The emission from light-emitting fluorescent molecules can return to the lens and then passes through the beam splitter and finally collected and digitalized by a CCD camera¹⁷².

As a classical way to present the microperfusion and leukocytes in the liver microcirculation, intravenous application of FITC-labeled dextran with 150 000 molecular weight was used to analyze the vitality of sinusoids. Rhodamine-6G was able to stain leukocytes. The hepatocytes could also be stained by rhodamine-6G so that the leukocytes could only be observed in post-sinusoidal venules, whereas the background signal in sinusoidal parenchyma was too high.

The limitation of epi-illumination is that the images contain signals not only from the focused layers but also the emission reflected by all layers of tissue. That may cause ambiguity when quantifying fluorescent cells. That was the reason to use IHC to further quantify the immune-cell recruitment in liver parenchyma and to utilize 2PM to analyze neutrophil-platelet interaction in hepatic sinusoids.

5.3 Two-photon microscopy

The 2PM owns a huge advantage compared to conventional single-photon imaging, because the absorption volume is much smaller at the focus at one time¹⁷³. That means 2PM causes much less photobleaching and phototoxicity on the liver tissue than a single-photon microscope. The longer wavelengths used by 2PM are less scattered by the specimen, enabling the observation deeper in the tissue than using a conventional microscope. It also excites less background autofluorescence. Moreover, several fluorochromes can be excited at one time, which enables live imaging without lagging from different channels after merging¹⁷⁴. To quantify the neutrophil-platelet interaction in sinusoids, a well-focused section of liver parenchyma is essential for reliable quantification. With a conventional or multi-channel fluorescence microscope, there is a significant lagging from channel to channel. When recording, only one fluorochrome can be excited and recorded at a time. This lagging causes displacement from object to object due to the micromovement of the liver so that the colocalization cannot be precisely analyzed. In contrast, 2PM ensured that the living objects could be captured at the same time without any displacement.

The *in vivo* images from 2PM thus provided a sharply focused section of liver parenchymal with very low phototoxicity to avoid regional inflammation and thrombosis.

5.4 results

5.4.1 Study I

This is so far the first attempt to use *in vivo* mouse model to observe the initial endothelial-leukocyte interaction and microvascular injury following the change of shear rate in the acute phase after PH. The first finding of this study was that the interaction between hepatic endothelial cells and leukocytes was immediately aggravated in response to the excessive shear rate following different extents of hepatectomy. This aggravation was reflected by an early augmentation of the leukocyte rolling and adhering to the wall of postsinusoidal venules. Interestingly, although greatly increased numbers of leukocytes and neutrophils were found in hepatic sinusoids in the 90%-PH group, as was showed from IHC analysis, a limited increase of adherent cells was found in postsinusoidal venules compared to the increase in the 60%-PH group. It was reported that leukocytes could roll on endothelium at shear stress from 1 to 10 dynes/cm²^{175,176}. Extremely excessive shear stress might compromise the initial capture and tethering of the leukocyte. This might indicate that leukocytes-endothelial interaction in hepatic sinusoids aggravates with the increase of shear rate, but the interaction can be hindered by an unphysiologically high shear rate in postsinusoidal venules

An attenuated leukocyte-endothelial interaction was found immediately from the baseline measurement after the treatment of aprotinin. The recruitment of leukocytes was largely inhibited in the presence of aprotinin. This finding demonstrated that SPs mediate the early leukocyte recruitment following the excessive shear rate in the remnant liver. Aprotinin is a broad-spectrum SP inhibitor that can inhibit fibrinolysis-related SPs like Plasmin, Plg activator, Kallikrein¹⁷⁷. By using Aprotinin, the Plg/plasmin pathway could be inhibited. Monocytes and Macrophages, like Kupffer cells, are rich in plasminogen receptors and uPA receptor. The plasmin can activate the Kupffer cell to

release many cytokines such as TNF- α , IL-1, and monocyte chemoattractant protein-1 to amplify the inflammatory response¹⁷⁸. Plasmin can also induce actin polymerization and chemotaxis in dendritic cells, which cause CD4+T cells to produce interferon- γ ¹⁷⁹. The former work of our group used an inflamed mouse cremaster model to quantify the leukocyte recruitment and transmigration. The treatment of aprotinin attenuated the number of recruited transmigrated leukocytes¹¹⁹.

It is generally accepted that sufficient perfusion of sinusoids is critical for the subsequent regeneration of the liver after PH¹⁸⁰. This underlines the importance of investigating the pathophysiological mechanism of hepatic microvascular injury before the regeneration is completely stimulated. Structural impairment of hepatic microcirculation in the acute phase was reported by studies featuring partial liver transplantation models^{64,181}. The hyperperfusion and a severe endothelial injury were reported following 90% PH based on a rat model reported by Li *et al.*¹⁸². A significant perfusion failure was reported in 90% PH in a rat model using a stepwise hepatectomy, according to Dold *et al.*¹⁶⁶.

In the current study, an early perfusion impairment was found immediately after PH using *in vivo* imaging. The inhibition of SPs improved sinusoidal perfusion instead of hindering it by prompting fibrin aggregation and blood clots. The anti-fibrinolysis is the main function of aprotinin¹⁸³. It is widely used in the prevention of bleeding from trauma and surgeries¹⁸⁴. Our finding demonstrated that SPs mediated the inflammatory process instead of prompt microthrombosis in sinusoids in the remnant liver without direct surgical trauma. Furthermore, the amelioration of inflammation further preserved liver function in the acute phase after PH.

Because aprotinin is a broad-spectrum SP inhibitor, the detailed function of individual SP, such as plasmin or thrombin, still needs to be addressed.

5.4.2 Study II

As reported by many studies, platelets are believed to be closely connected with inflammation^{109,185}. Although platelets are small anucleate fragments, several facts support that the platelet should be recognized as an immune cell¹⁸⁶⁻¹⁸⁸. Platelets express Toll-like receptors, which indicates a capacity to engage pathogens like leukocytes. One study reported that platelets could directly scavenge and collect bacteria¹⁷⁰. In a sterile liver injury model, platelets facilitated neutrophil extravasation in a GpIIb/IIIa dependent manner¹⁸⁹. Hence, we hypothesized that platelets induce leukocytes-mediated inflammation in the acute-phase liver injury after PH.

Using a platelet-depletion model, our results demonstrated that the early leukocyte-endothelial interaction was mediated by platelets. After platelet depletion, significantly fewer rolling leukocytes were found immediately after 60% PH and 2 hours after 60% PH. The leukocyte rolling is the classical step next to initial capture (tethering). P-selectin, largely involved in both leukocyte capture and rolling, is expressed by the platelets and endothelial cells. After being activated by the vWF, tissue factors, and thrombin released by injured endothelium, platelets can adhere to the endothelium. Predominantly with P-selectin and CD40-CD40L⁷⁰, the activated platelets can also bound to the flowing leukocytes¹⁹⁰. Hence, the adherent platelets form a bridge between leukocytes and endothelium so that the leukocyte capture and rolling are facilitated. The molecules involved in the platelet-leukocyte-endothelial interaction are described in Table 12. The decrease in the number of rolling leukocytes can also explain our next

finding that significantly fewer firm adherent leukocytes were found 2 hours after 60% PH because the leukocytes might not finally arrest and transmigrate without successful rolling process.

molecule	origin			ligand
	platelet	leukocyte	endothelial cell	
P-selectin	*		*	PSGL-1
E-selectin			*	PSGL-1; ESL-1; CD44
L-selectin		*		PSGL-1
ICAM-1		*	*	β 2-integrins
ICAM-2			*	β 2-integrins
VCAM-1			*	α 4-integrins
PECAM-1	*	*	*	PECAM-1
β 2-integrins		*		ICAM-1; ICAM-2; VCAM-1
β 3-integrins	*	*		fibrinogen; extracelular matrix
CD40	*	*	*	CD40L
CD40L	*	*	*	CD40L; α IIb β 3

Table 12: critical molecules and their ligands involved in the interaction among platelet, leukocyte, and endothelial cell

The result from the repressed leukocyte-endothelial interaction in the absence of platelets was that the acute inflammatory response after liver resection was attenuated. Our IHC analysis showed that the numbers of leukocytes and neutrophils were significantly reduced after platelet depletion within the sinusoids. Neutrophils were known as the first recruited leukocytes in acute inflammation. In the context of hepatectomy, the results from Study I showed significant recruitment of neutrophils in liver parenchyma in the acute phase after PH. The recruited neutrophils could initiate direct tissue damage after transmigration by releasing ROS, MPO, MMPs¹⁰⁵, and elastase¹⁹¹. Thus, this decrement in the number of neutrophils recruited in the liver parenchyma might contribute to the prevention of liver injury in the acute phase after liver resection.

Much effort has been made to investigate the role of platelets in the regeneration of the liver after liver resection. Murata *et al.* reported that the liver regenerates faster under thrombocytosis condition¹⁹². Matsuo *et al.* found that the liver/body weight ratio increased in the rats treated with platelet-rich plasma 24 hours after PH¹⁹³. Lopez *et al.* reported that platelet increased survival in a model of 90% PH in rats¹⁹⁴. Less attention has been paid to investigate the role of platelets in acute liver injury after liver resection. Husakura *et al.* used the pig-PH model and found that platelets could prevent acute liver damage after PH¹⁹⁵. However, within 6 hours, the AST from pigs with normal platelet counts was lower than the level from pigs treated with thrombopoietin. In the current study, the data showed that platelets could prompt leukocyte-

endothelial interaction that induced acute liver damage after liver resection. To prevent liver injury and preserve liver function after extended hepatectomy, it is unrealistic to perform surgery in the absence of platelets. In the next study, we further investigated the mechanism of how platelets mediated this inflammatory response and whether the activated platelets directly impair the sinusoidal perfusion by forming the microthrombi.

5.4.3 Study III

A critical finding was that the interaction between platelets and neutrophils was largely amplified after 60% PH. This implied that platelets might serve as an "assistant" to help neutrophils interact with endothelium and facilitate the hepatic neutrophil recruitment after PH. Serving as a reinforcement of our IHC, the *in vivo* imaging results showed a 4-fold increment in the number of recruited neutrophils in sinusoids two hours after hepatectomy. The neutrophils might be the most active cell component from innate immunity. They responded instantly after the PH. Neutrophils contribute to the direct tissue damage in PHLF in an MMP-9-dependent manner reported by Ohashi *et al.*¹⁰⁵.

By utilizing 2PM, we could quantify the thrombosis in hepatic microcirculation from consecutive images (scans). This is also the first attempt to quantify the microthrombosis in hepatic sinusoids in a real-time manner. Kirschbaum *et al.* reported that platelets aggregated in the remnant liver within 15 min after 70% PH¹⁹⁶. Our results showed that aggregated platelets tend to form microthrombi in sinusoids after PH. This finding can also explain the perfusion failure in the first study, which could be contributed by the microthrombi.

In this study, we also investigated whether platelets mediated neutrophil recruitment in a PAR-4-dependent manner, since platelets can be activated by thrombin via PAR-4¹⁴⁶. Our data showed that the inhibition of PAR-4 repressed the neutrophil-platelet interaction in the acute phase after PH. By using tcY-NH₂, a selective inhibitor of PAR-4, the activation from thrombin was inhibited. Platelet expresses much fewer adhesion molecules like p-selectin in an inactivated state. The “bridge” between the endothelium and neutrophil was weakened. The number of recruited neutrophils in sinusoids were decreased, but the difference was not significant compared to that in the vehicle-treated mice. This finding indicated the recruitment of neutrophils does not completely depend on platelet activation or neutrophil-platelet interaction, rather a more complicated mechanism.

The inhibition of platelet activation also resulted in a decrease in the number of microthrombi in sinusoids. This was followed by another exciting finding, that the inhibition of PAR-4 prevented the early liver injury after liver resection, which was reflected by the liver enzymes. Together with the further interaction of platelets and neutrophils, the activation of platelets accounted for acute liver injury after liver resection.

Epifluorescence microscope results showed that the inhibition of PAR-4 resulted in a reduction of firmly adherent leukocytes in postsinusoidal venules. Interestingly, it does not affect the number of rolling leukocytes in the venules. This indicated that the activation of platelet via PAR-4 is critical for the arrest of rolling leukocytes. Diacovo et al. reported that the adherent platelets on the neutrophils are essential for firm adhesion and further transmigration¹⁷⁵. PAR-

4 induced inflammation is reported in a neutrophil-dependent manner¹⁹⁷. Miyakawa *et al.* reported that early hepatic platelet accumulation within two hours was significantly reduced in PAR-4-deficient mice with acetaminophen (APAP)-induced liver injury compared to the wild-type mice. They found that depletion of platelets could also attenuate APAP-induced liver damage¹⁹⁸. Our research group reported that inhibition of PAR-4 alleviated platelet-endothelial interaction and platelet migration to the liver in IRI¹³⁹.

5.4.4 Study IV

In this set of experiments, significant early fibrinogen deposition was found after PH using *in vivo* imaging. This phenomenon suggested that the coagulation cascade responded in the first line following the shear stress alteration in hepatic microcirculation. This finding was in agreement with other studies suggesting an early engagement of coagulation system^{121,122} after PH.

Fibrin(ogen) can facilitate the leukocyte rolling and transmigration by acting as a ligand for various adhesion molecules, such as ICAM-1, VE-cadherin, and α IIb β 3, expressed by leukocytes, platelets, and endothelial cells¹⁹⁹. The accumulated fibrinogen could also facilitate the clot formation by the platelets. This can also explain the results from Study III that significantly more microthrombi were found in hepatic sinusoids after PH. Groeneveld *et al.* reported that fibrinogen deposition drives liver regeneration after PH in mice and humans²⁰⁰. The detailed function of fibrinogen regarding acute-phase liver injury is the future work of our research group.

5.5 Conclusions

The increased leukocyte-endothelial interaction and microcirculatory injury were two hallmarks in the acute phase after PH. The coagulation cascade was quickly activated after the increment of the shear rate reflected by the fibrinogen deposition. SPs and platelets play critical roles in this initial immune response. Platelets mediated the leukocyte-endothelial interaction by suppressing the expression of ICAM-1. The depletion of platelets resulted in a reduction in the number of recruited leukocytes in postsinusoidal venules, which improved the microcirculatory perfusion and prevented the parenchymal injury. PAR-4 played a critical role in the formation of acute liver injury after extended hepatectomy by regulating the leukocyte firm adhesion, the neutrophil-platelet interaction, and the microthrombosis in the hepatic microcirculation.

6. References

- 1 Morise, Z. & Wakabayashi, G. First quarter century of laparoscopic liver resection. *World J Gastroenterol* **23**, 3581-3588, doi:10.3748/wjg.v23.i20.3581 (2017).
- 2 Liu, C. Y., Chen, K. F. & Chen, P. J. Treatment of Liver Cancer. *Cold Spring Harb Perspect Med* **5**, a021535, doi:10.1101/cshperspect.a021535 (2015).
- 3 Orcutt, S. T. & Anaya, D. A. Liver Resection and Surgical Strategies for Management of Primary Liver Cancer. *Cancer Control* **25**, 1073274817744621, doi:10.1177/1073274817744621 (2018).
- 4 McGlynn, K. A., Petrick, J. L. & London, W. T. Global epidemiology of hepatocellular carcinoma: an emphasis on demographic and regional variability. *Clin Liver Dis* **19**, 223-238, doi:10.1016/j.cld.2015.01.001 (2015).
- 5 Petrick, J. L., Kelly, S. P., Altekruse, S. F., McGlynn, K. A. & Rosenberg, P. S. Future of Hepatocellular Carcinoma Incidence in the United States Forecast Through 2030. *J Clin Oncol* **34**, 1787-1794, doi:10.1200/JCO.2015.64.7412 (2016).
- 6 Massarweh, N. N. & El-Serag, H. B. Epidemiology of Hepatocellular Carcinoma and Intrahepatic Cholangiocarcinoma. *Cancer Control* **24**, 1073274817729245, doi:10.1177/1073274817729245 (2017).
- 7 de Jong, M. C. *et al.* Intrahepatic cholangiocarcinoma: an international multi-institutional analysis of prognostic factors and lymph node assessment. *J Clin Oncol* **29**, 3140-3145, doi:10.1200/JCO.2011.35.6519 (2011).
- 8 Brenner, H., Kloor, M. & Pox, C. P. Colorectal cancer. *Lancet* **383**, 1490-1502, doi:10.1016/S0140-6736(13)61649-9 (2014).
- 9 Akgul, O., Cetinkaya, E., Ersoz, S. & Tez, M. Role of surgery in colorectal cancer liver metastases. *World J Gastroenterol* **20**, 6113-6122, doi:10.3748/wjg.v20.i20.6113 (2014).
- 10 Chow, F. C. & Chok, K. S. Colorectal liver metastases: An update on multidisciplinary approach. *World J Hepatol* **11**, 150-172, doi:10.4254/wjh.v11.i2.150 (2019).
- 11 Garden, O. J. *et al.* Guidelines for resection of colorectal cancer liver metastases. *Gut* **55 Suppl 3**, iii1-8, doi:10.1136/gut.2006.098053 (2006).
- 12 Lyratzopoulos, G., Tyrrell, C., Smith, P. & Yelloly, J. Recent trends in liver resection surgery activity and population utilization rates in English regions. *HPB : the official journal of the International Hepato Pancreato Biliary Association* **9**, 277-280, doi:10.1080/13651820701504165 (2007).
- 13 Mandli, T. *et al.* [Evaluation of liver function before living donor liver transplantation and liver resection]. *Orv Hetil* **149**, 779-786, doi:10.1556/OH.2008.28316 (2008).
- 14 Adam, R., Hoti, E. & Bredt, L. C. [Oncosurgical strategies for metastatic liver cancer]. *Cir Esp* **89**, 10-19, doi:10.1016/j.ciresp.2010.10.007 (2011).

- 15 Hackl, C. *et al.* Split liver transplantation: Current developments. *World J Gastroenterol* **24**, 5312-5321, doi:10.3748/wjg.v24.i47.5312 (2018).
- 16 Samuel, D. & Coilly, A. Management of patients with liver diseases on the waiting list for transplantation: a major impact to the success of liver transplantation. *BMC Med* **16**, 113, doi:10.1186/s12916-018-1110-y (2018).
- 17 Shaib, Y. H., Davila, J. A., McGlynn, K. & El-Serag, H. B. Rising incidence of intrahepatic cholangiocarcinoma in the United States: a true increase? *J Hepatol* **40**, 472-477, doi:10.1016/j.jhep.2003.11.030 (2004).
- 18 Hashimoto, K. & Miller, C. M. Liver transplantation for intrahepatic cholangiocarcinoma. *J Hepatobiliary Pancreat Sci* **22**, 138-143, doi:10.1002/jhbp.159 (2015).
- 19 Tacke, F., Kroy, D. C., Barreiros, A. P. & Neumann, U. P. Liver transplantation in Germany. *Liver Transpl* **22**, 1136-1142, doi:10.1002/lt.24461 (2016).
- 20 Suri, J. S., Danford, C. J., Patwardhan, V. & Bonder, A. Mortality on the UNOS Waitlist for Patients with Autoimmune Liver Disease. *J Clin Med* **9**, doi:10.3390/jcm9020319 (2020).
- 21 Ray, S., Mehta, N. N., Golhar, A. & Nundy, S. Post hepatectomy liver failure - A comprehensive review of current concepts and controversies. *Ann Med Surg (Lond)* **34**, 4-10, doi:10.1016/j.amsu.2018.08.012 (2018).
- 22 Riddiough, G. E., Christophi, C., Jones, R. M., Muralidharan, V. & Perini, M. V. A systematic review of small for size syndrome after major hepatectomy and liver transplantation. *HPB : the official journal of the International Hepato Pancreato Biliary Association* **22**, 487-496, doi:10.1016/j.hpb.2019.10.2445 (2020).
- 23 Rahbari, N. N. *et al.* Posthepatectomy liver failure: a definition and grading by the International Study Group of Liver Surgery (ISGLS). *Surgery* **149**, 713-724, doi:10.1016/j.surg.2010.10.001 (2011).
- 24 Clavien, P. A. & Eshmunov, D. Small for size: Laboratory perspective. *Liver transplantation : official publication of the American Association for the Study of Liver Diseases and the International Liver Transplantation Society* **21 Suppl 1**, S13-14, doi:10.1002/lt.24309 (2015).
- 25 Dahm, F., Georgiev, P. & Clavien, P. A. Small-for-size syndrome after partial liver transplantation: definition, mechanisms of disease and clinical implications. *Am J Transplant* **5**, 2605-2610, doi:10.1111/j.1600-6143.2005.01081.x (2005).
- 26 Shimada, M. *et al.* Living-donor liver transplantation: present status and future perspective. *J Med Invest* **52**, 22-32 (2005).
- 27 Golse, N. *et al.* New paradigms in post-hepatectomy liver failure. *Journal of gastrointestinal surgery : official journal of the Society for Surgery of the Alimentary Tract* **17**, 593-605, doi:10.1007/s11605-012-2048-6 (2013).
- 28 Yagi, S. & Uemoto, S. Small-for-size syndrome in living donor liver transplantation. *Hepatobiliary Pancreat Dis Int* **11**, 570-576, doi:10.1016/s1499-3872(12)60227-6 (2012).
- 29 Yamada, T. *et al.* Selective hemi-portocaval shunt based on portal vein pressure for small-for-size graft in adult living donor liver transplantation. *Am J Transplant* **8**, 847-853, doi:10.1111/j.1600-6143.2007.02144.x (2008).
- 30 Botha, J. F. *et al.* Left lobe adult-to-adult living donor liver transplantation: small grafts and hemiportocaval shunts in the prevention of small-for-size syndrome. *Liver Transpl* **16**, 649-657, doi:10.1002/lt.22043 (2010).
- 31 Sato, Y. *et al.* Inferior mesenteric venous left renal vein shunting for decompression of excessive portal hypertension in adult living related liver transplantation. *Transplant Proc* **36**, 2234-2236, doi:10.1016/j.transproceed.2004.08.027 (2004).

- 32 Sato, Y. *et al.* Management of major portosystemic shunting in small-for-size adult living-related donor liver transplantation with a left-sided graft liver. *Surg Today* **36**, 354-360, doi:10.1007/s00595-005-3136-y (2006).
- 33 Cescon, M. *et al.* Restoration of portal vein flow by splenorenal shunt ligation and splenectomy after living-related liver transplantation. *Hepatogastroenterology* **48**, 1453-1454 (2001).
- 34 Shirouzu, Y. *et al.* How to handle a huge portosystemic shunt in adult living donor liver transplantation with a small-for-size graft: report of a case. *Surg Today* **39**, 637-640, doi:10.1007/s00595-008-3886-4 (2009).
- 35 Ren, Y. S. *et al.* Beneficial effects of splenectomy on liver regeneration in a rat model of massive hepatectomy. *Hepatobiliary Pancreat Dis Int* **11**, 60-65 (2012).
- 36 Eipel, C. *et al.* Splenectomy improves survival by increasing arterial blood supply in a rat model of reduced-size liver. *Transpl Int* **23**, 998-1007, doi:10.1111/j.1432-2277.2010.01079.x (2010).
- 37 Umeda, Y. *et al.* Effects of prophylactic splenic artery modulation on portal overperfusion and liver regeneration in small-for-size graft. *Transplantation* **86**, 673-680, doi:10.1097/TP.0b013e318181e02d (2008).
- 38 Rosado, B. & Kamath, P. S. Transjugular intrahepatic portosystemic shunts: an update. *Liver transplantation : official publication of the American Association for the Study of Liver Diseases and the International Liver Transplantation Society* **9**, 207-217, doi:10.1053/jlts.2003.50045 (2003).
- 39 Sellers, C. M., Nezami, N., Schilsky, M. L. & Kim, H. S. Transjugular intrahepatic portosystemic shunt as a bridge to liver transplant: Current state and future directions. *Transplant Rev (Orlando)* **33**, 64-71, doi:10.1016/j.tre.2018.10.004 (2019).
- 40 Saad, W. E. Transjugular Intrahepatic Portosystemic Shunt before and after Liver Transplantation. *Semin Intervent Radiol* **31**, 243-247, doi:10.1055/s-0034-1382791 (2014).
- 41 Selvaggi, G. & Tzakis, A. Surgical considerations in liver transplantation: small for size syndrome. *Panminerva Med* **51**, 227-233 (2009).
- 42 Samimi, F. *et al.* Role of splenectomy in human liver transplantation under modern-day immunosuppression. *Digestive diseases and sciences* **43**, 1931-1937 (1998).
- 43 Ishibe, A. *et al.* Prostaglandin E1 prevents liver failure after excessive hepatectomy in the rat by up-regulating Cyclin C, Cyclin D1, and Bclxl. *Wound Repair Regen* **17**, 62-70, doi:10.1111/j.1524-475X.2008.00442.x (2009).
- 44 Aiba, M. *et al.* Novel nitric oxide donor (FK409) ameliorates liver damage during extended liver resection with warm ischemia in dogs. *J Am Coll Surg* **193**, 264-271, doi:10.1016/s1072-7515(01)01002-x (2001).
- 45 Du, Z. *et al.* Octreotide prevents liver failure through upregulating 5'-methylthioadenosine in extended hepatectomized rats. *Liver international : official journal of the International Association for the Study of the Liver* **36**, 212-222, doi:10.1111/liv.12863 (2016).
- 46 Palmes, D. *et al.* Amelioration of microcirculatory damage by an endothelin A receptor antagonist in a rat model of reversible acute liver failure. *J Hepatol* **42**, 350-357, doi:10.1016/j.jhep.2004.11.019 (2005).
- 47 Shoreem, H. *et al.* Small for size syndrome difficult dilemma: Lessons from 10 years single centre experience in living donor liver transplantation. *World J Hepatol* **9**, 930-944, doi:10.4254/wjh.v9.i21.930 (2017).
- 48 Eipel, C., Abshagen, K. & Vollmar, B. Regulation of hepatic blood flow: the hepatic arterial buffer response revisited. *World J Gastroenterol* **16**, 6046-6057, doi:10.3748/wjg.v16.i48.6046 (2010).

- 49 Vollmar, B. & Menger, M. D. The hepatic microcirculation: mechanistic contributions and therapeutic targets in liver injury and repair. *Physiological reviews* **89**, 1269-1339, doi:10.1152/physrev.00027.2008 (2009).
- 50 Lauth, W. W., Legare, D. J. & Ezzat, W. R. Quantitation of the hepatic arterial buffer response to graded changes in portal blood flow. *Gastroenterology* **98**, 1024-1028 (1990).
- 51 Sancetta, S. M. Dynamic and neurogenic factors determining the hepatic arterial flow after portal occlusion. *Circ Res* **1**, 414-418 (1953).
- 52 Henderson, J. M. *et al.* Hemodynamics during liver transplantation: the interactions between cardiac output and portal venous and hepatic arterial flows. *Hepatology* **16**, 715-718 (1992).
- 53 Lauth, W. W. Regulatory processes interacting to maintain hepatic blood flow constancy: Vascular compliance, hepatic arterial buffer response, hepatorenal reflex, liver regeneration, escape from vasoconstriction. *Hepatol Res* **37**, 891-903, doi:10.1111/j.1872-034X.2007.00148.x (2007).
- 54 Kohler, A. *et al.* Portal hyperperfusion after major liver resection and associated sinusoidal damage is a therapeutic target to protect the remnant liver. *American journal of physiology. Gastrointestinal and liver physiology* **317**, G264-G274, doi:10.1152/ajpgi.00113.2019 (2019).
- 55 Poisson, J. *et al.* Liver sinusoidal endothelial cells: Physiology and role in liver diseases. *J Hepatol* **66**, 212-227, doi:10.1016/j.jhep.2016.07.009 (2017).
- 56 Becker, D. *et al.* Model Assisted Analysis of the Hepatic Arterial Buffer Response During Ex Vivo Porcine Liver Perfusion. *IEEE Trans Biomed Eng* **67**, 667-678, doi:10.1109/TBME.2019.2919413 (2020).
- 57 Gruttadauria, S., Pagano, D., Luca, A. & Gridelli, B. Small-for-size syndrome in adult-to-adult living-related liver transplantation. *World J Gastroenterol* **16**, 5011-5015 (2010).
- 58 Demetris, A. J. *et al.* Pathophysiologic observations and histopathologic recognition of the portal hyperperfusion or small-for-size syndrome. *Am J Surg Pathol* **30**, 986-993 (2006).
- 59 Paulsen, A. W. & Klintmalm, G. B. Direct measurement of hepatic blood flow in native and transplanted organs, with accompanying systemic hemodynamics. *Hepatology* **16**, 100-111 (1992).
- 60 Ito, T. *et al.* Changes in portal venous pressure in the early phase after living donor liver transplantation: pathogenesis and clinical implications. *Transplantation* **75**, 1313-1317, doi:10.1097/01.TP.0000063707.90525.10 (2003).
- 61 Imura, S., Shimada, M., Ikegami, T., Morine, Y. & Kanemura, H. Strategies for improving the outcomes of small-for-size grafts in adult-to-adult living-donor liver transplantation. *J Hepatobiliary Pancreat Surg* **15**, 102-110, doi:10.1007/s00534-007-1297-3 (2008).
- 62 Kelly, D. M. *et al.* Adenosine restores the hepatic artery buffer response and improves survival in a porcine model of small-for-size syndrome. *Liver transplantation : official publication of the American Association for the Study of Liver Diseases and the International Liver Transplantation Society* **15**, 1448-1457, doi:10.1002/lt.21863 (2009).
- 63 Soulis, J. V. *et al.* Molecular viscosity in the normal left coronary arterial tree. Is it related to atherosclerosis? *Angiology* **57**, 33-40, doi:10.1177/000331970605700105 (2006).
- 64 Man, K. *et al.* Liver transplantation in rats using small-for-size grafts: a study of hemodynamic and morphological changes. *Arch Surg* **136**, 280-285 (2001).
- 65 Braet, F. *et al.* Liver sinusoidal endothelial cell modulation upon resection and shear stress in vitro. *Comp Hepatol* **3**, 7, doi:10.1186/1476-5926-3-7 (2004).
- 66 Liu, J. *et al.* Impact of clinically significant portal hypertension on outcomes after partial hepatectomy for hepatocellular carcinoma: a systematic review and meta-analysis. *HPB* :

- the official journal of the International Hepato Pancreato Biliary Association*, doi:10.1016/j.hpb.2018.07.005 (2018).
- 67 Chen, X. *et al.* Severity of portal hypertension and prediction of postoperative liver failure after liver resection in patients with Child-Pugh grade A cirrhosis. *The British journal of surgery* **99**, 1701-1710, doi:10.1002/bjs.8951 (2012).
- 68 Shen, H., Kreisel, D. & Goldstein, D. R. Processes of sterile inflammation. *Journal of immunology* **191**, 2857-2863, doi:10.4049/jimmunol.1301539 (2013).
- 69 Chen, G. Y. & Nunez, G. Sterile inflammation: sensing and reacting to damage. *Nature reviews. Immunology* **10**, 826-837, doi:10.1038/nri2873 (2010).
- 70 Khandoga, A., Hanschen, M., Kessler, J. S. & Krombach, F. CD4+ T cells contribute to postischemic liver injury in mice by interacting with sinusoidal endothelium and platelets. *Hepatology* **43**, 306-315, doi:10.1002/hep.21017 (2006).
- 71 Kubes, P. & Mehal, W. Z. Sterile inflammation in the liver. *Gastroenterology* **143**, 1158-1172, doi:10.1053/j.gastro.2012.09.008 (2012).
- 72 Carrick, J. B. & Begg, A. P. Peripheral blood leukocytes. *Vet Clin North Am Equine Pract* **24**, 239-259, v, doi:10.1016/j.cveq.2008.05.003 (2008).
- 73 Breedveld, A., Groot Kormelink, T., van Egmond, M. & de Jong, E. C. Granulocytes as modulators of dendritic cell function. *Journal of leukocyte biology* **102**, 1003-1016, doi:10.1189/jlb.4MR0217-048RR (2017).
- 74 Laschke, M. W., Dold, S., Menger, M. D., Jeppsson, B. & Thorlacius, H. Platelet-dependent accumulation of leukocytes in sinusoids mediates hepatocellular damage in bile duct ligation-induced cholestasis. *British journal of pharmacology* **153**, 148-156, doi:10.1038/sj.bjp.0707578 (2008).
- 75 Khandoga, A. *et al.* Junctional adhesion molecule-A deficiency increases hepatic ischemia-reperfusion injury despite reduction of neutrophil transendothelial migration. *Blood* **106**, 725-733, doi:10.1182/blood-2004-11-4416 (2005).
- 76 Eipel, C., Bordel, R., Nickels, R. M., Menger, M. D. & Vollmar, B. Impact of leukocytes and platelets in mediating hepatocyte apoptosis in a rat model of systemic endotoxemia. *American journal of physiology. Gastrointestinal and liver physiology* **286**, G769-776, doi:10.1152/ajpgi.00275.2003 (2004).
- 77 Corso, C. O., Okamoto, S., Ruttinger, D. & Messmer, K. Hypertonic saline dextran attenuates leukocyte accumulation in the liver after hemorrhagic shock and resuscitation. *The Journal of trauma* **46**, 417-423 (1999).
- 78 Chosay, J. G., Essani, N. A., Dunn, C. J. & Jaeschke, H. Neutrophil margination and extravasation in sinusoids and venules of liver during endotoxin-induced injury. *Am J Physiol* **272**, G1195-1200, doi:10.1152/ajpgi.1997.272.5.G1195 (1997).
- 79 Amulic, B., Cazalet, C., Hayes, G. L., Metzler, K. D. & Zychlinsky, A. Neutrophil function: from mechanisms to disease. *Annual review of immunology* **30**, 459-489, doi:10.1146/annurev-immunol-020711-074942 (2012).
- 80 Winterbourn, C. C., Kettle, A. J. & Hampton, M. B. Reactive Oxygen Species and Neutrophil Function. *Annu Rev Biochem* **85**, 765-792, doi:10.1146/annurev-biochem-060815-014442 (2016).
- 81 Mutua, V. & Gershwin, L. J. A Review of Neutrophil Extracellular Traps (NETs) in Disease: Potential Anti-NETs Therapeutics. *Clin Rev Allergy Immunol* **61**, 194-211, doi:10.1007/s12016-020-08804-7 (2021).
- 82 Kolaczowska, E. & Kubes, P. Neutrophil recruitment and function in health and inflammation. *Nature reviews. Immunology* **13**, 159-175, doi:10.1038/nri3399 (2013).

- 83 Kubes, P. The enigmatic neutrophil: what we do not know. *Cell Tissue Res* **371**, 399-406, doi:10.1007/s00441-018-2790-5 (2018).
- 84 Ley, K., Laudanna, C., Cybulsky, M. I. & Nourshargh, S. Getting to the site of inflammation: the leukocyte adhesion cascade updated. *Nature reviews. Immunology* **7**, 678-689, doi:10.1038/nri2156 (2007).
- 85 Woollard, K. J. *et al.* Pathophysiological levels of soluble P-selectin mediate adhesion of leukocytes to the endothelium through Mac-1 activation. *Circ Res* **103**, 1128-1138, doi:10.1161/CIRCRESAHA.108.180273 (2008).
- 86 Petri, B., Phillipson, M. & Kubes, P. The physiology of leukocyte recruitment: an in vivo perspective. *Journal of immunology* **180**, 6439-6446 (2008).
- 87 Kum, W. W. *et al.* Lack of functional P-selectin ligand exacerbates Salmonella serovar typhimurium infection. *Journal of immunology* **182**, 6550-6561, doi:10.4049/jimmunol.0802536 (2009).
- 88 Gotsch, U., Jager, U., Dominis, M. & Vestweber, D. Expression of P-selectin on endothelial cells is upregulated by LPS and TNF-alpha in vivo. *Cell adhesion and communication* **2**, 7-14 (1994).
- 89 Ala, A., Dhillon, A. P. & Hodgson, H. J. Role of cell adhesion molecules in leukocyte recruitment in the liver and gut. *International journal of experimental pathology* **84**, 1-16, doi:10.1046/j.1365-2613.2003.00235.x (2003).
- 90 Speyer, C. L. & Ward, P. A. Role of endothelial chemokines and their receptors during inflammation. *Journal of investigative surgery : the official journal of the Academy of Surgical Research* **24**, 18-27, doi:10.3109/08941939.2010.521232 (2011).
- 91 Sokol, C. L. & Luster, A. D. The chemokine system in innate immunity. *Cold Spring Harb Perspect Biol* **7**, doi:10.1101/cshperspect.a016303 (2015).
- 92 Henderson, R. B. *et al.* The use of lymphocyte function-associated antigen (LFA)-1-deficient mice to determine the role of LFA-1, Mac-1, and alpha4 integrin in the inflammatory response of neutrophils. *J Exp Med* **194**, 219-226 (2001).
- 93 Vestweber, D. How leukocytes cross the vascular endothelium. *Nature reviews. Immunology* **15**, 692-704, doi:10.1038/nri3908 (2015).
- 94 Filippi, M. D. Neutrophil transendothelial migration: updates and new perspectives. *Blood* **133**, 2149-2158, doi:10.1182/blood-2018-12-844605 (2019).
- 95 Vestweber, D. Adhesion and signaling molecules controlling the transmigration of leukocytes through endothelium. *Immunological reviews* **218**, 178-196, doi:10.1111/j.1600-065X.2007.00533.x (2007).
- 96 McCluney, S. J. *et al.* Neutrophil: Lymphocyte ratio as a method of predicting complications following hepatic resection for colorectal liver metastasis. *J Surg Oncol* **117**, 1058-1065, doi:10.1002/jso.24996 (2018).
- 97 Ma, Z. Y. *et al.* Inhibition of matrix metalloproteinase-9 attenuates acute small-for-size liver graft injury in rats. *Am J Transplant* **10**, 784-795, doi:10.1111/j.1600-6143.2009.02993.x (2010).
- 98 Ohtsuka, M., Miyazaki, M., Kondo, Y. & Nakajima, N. Neutrophil-mediated sinusoidal endothelial cell injury after extensive hepatectomy in cholestatic rats. *Hepatology* **25**, 636-641, doi:10.1002/hep.510250324 (1997).
- 99 Rao, R. *et al.* Interleukin 17-producing gammadeltaT cells promote hepatic regeneration in mice. *Gastroenterology* **147**, 473-484 e472, doi:10.1053/j.gastro.2014.04.042 (2014).
- 100 Tumanov, A. V. *et al.* T cell-derived lymphotoxin regulates liver regeneration. *Gastroenterology* **136**, 694-704 e694, doi:10.1053/j.gastro.2008.09.015 (2009).

- 101 Nakashima, H. *et al.* Activation of mouse natural killer T cells accelerates liver regeneration after partial hepatectomy. *Gastroenterology* **131**, 1573-1583, doi:10.1053/j.gastro.2006.08.028 (2006).
- 102 Yin, S. *et al.* Activation of invariant natural killer T cells impedes liver regeneration by way of both IFN-gamma- and IL-4-dependent mechanisms. *Hepatology* **60**, 1356-1366, doi:10.1002/hep.27128 (2014).
- 103 Selzner, N. *et al.* ICAM-1 triggers liver regeneration through leukocyte recruitment and Kupffer cell-dependent release of TNF-alpha/IL-6 in mice. *Gastroenterology* **124**, 692-700, doi:10.1053/gast.2003.50098 (2003).
- 104 Minagawa, M. *et al.* Intensive expansion of natural killer T cells in the early phase of hepatocyte regeneration after partial hepatectomy in mice and its association with sympathetic nerve activation. *Hepatology* **31**, 907-915, doi:10.1053/he.2000.5850 (2000).
- 105 Ohashi, N. *et al.* Matrix metalloproteinase-9 in the initial injury after hepatectomy in mice. *World J Gastroenterol* **19**, 3027-3042, doi:10.3748/wjg.v19.i20.3027 (2013).
- 106 Rudich, N. *et al.* Focal liver necrosis appears early after partial hepatectomy and is dependent on T cells and antigen delivery from the gut. *Liver international : official journal of the International Association for the Study of the Liver* **29**, 1273-1284, doi:10.1111/j.1478-3231.2009.02048.x (2009).
- 107 Sato, Y. *et al.* Activation of extrathymic T cells in the liver during liver regeneration following partial hepatectomy. *Immunology* **78**, 86-91 (1993).
- 108 Kato, T. *et al.* Involvement of natural killer T cells and granulocytes in the inflammation induced by partial hepatectomy. *J Hepatol* **40**, 285-290 (2004).
- 109 Margraf, A. & Zarbock, A. Platelets in Inflammation and Resolution. *Journal of immunology* **203**, 2357-2367, doi:10.4049/jimmunol.1900899 (2019).
- 110 Foley, J. H. & Conway, E. M. Cross Talk Pathways Between Coagulation and Inflammation. *Circ Res* **118**, 1392-1408, doi:10.1161/CIRCRESAHA.116.306853 (2016).
- 111 Carter, P. & Wells, J. A. Dissecting the catalytic triad of a serine protease. *Nature* **332**, 564-568, doi:10.1038/332564a0 (1988).
- 112 Henkel, A. S., Khan, S. S., Olivares, S., Miyata, T. & Vaughan, D. E. Inhibition of Plasminogen Activator Inhibitor 1 Attenuates Hepatic Steatosis but Does Not Prevent Progressive Nonalcoholic Steatohepatitis in Mice. *Hepatol Commun* **2**, 1479-1492, doi:10.1002/hep4.1259 (2018).
- 113 Okada, K., Ueshima, S., Imano, M., Kataoka, K. & Matsuo, O. The regulation of liver regeneration by the plasmin/alpha 2-antiplasmin system. *J Hepatol* **40**, 110-116, doi:10.1016/j.jhep.2003.09.016 (2004).
- 114 Avalos-de Leon, C. G., Jimenez-Castro, M. B., Cornide-Petronio, M. E., Casillas-Ramirez, A. & Peralta, C. The Role of GLP1 in Rat Steatotic and Non-Steatotic Liver Transplantation from Cardiocirculatory Death Donors. *Cells* **8**, doi:10.3390/cells8121599 (2019).
- 115 Gao, S., Silasi-Mansat, R., Behar, A. R., Lupu, F. & Griffin, C. T. Excessive Plasmin Compromises Hepatic Sinusoidal Vascular Integrity After Acetaminophen Overdose. *Hepatology* **68**, 1991-2003, doi:10.1002/hep.30070 (2018).
- 116 Law, R. H., Abu-Ssaydeh, D. & Whisstock, J. C. New insights into the structure and function of the plasminogen/plasmin system. *Curr Opin Struct Biol* **23**, 836-841, doi:10.1016/j.sbi.2013.10.006 (2013).
- 117 Weisel, J. W. & Litvinov, R. I. Fibrin Formation, Structure and Properties. *Subcell Biochem* **82**, 405-456, doi:10.1007/978-3-319-49674-0_13 (2017).

- 118 Praetner, M. *et al.* Plasminogen Activator Inhibitor-1 Promotes Neutrophil Infiltration and Tissue Injury on Ischemia-Reperfusion. *Arteriosclerosis, thrombosis, and vascular biology* **38**, 829-842, doi:10.1161/ATVBAHA.117.309760 (2018).
- 119 Lerchenberger, M. *et al.* Matrix metalloproteinases modulate ameboid-like migration of neutrophils through inflamed interstitial tissue. *Blood* **122**, 770-780, doi:10.1182/blood-2012-12-472944 (2013).
- 120 Mangnall, D., Smith, K., Bird, N. C. & Majeed, A. W. Early increases in plasminogen activator activity following partial hepatectomy in humans. *Comp Hepatol* **3**, 11, doi:10.1186/1476-5926-3-11 (2004).
- 121 Mars, W. M. *et al.* Immediate early detection of urokinase receptor after partial hepatectomy and its implications for initiation of liver regeneration. *Hepatology* **21**, 1695-1701 (1995).
- 122 Watanabe, K. *et al.* PAI-1 plays an important role in liver failure after excessive hepatectomy in the rat. *J Surg Res* **143**, 13-19, doi:10.1016/j.jss.2007.04.041 (2007).
- 123 Inagaki, H. *et al.* Effects of nafamostat mesilate, a synthetic protease inhibitor, on immunity and coagulation after hepatic resection. *Hepatogastroenterology* **46**, 3223-3228 (1999).
- 124 Gotohda, N. *et al.* The role of a protease inhibitor against hepatectomy. *Hepatogastroenterology* **53**, 115-119 (2006).
- 125 Draxler, D. F. *et al.* Tranexamic acid modulates the immune response and reduces postsurgical infection rates. *Blood Adv* **3**, 1598-1609, doi:10.1182/bloodadvances.2019000092 (2019).
- 126 Tangelder, G. J., Teirlinck, H. C., Slaaf, D. W. & Reneman, R. S. Distribution of blood platelets flowing in arterioles. *Am J Physiol* **248**, H318-323, doi:10.1152/ajpheart.1985.248.3.H318 (1985).
- 127 Woldhuis, B., Tangelder, G. J., Slaaf, D. W. & Reneman, R. S. Concentration profile of blood platelets differs in arterioles and venules. *Am J Physiol* **262**, H1217-1223, doi:10.1152/ajpheart.1992.262.4.H1217 (1992).
- 128 Yun, S. H., Sim, E. H., Goh, R. Y., Park, J. I. & Han, J. Y. Platelet Activation: The Mechanisms and Potential Biomarkers. *Biomed Res Int* **2016**, 9060143, doi:10.1155/2016/9060143 (2016).
- 129 Periyah, M. H., Halim, A. S. & Mat Saad, A. Z. Mechanism Action of Platelets and Crucial Blood Coagulation Pathways in Hemostasis. *Int J Hematol Oncol Stem Cell Res* **11**, 319-327 (2017).
- 130 Morrell, C. N., Aggrey, A. A., Chapman, L. M. & Modjeski, K. L. Emerging roles for platelets as immune and inflammatory cells. *Blood* **123**, 2759-2767, doi:10.1182/blood-2013-11-462432 (2014).
- 131 Bombeli, T., Schwartz, B. R. & Harlan, J. M. Adhesion of activated platelets to endothelial cells: evidence for a GPIIb/IIIa-dependent bridging mechanism and novel roles for endothelial intercellular adhesion molecule 1 (ICAM-1), alpha_vbeta₃ integrin, and GPIIb/IIIa. *J Exp Med* **187**, 329-339, doi:10.1084/jem.187.3.329 (1998).
- 132 Lievens, D. *et al.* Platelet CD40L mediates thrombotic and inflammatory processes in atherosclerosis. *Blood* **116**, 4317-4327, doi:10.1182/blood-2010-01-261206 (2010).
- 133 Kuijper, P. H. *et al.* Platelet associated fibrinogen and ICAM-2 induce firm adhesion of neutrophils under flow conditions. *Thromb Haemost* **80**, 443-448 (1998).
- 134 Simon, D. I. *et al.* Platelet glycoprotein Iba1 is a counterreceptor for the leukocyte integrin Mac-1 (CD11b/CD18). *J Exp Med* **192**, 193-204 (2000).

- 135 Zarbock, A., Polanowska-Grabowska, R. K. & Ley, K. Platelet-neutrophil-interactions: linking hemostasis and inflammation. *Blood Rev* **21**, 99-111, doi:10.1016/j.blre.2006.06.001 (2007).
- 136 Savage, B., Saldivar, E. & Ruggeri, Z. M. Initiation of platelet adhesion by arrest onto fibrinogen or translocation on von Willebrand factor. *Cell* **84**, 289-297 (1996).
- 137 Rumbaut, R. E., Randhawa, J. K., Smith, C. W. & Burns, A. R. Mouse cremaster venules are predisposed to light/dye-induced thrombosis independent of wall shear rate, CD18, ICAM-1, or P-selectin. *Microcirculation* **11**, 239-247, doi:10.1080/10739680490425949 (2004).
- 138 Ruggeri, Z. M., Orje, J. N., Habermann, R., Federici, A. B. & Reininger, A. J. Activation-independent platelet adhesion and aggregation under elevated shear stress. *Blood* **108**, 1903-1910, doi:10.1182/blood-2006-04-011551 (2006).
- 139 Mende, K. *et al.* Targeting platelet migration in the postischemic liver by blocking protease-activated receptor 4. *Transplantation* **97**, 154-160, doi:10.1097/01.TP.0000437430.89485.a0 (2014).
- 140 Khandoga, A., Biberthaler, P., Messmer, K. & Krombach, F. Platelet-endothelial cell interactions during hepatic ischemia-reperfusion in vivo: a systematic analysis. *Microvascular research* **65**, 71-77 (2003).
- 141 Khandoga, A. *et al.* P-selectin mediates platelet-endothelial cell interactions and reperfusion injury in the mouse liver in vivo. *Shock* **18**, 529-535 (2002).
- 142 Khandoga, A. *et al.* Platelet adhesion mediated by fibrinogen-intercellular adhesion molecule-1 binding induces tissue injury in the postischemic liver in vivo. *Transplantation* **74**, 681-688, doi:10.1097/00007890-200209150-00016 (2002).
- 143 Coughlin, S. R. Thrombin signalling and protease-activated receptors. *Nature* **407**, 258-264, doi:10.1038/35025229 (2000).
- 144 Rezaie, A. R. Protease-activated receptor signalling by coagulation proteases in endothelial cells. *Thromb Haemost* **112**, 876-882, doi:10.1160/TH14-02-0167 (2014).
- 145 O'Brien, P. J., Molino, M., Kahn, M. & Brass, L. F. Protease activated receptors: theme and variations. *Oncogene* **20**, 1570-1581, doi:10.1038/sj.onc.1204194 (2001).
- 146 Bahou, W. F. Protease-activated receptors. *Curr Top Dev Biol* **54**, 343-369, doi:10.1016/s0070-2153(03)54014-5 (2003).
- 147 Fender, A. C., Rauch, B. H., Geisler, T. & Schror, K. Protease-Activated Receptor PAR-4: An Inducible Switch between Thrombosis and Vascular Inflammation? *Thromb Haemost* **117**, 2013-2025, doi:10.1160/TH17-03-0219 (2017).
- 148 Rigg, R. A. *et al.* Protease-activated receptor 4 activity promotes platelet granule release and platelet-leukocyte interactions. *Platelets* **30**, 126-135, doi:10.1080/09537104.2017.1406076 (2019).
- 149 Massberg, S. *et al.* Fibrinogen deposition at the postischemic vessel wall promotes platelet adhesion during ischemia-reperfusion in vivo. *Blood* **94**, 3829-3838 (1999).
- 150 Brown, J. H., Volkmann, N., Jun, G., Henschen-Edman, A. H. & Cohen, C. The crystal structure of modified bovine fibrinogen. *Proc Natl Acad Sci U S A* **97**, 85-90, doi:10.1073/pnas.97.1.85 (2000).
- 151 Weisel, J. W. Fibrinogen and fibrin. *Adv Protein Chem* **70**, 247-299, doi:10.1016/S0065-3233(05)70008-5 (2005).
- 152 Lishko, V. K. *et al.* Multiple binding sites in fibrinogen for integrin alphaMbeta2 (Mac-1). *J Biol Chem* **279**, 44897-44906, doi:10.1074/jbc.M408012200 (2004).
- 153 Hori, T. *et al.* Simple and reproducible hepatectomy in the mouse using the clip technique. *World J Gastroenterol* **18**, 2767-2774, doi:10.3748/wjg.v18.i22.2767 (2012).

- 154 Tian, Y., Graf, R., Jochum, W. & Clavien, P. A. Arterialized partial orthotopic liver transplantation in the mouse: a new model and evaluation of the critical liver mass. *Liver Transpl* **9**, 789-795, doi:10.1053/jlts.2003.50170 (2003).
- 155 Schneider, C. A., Rasband, W. S. & Eliceiri, K. W. NIH Image to ImageJ: 25 years of image analysis. *Nat Methods* **9**, 671-675, doi:10.1038/nmeth.2089 (2012).
- 156 Creasy, J. M. *et al.* The Impact of Primary Tumor Location on Long-Term Survival in Patients Undergoing Hepatic Resection for Metastatic Colon Cancer. *Ann Surg Oncol* **25**, 431-438, doi:10.1245/s10434-017-6264-x (2018).
- 157 Tian, Y. *et al.* Kupffer cell-dependent TNF-alpha signaling mediates injury in the arterIALIZED small-for-size liver transplantation in the mouse. *Proc Natl Acad Sci U S A* **103**, 4598-4603, doi:10.1073/pnas.0600499103 (2006).
- 158 Jin, X., Zhang, Z., Beer-Stolz, D., Zimmers, T. A. & Koniaris, L. G. Interleukin-6 inhibits oxidative injury and necrosis after extreme liver resection. *Hepatology* **46**, 802-812, doi:10.1002/hep.21728 (2007).
- 159 Serenari, M., Cescon, M., Cucchetti, A. & Pinna, A. D. Liver function impairment in liver transplantation and after extended hepatectomy. *World J Gastroenterol* **19**, 7922-7929, doi:10.3748/wjg.v19.i44.7922 (2013).
- 160 Zelaya, H., Rothmeier, A. S. & Ruf, W. Tissue factor at the crossroad of coagulation and cell signaling. *J Thromb Haemost* **16**, 1941-1952, doi:10.1111/jth.14246 (2018).
- 161 Witkowski, M., Landmesser, U. & Rauch, U. Tissue factor as a link between inflammation and coagulation. *Trends Cardiovasc Med* **26**, 297-303, doi:10.1016/j.tcm.2015.12.001 (2016).
- 162 Levi, M. & van der Poll, T. Inflammation and coagulation. *Crit Care Med* **38**, S26-34, doi:10.1097/CCM.0b013e3181c98d21 (2010).
- 163 Higgins GM, A. R. Experimental pathology of liver. I. Restoration of liver of white rat following partial surgical removal. *Arch Pathol*, 186-202 (1931).
- 164 Nevzorova, Y. A., Tolba, R., Trautwein, C. & Liedtke, C. Partial hepatectomy in mice. *Laboratory animals* **49**, 81-88, doi:10.1177/0023677215572000 (2015).
- 165 Nikfarjam, M., Malcontenti-Wilson, C., Fanartzis, M., Daruwalla, J. & Christophi, C. A model of partial hepatectomy in mice. *Journal of investigative surgery : the official journal of the Academy of Surgical Research* **17**, 291-294, doi:10.1080/08941930490502871 (2004).
- 166 Dold, S. *et al.* Portal Hyperperfusion after Extended Hepatectomy Does Not Induce a Hepatic Arterial Buffer Response (HABR) but Impairs Mitochondrial Redox State and Hepatocellular Oxygenation. *Plos One* **10**, e0141877, doi:10.1371/journal.pone.0141877 (2015).
- 167 Pühr-Westerheide, D. *et al.* Neutrophils promote venular thrombosis by shaping the rheological environment for platelet aggregation. *Sci Rep* **9**, 15932, doi:10.1038/s41598-019-52041-8 (2019).
- 168 Antunes, M. M., Carvalho, E. & Menezes, G. B. DIY: "Do Imaging Yourself" - Conventional microscopes as powerful tools for in vivo investigation. *Int J Biochem Cell Biol* **94**, 1-5, doi:10.1016/j.biocel.2017.11.004 (2018).
- 169 Sanger, C. *et al.* Intrahepatic Vascular Anatomy in Rats and Mice--Variations and Surgical Implications. *Plos One* **10**, e0141798, doi:10.1371/journal.pone.0141798 (2015).
- 170 Gaertner, F. *et al.* Migrating Platelets Are Mechano-scavengers that Collect and Bundle Bacteria. *Cell* **171**, 1368-1382 e1323, doi:10.1016/j.cell.2017.11.001 (2017).

- 171 Park, S. A., Choe, Y. H., Lee, S. H. & Hyun, Y. M. Two-photon Intravital Imaging of Leukocytes During the Immune Response in Lipopolysaccharide-treated Mouse Liver. *J Vis Exp*, doi:10.3791/57191 (2018).
- 172 Webb, D. J. & Brown, C. M. Epi-fluorescence microscopy. *Methods Mol Biol* **931**, 29-59, doi:10.1007/978-1-62703-056-4_2 (2013).
- 173 So, P. T., Dong, C. Y., Masters, B. R. & Berland, K. M. Two-photon excitation fluorescence microscopy. *Annu Rev Biomed Eng* **2**, 399-429, doi:10.1146/annurev.bioeng.2.1.399 (2000).
- 174 Diaspro, A., Chirico, G. & Collini, M. Two-photon fluorescence excitation and related techniques in biological microscopy. *Q Rev Biophys* **38**, 97-166, doi:10.1017/S0033583505004129 (2005).
- 175 Diacovo, T. G., Roth, S. J., Buccola, J. M., Bainton, D. F. & Springer, T. A. Neutrophil rolling, arrest, and transmigration across activated, surface-adherent platelets via sequential action of P-selectin and the beta 2-integrin CD11b/CD18. *Blood* **88**, 146-157 (1996).
- 176 Sundd, P., Pospieszalska, M. K., Cheung, L. S., Konstantopoulos, K. & Ley, K. Biomechanics of leukocyte rolling. *Biorheology* **48**, 1-35, doi:10.3233/BIR-2011-0579 (2011).
- 177 Robert, S., Wagner, B. K., Boulanger, M. & Richer, M. Aprotinin. *Ann Pharmacother* **30**, 372-380, doi:10.1177/106002809603000410 (1996).
- 178 Syrovets, T., Jendrach, M., Rohwedder, A., Schule, A. & Simmet, T. Plasmin-induced expression of cytokines and tissue factor in human monocytes involves AP-1 and IKKbeta-mediated NF-kappaB activation. *Blood* **97**, 3941-3950, doi:10.1182/blood.v97.12.3941 (2001).
- 179 Li, X. *et al.* Plasmin triggers chemotaxis of monocyte-derived dendritic cells through an Akt2-dependent pathway and promotes a T-helper type-1 response. *Arteriosclerosis, thrombosis, and vascular biology* **30**, 582-590, doi:10.1161/ATVBAHA.109.202044 (2010).
- 180 Greene, A. K. *et al.* Endothelial-directed hepatic regeneration after partial hepatectomy. *Ann Surg* **237**, 530-535, doi:10.1097/01.SLA.0000059986.96051.EA (2003).
- 181 Li, J. *et al.* Sinusoidal microcirculatory changes after small-for-size liver transplantation in rats. *Transpl Int* **23**, 924-933, doi:10.1111/j.1432-2277.2010.01058.x (2010).
- 182 Li, C. H. *et al.* Laser speckle contrast imaging and Oxygen to See for assessing microcirculatory liver blood flow changes following different volumes of hepatectomy. *Microvasc Res* **110**, 14-23, doi:10.1016/j.mvr.2016.11.004 (2017).
- 183 Moore, E. E. *et al.* Postinjury fibrinolysis shutdown: Rationale for selective tranexamic acid. *J Trauma Acute Care Surg* **78**, S65-69, doi:10.1097/TA.0000000000000634 (2015).
- 184 Roberts, I. Tranexamic acid in trauma: how should we use it? *J Thromb Haemost* **13 Suppl 1**, S195-199, doi:10.1111/jth.12878 (2015).
- 185 Franco, A. T., Corken, A. & Ware, J. Platelets at the interface of thrombosis, inflammation, and cancer. *Blood* **126**, 582-588, doi:10.1182/blood-2014-08-531582 (2015).
- 186 Weyrich, A. S. & Zimmerman, G. A. Platelets: signaling cells in the immune continuum. *Trends Immunol* **25**, 489-495, doi:10.1016/j.it.2004.07.003 (2004).
- 187 Vieira-de-Abreu, A., Campbell, R. A., Weyrich, A. S. & Zimmerman, G. A. Platelets: versatile effector cells in hemostasis, inflammation, and the immune continuum. *Semin Immunopathol* **34**, 5-30, doi:10.1007/s00281-011-0286-4 (2012).
- 188 Semple, J. W., Italiano, J. E., Jr. & Freedman, J. Platelets and the immune continuum. *Nature reviews. Immunology* **11**, 264-274, doi:10.1038/nri2956 (2011).

- 189 Slaba, I. *et al.* Imaging the dynamic platelet-neutrophil response in sterile liver injury and repair in mice. *Hepatology* **62**, 1593-1605, doi:10.1002/hep.28003 (2015).
- 190 Ed Rainger, G. *et al.* The role of platelets in the recruitment of leukocytes during vascular disease. *Platelets* **26**, 507-520, doi:10.3109/09537104.2015.1064881 (2015).
- 191 Rosales, C. Neutrophil: A Cell with Many Roles in Inflammation or Several Cell Types? *Front Physiol* **9**, 113, doi:10.3389/fphys.2018.00113 (2018).
- 192 Murata, S. *et al.* Platelets promote liver regeneration in early period after hepatectomy in mice. *World J Surg* **31**, 808-816, doi:10.1007/s00268-006-0772-3 (2007).
- 193 Matsuo, R., Nakano, Y. & Ohkohchi, N. Platelet administration via the portal vein promotes liver regeneration in rats after 70% hepatectomy. *Ann Surg* **253**, 759-763, doi:10.1097/SLA.0b013e318211caf8 (2011).
- 194 Lopez, M. L. *et al.* Platelet increases survival in a model of 90% hepatectomy in rats. *Liver international : official journal of the International Association for the Study of the Liver* **34**, 1049-1056, doi:10.1111/liv.12326 (2014).
- 195 Hisakura, K. *et al.* Platelets prevent acute liver damage after extended hepatectomy in pigs. *J Hepatobiliary Pancreat Sci* **17**, 855-864, doi:10.1007/s00534-010-0276-2 (2010).
- 196 Kirschbaum, M. *et al.* Transient von Willebrand factor-mediated platelet influx stimulates liver regeneration after partial hepatectomy in mice. *Liver international : official journal of the International Association for the Study of the Liver* **37**, 1731-1737, doi:10.1111/liv.13386 (2017).
- 197 Slofstra, S. H. *et al.* Protease-activated receptor-4 inhibition protects from multiorgan failure in a murine model of systemic inflammation. *Blood* **110**, 3176-3182, doi:10.1182/blood-2007-02-075440 (2007).
- 198 Miyakawa, K. *et al.* Platelets and protease-activated receptor-4 contribute to acetaminophen-induced liver injury in mice. *Blood* **126**, 1835-1843, doi:10.1182/blood-2014-09-598656 (2015).
- 199 Luyendyk, J. P., Schoenecker, J. G. & Flick, M. J. The multifaceted role of fibrinogen in tissue injury and inflammation. *Blood* **133**, 511-520, doi:10.1182/blood-2018-07-818211 (2019).
- 200 Groeneveld, D. *et al.* Intrahepatic fibrin(ogen) deposition drives liver regeneration after partial hepatectomy in mice and humans. *Blood* **133**, 1245-1256, doi:10.1182/blood-2018-08-869057 (2019).

Danksagung

In erster Linie danke ich Herrn Prof. Dr. med Alexander Baethmann für die freundliche Einladung in das Walter-Brendel-Zentrum. Sein mehrjähriger Beitrag zu der CSC-LMU-Kooperation ermöglichte zahlreichen chinesischen Doktoranden an der Ludwig-Maximilians-Universität promovieren zu dürfen.

In höchstem Maße danke ich Herrn Prof. Dr. med Andrej Khandoga für die Aufnahme in seine Arbeitsgruppe und die Überlassung des interessanten Themas der vorliegenden Arbeit. Die exzellent etablierte Arbeitsumgebung und Teamdynamik erleichterten den komplizierten Ablauf des Experiments. Seine hervorragende akademische Leistung und sein wissenschaftlicher Anspruch werden für mich in meiner Karriere immer ein Ansporn sein.

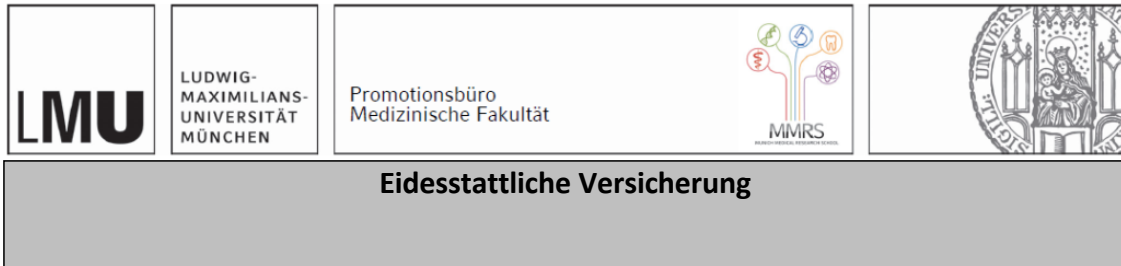
Insbesondere möchte ich mich bei Herrn Dr. med. Maximilian Lerchenberger bedanken. Unter seiner freundschaftlichen Betreuung konnte ich umfangreiche wissenschaftliche Fähigkeiten erlernen. Durch sein Vertrauen in mich konnte ich selbständig arbeiten und meine eigenen Ideen durchführen. Die fast grenzenlose Geduld und der ständige persönliche Einsatz von ihm machten den Weg für meinen ersten Kongressvortrag auf Deutsch frei. Darüber hinaus war er mir in Deutschland ein großes Vorbild, als Chirurg, Wissenschaftler, und Lehrer. Die Zusammenarbeit mit ihm ist eine Ehre und wird in bester Erinnerung gehalten.

Ebenso danke ich meinem Kollegen Dr. med. Marc Praetner für die freundliche Einarbeitung in das Projekt sowie Patrick Huber für die erfolgreiche Zusammenarbeit. Frau Prof. Dr. med.

Dr. rer. nat. Lesca Holdt, Frau Britta Pauli und Frau Dr. med. Dorothea Fichtl danke ich für die kompetente und zuverlässige laboratorische Unterstützung. Dr. Shakarami und seinem Team aus der Tierhaltung möchte ich ebenfalls meinen Dank aussprechen. Ohne ihre Hilfe wäre diese Doktorarbeit nicht möglich gewesen.

Nicht zuletzt möchte ich ein herzliches Dankeschön an meine Eltern, Weidong Zhang und Ye Zou, sowie an meine Großeltern für den Rückhalt in der Familie richten. Tina Wimmer danke ich für die liebevolle Unterstützung und den motivierenden Zuspruch. Unter anderem Lih Qi Tan und Tim Walter danke ich für eine tolle Freundschaft, die ich zu jedem Zeitpunkt schätzen und respektieren werde. Der Familie Bleckmann danke ich, für die wunderschönen ersten Einblicke in die Kultur und Traditionen Deutschlands, die mir einen reibungslosen Beginn in München ermöglichten.

Affidavit



Zhang, Yunjie

Name, Vorname

Ich erkläre hiermit an Eides statt, dass ich die vorliegende Dissertation mit dem Titel:

The influence of coagulation system on early leukocyte recruitment and acute microcirculatory injury after extended hepatectomy

selbständig verfasst, mich außer der angegebenen keiner weiteren Hilfsmittel bedient und alle Erkenntnisse, die aus dem Schrifttum ganz oder annähernd übernommen sind, als solche kenntlich gemacht und nach ihrer Herkunft unter Bezeichnung der Fundstelle einzeln nachgewiesen habe.

Ich erkläre des Weiteren, dass die hier vorgelegte Dissertation nicht in gleicher oder in ähnlicher Form bei einer anderen Stelle zur Erlangung eines akademischen Grades eingereicht wurde.

München, 30.10.2023
Ort, Datum

Yunjie Zhang
Unterschrift Doktorandin bzw. Doktorand

Lebenslauf

Name: Yunjie Zhang
Geburtsdatum: 13. Juni 1992
Geburtsort: Shanghai, China

Schulische Ausbildung

1998-2008 In Shanghai, China
Jun 2010 Abitur

Universitäre Ausbildung

Sep 2010 – Jun 2015 Bachelor-Studium der Humanmedizin an der Tongji
Universität, Shanghai, China

Sep 2015 – Jun 2018 Master-Studium der Humanmedizin mit Schwerpunkt
der Chirurgie an der Fudan-Universität, Shanghai, China
mit Auszeichnung

Sep 2018 – heute Promotion an der Ludwig-Maximilians-Universität,
München, Deutschland

Mai 2021 – heute Assistenzarzt des Muskuloskelettalen Universitätszentrums München

Staatliche Qualifikation

Okt 2018	Staatsexamen
Mär 2020	Ärztliche Approbation, Tianjin, China
Nov 2021	Ärztliche Approbation, Oberbayern, Deutschland

Publikationen

- 1 **Zhang, Y.**, Wang, X., Shao, Y. & Xia, Q. The orientation of the surgical epicondylar axis varies in varus and non-varus knees in the coronal plane. *Knee Surg Sports Traumatol Arthrosc*, doi:10.1007/s00167-016-4386-5 (2016).
- 2 **Zhang, Y.**, Wang, X., Wu, Z., Xia, Q. & Shao, Y. Highly Variable Femoral Morphology in Osteoarthritic Chinese: Are Prostheses Today Sufficiently Suitable? *J Knee Surg* **30**, 936-942, doi:10.1055/s-0037-1599250 (2017).
- 3 **Zhang, Y. J. et al.** MicroRNAmRNA integrated analysis based on a case of welldifferentiated thyroid cancer with both metastasis and metastatic recurrence. *Oncol Rep* **40**, 3803-3811, doi:10.3892/or.2018.6739 (2018).
- 4 Song, Y. C. *et al.* Proteogenomic characterization and integrative analysis of glioblastoma multiforme. *Oncotarget* **8**, 97304-97312, doi:10.18632/oncotarget.21937 (2017).

- 5 Ma, Y. S. *et al.* Inhibition of USP14 Deubiquitinating Activity as a Potential Therapy for Tumors with p53 Deficiency. *Mol Ther Oncolytics* **16**, 147-157, doi:10.1016/j.omto.2019.12.013 (2020).

Vorträge

- 1 **Zhang, Y. et al.** Small-for-Size Syndrom: Murines IVM Modell zeigt Leukozytenrekutierung und Mikrozirkulationsstörung nach erweiterter Hepatektomie. Viszeralmedizin 2019
- 2 **Zhang, Y. et al.** Cross-talk between Initial Immune Response and Hemodynamical Change in the Acute-phase Liver Injury after Partial Hepatectomy. 23. Chirurgische Forschungstage 2019